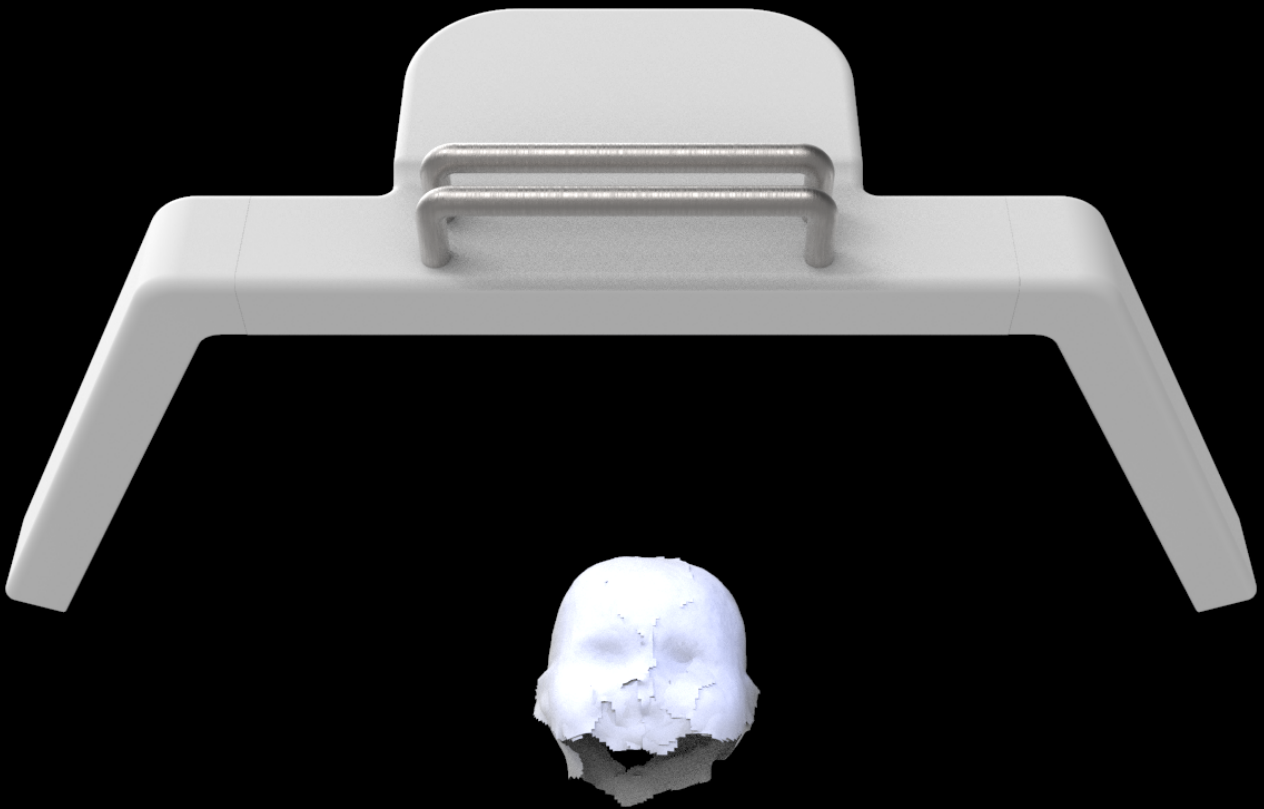


MONITOR3D

DESIGN OF A 3D SCANNER FOR MEASURING PRETERM
INFANT HEAD CIRCUMFERENCE



MASTER THESIS
ALEX ZEVENBERGEN



Author

Alex Zevenbergen

Supervisory Team

Chair

Dr. Yu (Wolf) Song

Mentor TU Delft

Dr. Toon Huysmans

Mentor Vectory3

Pieter van der Zwan

Special thanks to:

Ronald van Gils

For his support and cooperation in this project

Integrated Product Design

Faculty of Design Engineering

Delft University of Technology

10th of December 2020

SUMMARY

In 2010, an estimated 15 million infants were born prematurely, which makes up 10% of all childbirths that year. Just in the Netherlands there were 11,530 preterm births in 2018. Since these children should be spending additional months inside of the uterus, they are delicate and need to grow until near regular gestational age inside of an incubator in the neonatal intensive care unit (NICU), which provides these children with clean, humid, and warm air.

One important part of the care of these infants is keeping track of their development, in order to adjust nourishment, as well as spot possible complications early. A regular part of these measurements is the head circumference (HC) measurement. This measurement is performed by two nurses, one holding the infant still while another winds a tape measure around the delicate head, in order to take the measurement.

Unfortunately, this process causes the infant to stress, which is correlated to an increased chance in reduced neurological development of the infant. Therefore, Vectory3, a company specialized in 3D scanning for healthcare, commissioned a project to create an alternative way to take this measurement, which would cause the infant less stress than the current method.

During this project, this alternative has been conceived and developed into a functional prototype: MONITOR3D. MONITOR3D makes use of 3 hybrid photogrammetry cameras in order to take a contactless 3D capture of the infant's head, allowing NICU staff to measure the 3D model after acquisition, instead of measuring the child directly.

MONITOR3D's cameras are housed in an unobtrusive shell which is placed on top of the incubator hood, staying outside of the hygienical zone of the child during use.

Though the hardware for MONITOR3D is already in a functional state, providing higher accuracy than the current tape measure-based measurements, the software still consists of unmodified open-source software, for which a simple but relatively time consuming (compared to tape measuring) workflow has been developed. The current prototype of MONITOR3D is thus not ready to be used by regular in a NICU setting. However, it can possibly be used for research purposes in its current state.

Future developments should focus mainly on the software part of the product, automating as many of the mesh processing steps as possible, in order to make the device usable in a live NICU environment as alternative to the current tape measure.

TABLE OF CONTENTS

1. Introduction.....	1
1.1 The Problem.....	1
1.2 Objective.....	2
1.3 Report Structure/Design Process.....	2
1.4 Acknowledgements.....	2
2. Analysis.....	4
2.1 NICU.....	5
2.1.1 Equipment.....	5
2.1.2 Dimensions.....	13
2.1.3 Light at Erasmus MC.....	13
2.1.4 Conclusion.....	15
2.2 Infant Sensitivities.....	16
2.2.1 Light.....	16
2.2.2 Sound.....	21
2.2.3 Conclusion.....	22
2.3 Growth Monitoring.....	23
2.3.1 Methods.....	23
2.3.2 Conclusion.....	29
2.4 Program of Requirements.....	31
1. Performance.....	31
2. Maintenance.....	31
3. Aesthetic, Appearance & Finish.....	31
4. Ergonomics.....	31
5. Safety.....	32
6. Product policy.....	32
2.5 Technology Overview.....	33
2.5.1 Types of acquisition.....	33
2.5.2 Overview.....	34
2.5.3 Conclusion.....	41
2.6 Technology choice.....	44
2.6.1 Hardware.....	44
2.6.2 Plane Fit.....	45
2.6.3 Reconstruction Accuracy.....	46
2.6.4 Conclusion.....	51

3. Design	52
3.1 Concepts	53
3.1.1 LiveScan	53
3.1.2 FlexScan	53
3.1.3 Monitor3d	55
3.1.4 Concept Choice	55
3.2 Embodiement	58
3.2.1 Scanning Hardware	58
3.2.2 Module settings	58
3.2.3 Scanner Module Layout	59
3.2.4. Construction	61
3.2.5 Software	67
4. Evaluation	70
4.1 Prototype	71
4.1.1 Hardware	71
4.1.2 Software	73
4.2 Measure Accuracy	78
4.2.1 Method	78
4.2.3 Results	79
4.2.4 Discussion	81
4.2.3 Conclusion	82
4.3 User Experience: Positioning	83
4.3.1 Research questions	83
4.3.2 Method	83
4.3.3 Results	84
4.3.4 Discussion	85
4.3.5 Conclusion	86
4.4 User Experience: Mesh Processing	87
4.4.1 Research question	87
4.4.2 Method	87
4.4.3 Results & Discussion	87
4.4.4 Conclusion	89
5. Conclusion & Recommendations	90
6. References	91

1. INTRODUCTION

1.1 THE PROBLEM

Though most pregnancies are full-term, meaning between 39 and 40 weeks long, sometimes a child is born earlier than that. When born before the 37th week of pregnancy, the infant is considered to be born "preterm" (Spong, 2013).

In 2010, an estimated 15 million infants were born prematurely (Blencowe et al., 2012), which makes up 10% of all childbirths that year. Just in the Netherlands there were 11,530 preterm births in 2018 (*Perined | Home*, 2020).

Worldwide, complications as a result of preterm birth are the number one cause in neonatal deaths (35.3%) (Liu et al., 2016). The risks of these complications being fatal increases with every week that the infant is born earlier. A 2011 study in France showed that survival rate until discharge from the hospital in preterm infants is 72% at 26 weeks, which drops to just 1% at 23 weeks (Ancel et al., 2015).

To safeguard the infant, it is held in an incubator (Figure 1). The incubator creates a controlled environment for the infant, while at the same time allowing for life-supporting and monitoring equipment to be applied. Additionally, the infant is measured regularly by hospital staff in order to monitor growth, which indicates proper development of the infant (Erasmus, 2019)



Figure 1 - Incubator in the NICU



Figure 2 - Infant body length measurement

Erasmus MC in Rotterdam, the Netherlands currently employs two methods for monitoring infant development. The first method uses an "infant measuring rod", which can be described as a large pair of callipers (Figure 2). The measuring rod is put into the incubator with the infant. The nurse then tries to carefully straighten out the limbs of the infant, while holding the measuring rod, in order to get an accurate reading of the infant's length from head to toes.

A contact-heavy method for measuring development in infants is through the circumference of the head. This is done with a simple tape measure. Multiple of these measurements over the stay of the infant can be used to monitor infant growth, and thus development.

Unfortunately, these methods stress the infant because of the extended physical contact needed to keep the infant in position. This stress is correlated to an increased chance on decreased neurological development of the infant (G. C. Smith et al., 2011).

1.2 OBJECTIVE

This project aims to reduce this stress by creating a new tool that allows hospital staff to monitor the growth of the infant without physical contact. This tool will create a 3D scan of (part of) the infant to determine the infant's growth, be that through circumference of the infant's head or other measurable features.

I aim to deliver a design that can be produced by the company Vectory3. This product will be a 3D scanner which makes scans of preterm infants in the incubator. I will create a functional prototype of this scanner which allows me to test the scanner with stakeholders to prove the scanner's functioning. Because the scanner will not make physical contact with the infant, stress levels of the infant will be kept to a minimum during the measurement process. From a usability point of view, the scanner (to be designed) will be as easy or easier to use by hospital staff than the current measuring methods. I expect this scanner to fit in Vectory3's current product-service system by making use of a pay-per-scan system similar to that of the current Vectory3 Curatio scanner.

1.3 REPORT STRUCTURE/DESIGN PROCESS

The structure of this report consists of the following four phases: Introduction, Analysis, Design, and Evaluation

The Analysis phase covers literature research, interviews, and experiments with the goal of determining the context of the product. This phase concludes with the *Program of Requirements (PoR)*, a list of requirements and wishes that describe the needed and wanted functionality of the product.

The Design phase covers the ideation, conceptualization and prototyping of the product. Here, both hardware and software aspects of the design are covered, as well as the limitations and initial findings of the final prototype.

The Evaluation phase covers experiments performed with the prototype, in order to validate what parts of the PoR are met. This way it is determined whether the current design meets the goal that was originally set out, or if it has any potential to do so in the future. Additionally, it is discussed what further action should be taken to improve upon the current design.

1.4 ACKNOWLEDGEMENTS

This research is an integrated product design (IPD) master graduation project from Delft University of Technology, faculty of Industrial Design Engineering. Dr. Yu (Wolf) Song acted as chair of the project, with Dr. Toon Huysmans acting as mentor.

This product will be designed for, and with the help of, Pieter van der Zwan of the commissioning party of this project, Vectory3 BV. Vectory3 has experience in using surface 3D scanning in medical settings. Specifically, their "Curatio" hand and arm scanner uses photogrammetry to construct a 3D model of the patient's limb from multiple 2D images taken from various angles.

Additionally, this project is supported by Erasmus MC and Ronald van Gils from Create4Care. The findings and resulting prototype from this study will be used by Ronald van Gils for his ongoing PhD project.

2. ANALYSIS

This chapter is divided into 4 sections. **2.1 NICU** gives an overview of what features of the neonatal intensive care unit, and its equipment, the product should take into account. **2.2 Infant Sensitivities** describes the susceptibility of preterm infants to certain stimuli, and how these stimuli affect the development of the infant. Knowing these sensitivities, Afterwards, **2.3 Growth Monitoring** explains the why and how of measuring preterm infants, and the accompanying difficulties caused by those sensitivities. **2.4 Program of Requirements** provides a summary of all relevant requirements and wishes for the product, based on the performed research. **2.5 Technology Overview** describes the different technologies that are available to be used in the product for the 3D capture of the infant's head. **2.6 Technology Choice** compares the two best fitting candidates from this overview through two experiments.

2.1 NICU

The neonatal intensive care unit (NICU) specialises in the care of premature or otherwise ill new-borns. It features specialised equipment like the incubator, as well as specialised staff to aid in this goal. In this chapter the environment in the NICU is discussed, as well as its possible implications on the design of the product. This environment has been based on observations at Erasmus MC where possible, and literature where not.

2.1.1 EQUIPMENT



Figure 3 - NICU nurses performing head circumference measurement

Firstly, the equipment inside the NICU is discussed, focussing on a single unit or cell, which is used to take care of a single infant. Special attention is paid to the incubator, it being perhaps the most vital piece of equipment in the room, keeping the baby in a controlled atmosphere. Afterwards, supporting equipment is briefly mentioned, including any possible effect this equipment has on the design of the product.

2.1.1.1 THE INCUBATOR



Figure 4 - Draeger Caleo incubator

Since the preterm infant no longer has the safety and protection of the uterus, it needs to be carefully protected after birth. This is accomplished through the use of an incubator (Figure 4). An incubator can be described as a see-through, plastic box that creates an isolated, protective environment within for the preterm infant. It is an integral part of the NICU. Though this product is to be made universal in a way that it works with most incubators, for the purpose of this report the focus will be on the Draeger Caleo and Draeger Babyleo, which are Erasmus MC's current and near-future incubator models respectively. This is done for accessibility, which aids analysis, prototyping and validation.

FUNCTIONALITY

Though many different incubator designs are developed and produced by different companies, all incubators possess the same set of basic functionalities. These are:

- Keeping a filtered internal airflow
- Maintaining a set internal atmospheric humidity (usually higher than outside)
- Maintaining a set internal temperature
- Allowing for monitoring equipment to be fed inside the incubator, without compromising its isolating qualities
- Allowing for life support equipment (such as ventilator and nutrition tubing) to be fed into the incubator without compromising its isolating quantity
- Allow quick and easy access to the infant for (emergency) procedures.

In addition to this, modern incubators, like those by Draeger also allow for the following:

- Monitoring the weight of the child through a built-in scale
- Height adjustable and tilting the bed for optimal access to the infant
- Air curtain thermoregulation, allowing for the internal temperature and humidity to stay stable even with the access hatches opened

DIMENSIONS

In order to design a product that resides either in or on the incubator, its dimensions must be known. However, incubator dimensions are as varied as the amount of incubator models that are produced, since no incubator design standards or best-practices have ever been published. Even in within the same model by the same maker, important dimensions can diver due to accessories. This is especially true for the inside of the incubator, where space is at a premium.

For example, an important internal measurement is that of the distance between the top of the forehead of the infant, and the inside of the top casing of the incubator. This measurement determines what, if anything, can be placed above the infant's head while staying inside the incubator. Even if this measurement is taken with 5 Draeger Caleo, the results will vary because of the influence of

- The size of the infant
- The height of the height-adjustable bed
- The thickness of the mattress used
- The amount of monitoring or tubing already in-place

This makes it impossible to say with any certainty what amount of space may be expected for the product to exist in, without even considering other models of incubator.

INTERNAL ENVIRONMENT

The incubator keeps a controlled internal environment to protect the preterm infant. The air is filtered for allergens and other particle, and a constant temperature and humidity are kept up. The amount of humidity and heat that get circulated depends on the age and week of gestation of the infant. A New Zealand New-born Service Clinical Guideline recommend starting out with a humidity of 80%, while letting the incubator itself regulate the internal temperature with a temperature probe connected to the infant, set for a temperature between 36.5°C and 37.2°C (*NW Newborn Clinical Guideline - Care of the Baby in an Incubator, n.d.*).

Though it is certainly possible to deploy an electronic product in such an environment, considerable care would have to be taken in the water resistance of the case design or conformal coating of the PCB. Additionally, attention should be paid to the thermal design if the product were to reside inside the hot incubator, especially now that it has been determined that the device will not feature any type of active cooling due to NICU sound levels already being surpassed without the product.

INFANT POSITION

The preterm infant, outside of moving its limbs, is too weak to make any meaningful changes to its position. Therefore, it is important that the nurse puts the infant in a position that is both healthy and comfortable.



Figure 5 - Infant in prone position



Figure 6 - Infant in supine position

There are two main positions that an infant can be placed in: a prone position and the supine position. In the prone position (figure 5) the infant lies on its stomach with its head turned to one side, while in the supine position (figure 6) the infant is on its back with its head either to one side, or stabilised to look straight up using a soft folded towel (*Positioning Your Premature Baby*, 2016)

More recent research suggests that the prone position enables more rapid growth and less energy expenditure (Willinger et al., 1998), better oxygenation of the infant (Rivas-Fernandez et al., 2016) and improved sleep patterns and lowered stress (Jarus et al., 2011). However multiple older study found that a correlation exists between sudden infant dead syndrome (SIDS) and positioning the infant in a prone position (Willinger et al., 1998). And even though no causality could be proven, the American Academy of Paediatrics published a guideline recommending that the prone position be avoided in favour of the supine position, in order to prevent SIDS ("American Academy of Pediatrics AAP Task Force on Infant Positioning and SIDS: Positioning and SIDS,," 1992). Because of this, most infants are now placed in the supine position.

Very preterm infants do not have the strength to move themselves. Their heads would stay laying in the same position if no action is taken by a nurse. This can cause plagiocephaly (flat head syndrome) since the soft skulls of the preterm infants can easily deform under their own weight. To prevent this from happening, hospital staff must periodically turn the head of the infant to another side, in order to equally distribute the pressure of laying down on all sides (Ifflaender, Rüdiger, Konstantelos, et al., 2013). No recommendations are given regarding this interval.

OBSTRUCTIONS

In an ideal world, the infant would be placed on a perfectly transparent surface, with no object around it limiting view, allowing for scanner equipment to be placed wherever it would be optimal for image quality. Unfortunately, in reality the (head of the) infant is mostly obscured by equipment, cover and bedding. Here the most frequently encountered forms of obstruction are discussed.

MATTRESS

Though obvious, the mattress is the first and biggest obstacle for a HC measurement through 3D scanning: Since the baby is lying down, and the mattress is opaque, the side of the head lying on the mattress can never be scanned.

HEAD SUPPORT



Figure 7 - infant in head supporting towel

Since very preterm infants in the NICU do not have the strength to keep their heads in position, a supportive towel is rolled up and put around the head of the infant in an 'U' shape (figure 7). The height of this towel obscures parts of the sides of the head of the infant.

OXYGEN TUBE



Figure 8 - Infant connected to oxygen tube

If an infant's blood oxygen level is too low, they may be fitted an oxygen tube. This thin, translucent tube spans the circumference of the head below the nose and supplies the child with oxygen (figure 8). Though the tube itself lies below the cranium, and thus in theory not obscuring relevant details from scanners, the extension of it can be an obstruction if not properly guided through the incubator.

CPAP



Figure 9 - Infant connected to CPAP mask

Continuous positive air pressure (CPAP) refers to the breathing equipment used on some preterm infants who do not yet have the development to breath themselves. These masks are relatively large and, depending on the model used, can cover the head of the infant, obscuring the cranium from the scanner (figure 9). Though hospitals like Erasmus use CPAP solutions that do not cover the cranium, if a solution that does is used by a hospital, it will most likely have to be removed or the obstruction otherwise held out of the way of the scanner during acquisition.

CAPS, HATS AND OTHER HEAD COVERS

Some hospitals put small caps over the cranium of the infant. Though this is not always the case, such caps might interfere with the measuring process, since they add additional bulk to the outside of the head. Depending on the thickness/form-fittingness of the cap, and the hospital's measuring protocol, the cap might have to be removed by caretakers before an acquisition can be made.

In order to prevent additional stress from this removal of the cap, image acquisition may be combined with other interventions that require the cap to be removed. This way the acquisition itself does not add to the stress levels of the infant.

HOOD DESIGN



Figure 10 - Two models of incubator showing similar hood design

Appendix C features an overview of currently available incubator designs, which shows that even though the exact measurements differ, a distinct archetype can be described that fits most of these designs: Most modern freestanding incubators use a design like the Draeger Caleo currently used by Erasmus. This means that the incubator, in addition to the horizontal top and vertical sides, also features two diagonal sides for easy viewing of the infant while standing in the NICU (Figure 10). The only big exceptions are units made for wall placement. These units only feature a single angled pane, with the wall-side of the incubator being completely vertical.

SCUFFS & SCRATCHES



Figure 11 - Two photos showing scuffs and scratches on an incubator hood

Scratches and scuffs on the hood of the incubator can cause blind-spots for the scanner if one in places in its line-of-sight. A hood that was lend to me by Erasmus MC features a number of these scratches and scuffs (figure 11). Nurses of the NICU confirmed that the number of marks this unit has in comparable to ones still in operation, though any deeper scratches than this would cause the hood to be decommissioned, since dirt and other contaminants could collect in the hard to clean gaps.

2.1.1.2 OTHER EQUIPMENT

In addition to the incubator, the NICU features supportive and diagnostic hardware that interacts with the incubator or the infant itself. Figure 3 shows a single cell with an incubator. At the time the picture was taken, two nurses were performing an HC measurement. The following is an overview of relevant hardware visible in this image, from left to right.

- There are two monitors on the left side of each incubator. The top one is used for infant diagnostics, including heart rate, blood pressure, blood oxygen level, etc. The leads connected to sensors that measure this data from the infant enter the incubator through the head-side access ports.
- The monitor below is used for entering and retrieving patient data to and from the database.
- The column to the right of the monitors features power sockets to power the incubator and other equipment. It also features the gas hook-ups for, for example, oxygen flow to the infant. The tubes from these hook-ups enter the incubator from the head-side access ports.

- On top of the incubator itself is a green tarp. At Erasmus, this is used to cover the incubator whenever there is no intervention or other handling of the infant necessary, in order to keep it in complete darkness for as long as possible.
- The monitor visible beneath the green tarp is fixed to the incubator itself. It features information about the status of the incubator.
- Below that, a small mobile desk can be seen. This is used to hold whatever tools the caretakers need to have at hand during interventions, as well as paperwork and disposables like gloves.
- To the right 4 infusion pumps are suspended from a rail that is mounted on the ceiling of the NICU. Their leads enter the incubator through the rear access ports.
- Finally, a curtain closable surrounds the entire cell. This allows for privacy when parents visit.

2.1.2 DIMENSIONS

When developing the mounting solution of the product, the working space of the NICU personnel must be considered to ensure that the product can be handled within the given space constraints. To make sure that adequate space around the Incubator is available, measurements have been taken of a typical Erasmus MC NICU cell. A top-down layout of the single NICU cell at Erasmus MC can be seen in figure 12. All measurements are in mm.

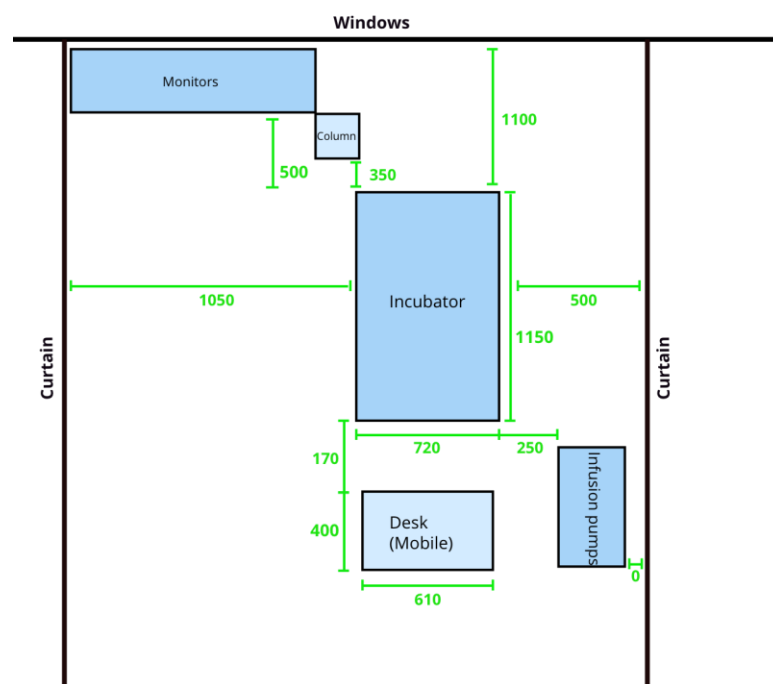


Figure 12 - Top down map of a single NICU care unit

2.1.3 LIGHT AT ERASMUS MC



Figure 13 - Erasmus NICU showing incubators covered in light blocking tarps

The performance of the technology used for 3D scanning in this product might be dependent on environmental light. In a previous chapter the lighting conditions in multiple NICUs were discussed based on literature research. Observations at Erasmus MC, however, show lighting conditions which are quite different from those discussed.

Current research and guidelines recommend the implementation of a day-night cycle for improved development of the preterm infant. However, Erasmus MC still operates according to the old paradigm that, since the inside of the uterus is supposedly dark, the best treatment for a preterm infant is to keep it in as dark an environment for as long as possible. This, of course, has been disproven since it is now known that a biological clock already develops while the infant is in-uterus (Akiyama et al., 2010).

Erasmus MC keeps the artificial lighting off and windows blinded for as long as possible, only opening one or more windows if light is needed for interventions and other work (figure 13). The same image shows that all incubators are covered with a darkening tarp whenever the infant is not being checked-up or otherwise handled. To prevent infant stress from lifting the tarp for routine visual checks, thus suddenly increasing the brightness, the nurses use a small camera attached to the outside of each incubator, which allows them to visually monitor the children from their desk without lifting the tarp.

When additional lighting is needed, this is kept to the minimum level necessary for performing the task. For example. During a HC measurement, the window blind of one window next to the incubator was opened. This caused a measured illumination near the infant of 55.5lux. During normal operation, when there are no handling activities in the NICU, measured light levels were 17.3lux. Though no measurements have been taken underneath the tarps, it can be assumed that the light level inside the incubator is near 0lux.

2.1.4 CONCLUSION

Regarding the incubator, it seems preferable to design the product to be used on the outside of the device. This means the hot, humid internal atmosphere can be disregarded, simplifying the design. Additionally, this means that the unknowns of the internal dimensions of the incubator no longer have to be taken into account. However, this also brings possible downsides, like image distortion due to the curvature of the incubator hood. Additionally, scuff marks, scratches and other imperfections of the see-through hood could impair data acquisition.

Regarding the position of the infant. Since it is recommended for the child to put in a supine position to prevent SIDS, this position will be assumed for the design of the product. Furthermore, it might be possible to make use of the periodical head-turning of the infant by the staff, in order to acquire data that was previously out of view.

Though it is impossible to prevent all forms of obstruction, a clever placement of the scanners(s) in combination with a quick 'best practices' instruction might be enough to solve most of the problem.

Equipment surrounding the incubator is placed far away enough to not interfere with any products placed directly on the hood of it. Yet, the wires and tubes coming from this equipment might obscure the line of sight between the scanner and the infant. Though the incubator in this observation offers enough possibilities for cables and tubes to be routed in an unobtrusive way, it is still up to the staff of the NICU to make sure that these features are made use of. Making this clear might become a requirement of the product if many cases of improper cable and tube management are found.

Though not cramped, the room around the incubator is compact. Especially on the side of the infusion pumps. Nevertheless, this should not affect the design of the product. If the product were large enough for the room around the incubator to cause a problem, it would most likely be too large for the NICU staff to handle anyway.

To keep stress levels for the infant during data acquisition as low as possible, the illumination in the incubator should ideally not be increased from the standard environmental illumination. However, at Erasmus this level is 0lux, with 55.5lux only being attained when the tarp is removed for handling which already induces stress. Depending on the chosen technology, IR-A illumination might be solution to this problem, since it slows for the increase in illumination for the scanner, without increasing visible illumination for the infant. If this turns out to not be possible, however, a solution is requiring the removal of the tarp. Though this does increase stress levels of the infant, the rest of the process requires no physical handling of the infant as opposed to traditions tape HC measurements. This till results in a net reduction of total procedure infant stress levels.

2.2 INFANT SENSITIVITIES

With the too-early birth of preterm children come numerous complications that make the handling of the infants challenging. After all, the time the infant is now spending outside was supposed to be time spent in the protective womb of the mother. The infant is thus not yet fully developed to deal with the conditions of the outside world. It is sensitive to certain outside stimuli. In this chapter, stimuli relevant to the design of the product (light, sound, touch) are explored in order to find requirements and limits for the product.

2.2.1 LIGHT

Optical scanners, by definition, require a light source (either visible or invisible) to function. The specifics and requirements of this light source differ per technology. In order to choose a suitable technology, the influence light has on the premature infant must first be explored.

2.2.1.1 VISIBLE LIGHT

Very preterm infants are already sensitive to light and respond to changes in environmental light intensity by, amongst others, increasing their respiratory rate (Kuhn et al., 2012). This means that even for very-preterm infants, the lighting conditions in the NICU need to be controlled. An illuminance of 600 lux maximum, measured near the infant, is recommended as environmental lighting in the NICU (White et al., 2013). Above this intensity protective eye covers are recommended. These are readily available in any NICU, since they are applied whenever an infant receives blue-light treatment against Jaundice (Robinson et al., 1990)(Figure 14). Even though prolonged exposure to higher intensities than 600lux has not been proven to cause ocular damage to infants (Hamer et al., 1984), it has been observed that light may cause stress in the infant (Newnham et al., 2009).

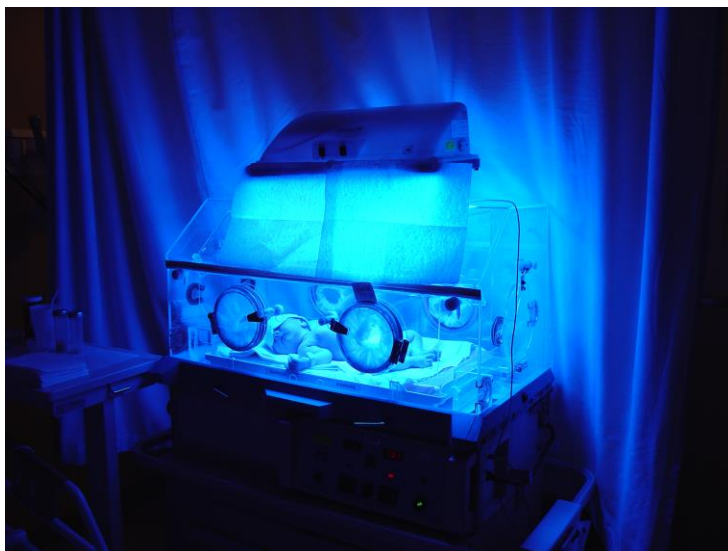


Figure 14 - Incubator lit by a *bili light*, which treats jaundice in infants

The amount of light reaching the infant is not only influenced by the product, but also by the infant's environment. Though the 600lux recommendation is given, research shows NICU illumination between hospitals vary from 192lux to 905lux (Robinson et al., 1990), with a more recent paper citing a measured value of 325lux in the NICU (Szczepański & Kamianowska, 2008). To ensure the total amount of illuminance of the infant (without eye protection) does not exceed 600 lux, the product must consider local environmental lighting conditions.

Though at first it was thought that, since it must be completely dark in uterus, the preterm infant must be kept in as much darkness as possible. Current understanding of the development of the foetus in the uterus shows that there is a circadian rhythm being kept (Akiyama et al., 2010). This rhythm is important for the neurological development of the infant (Rivkees, 2004), thus it is recommended that a day-night cycle is introduced into the NICU to support the development of this rhythm (Watanabe et al., 2013). Though no exact illuminance value is given, environmental lighting is to be kept to a minimum during the night cycle. Brandon D. observed a brightness of between 5lux and 30lux during the night cycle in the NICU in her study regarding the introduction of cycled light for extreme infants (Brandon et al., 2017). A scanner operating using visible light could thus be rendered inoperable during this time.

2.2.1.2 NON-VISIBLE LIGHT

Some scanning methods allow for the usage of light outside the visible spectrum of humans. A product using non-visible light would use light in the near-infrared spectrum (IR-A, 700nm – 1400nm) (Henderson, 2006), since ultraviolet (UV) spectrum light can cause skin damage at a high enough intensity (Ichihashi et al., 2003) in addition to causing eye damage such as cataracts, even in adults (Sloney, 1994).

Unlike UV, IR can only cause damage to the eyes and other tissues through thermal damage (Hamer et al., 1984). This means that for it to be safe, only the power of the IR radiation must be considered. Though research suggests that an irradiance of 1 kW/m² does not raise the temperature of the retina by more than 1 degree Celsius (Vos & Van Norren, 1994), the International Commission on Non-Ionizing Radiation Protection (ICNIRP) has created a guideline for IR-A exposure (Ziegelberger, 2013b).

In this guideline, only UV-A sources are seen as more damaging to infants than to adults due to photochemical damage they can cause. For thermal damage no such differentiation is made, thus the IR-A guidelines set are applicable to both adults and infants.

For incoherent light (most any light source outside of lasers), the allowable intensity of the source is given as a measure of Radiance (L_R) in watts per square meter per steradian ($W\ m^{-2}\ sr^{-1}$) and radiance dose (D_R) in joules per square meter per steradian ($J\ m^{-2}\ sr^{-1}$). The exposure limit is a function of the exposure time t in seconds, the angular subtense of the source α in radian, and a constant C found by the ICNIRP through testing, which itself is determined by source size α and exposure time t .

This gives a basic retinal thermal exposure limit of

$$L_R^{EL} = C \times \alpha^{-1} \times t^{-0.25}$$

$$D_R^{EL} = C \times \alpha^{-1} \times t^{0.75}$$

See table 1 for all exposure limit equations.

Table 1 - Thermal exposure limit equations

	Exposure duration t (s)	Source size α radians	Exposure limit (EL)		Reference note
			Radiance L_R^{EL} $W m^{-2} sr^{-1}$ (t in s and α in rad)	Radiance dose D_R^{EL} $J m^{-2} sr^{-1}$ (t in s and α in rad)	
Basic exposure limit	$1 \times 10^{-6} s \leq t < 0.25 s$	$\alpha_{min} \leq \alpha \leq \alpha_{max}$	$2.0 \times 10^4 \cdot \alpha^{-1} \cdot t^{-0.25}$	$2.0 \times 10^4 \cdot \alpha^{-1} \cdot t^{0.75}$	1, 2, 3, 4, 5
	$t < 1 \times 10^{-6} s$	$\alpha_{min} \leq \alpha \leq \alpha_{max}$	—	$0.63 \cdot \alpha^{-1}$	1, 2, 3
	$t \geq 0.25 s$	$\alpha_{min} \leq \alpha \leq \alpha_{max}$	$2.8 \times 10^4 \cdot \alpha^{-1}$	$0.71 \times 10^4 \cdot \alpha^{-1}$	1, 2, 4
Small sources	$t < 1 \times 10^{-6} s$	$\alpha \leq \alpha_{min}$	—	420	2,3
	$1 \times 10^{-6} s \leq t < 0.25 s$	$\alpha \leq \alpha_{min}$	$1.3 \times 10^7 \cdot t^{-0.25}$	$1.3 \times 10^7 \cdot t^{0.75}$	1, 2,3
	$t \geq 0.25 s$	$\alpha \leq \alpha_{min}$	1.9×10^7	—	2,4
Large sources	$t < 1 \times 10^{-6} s$	$\alpha \geq \alpha_{max}$	—	130	3, 5
	$1 \times 10^{-6} s \leq t < 625 \times 10^{-6} s$	$\alpha \geq \alpha_{max}$	—	$4.0 \times 10^6 \cdot t^{0.75}$	1, 5, 6
	$625 \times 10^{-6} s \leq t < 0.25 s$	$\alpha \geq \alpha_{max}$	—	$10 \times 10^4 \cdot t^{0.25}$	1, 5, 6
	$t \geq 0.25 s$	$\alpha \geq \alpha_{max}$	28×10^4	—	4, 5

Notes:

1. To calculate exposure limits, L_R^{EL} and D_R^{EL} , must be in seconds and α must be in radians;
2. $\alpha_{min} = 0.0015$ radian. If $\alpha \leq \alpha_{min}$, then $\alpha = \alpha_{min}$ for calculating the exposure limit;
3. If $t < 10^{-6}$ s, then $t = 10^{-6}$ s for calculation of the exposure limit in the radiance dose, D_R^{EL} ;
4. If $t > 0.25$ s, then $t = 0.25$ s for calculation of the exposure limit, L_R^{EL} ;
5. For $1 \times 10^{-6} s \leq t < 625 \times 10^{-6} s$, then $\alpha_{max} = 0.005$ radian. If $625 \times 10^{-6} s \leq t < 0.25 s$, then $\alpha_{max} = 0.2 \times t^{0.5}$. If $t \geq 0.25$ s, then $\alpha_{max} = 0.1$ radian; and
6. If 0.1 radian $> \alpha_{max}$, then $\alpha = \alpha_{max}$.

Note: Table reprinted from Ziegelberger, G. (2013). ICNIRP guidelines on limits of exposure to laser radiation of wavelengths between 180 nm and 1,000 μm . *Health Physics*.
<https://doi.org/10.1097/HP.0b013e3182983fd4>

Having calculated the radiance and radiance dose limit, the effective retinal thermal radiance L_R ($W m^{-2} sr^{-1}$) can be acquired by the summation of the product of the spectral radiance, L_λ ($W m^{-2} sr^{-1} nm^{-1}$) and the thermal biological weighing function $R(\lambda)$ (table 2) over the IR-A wavelength range of the source $\Delta\lambda$ (nm)

$$L_R = \sum_{700}^{1400} L_\lambda \times R(\lambda) \times \Delta\lambda$$

Table 2 - Retinal thermal hazard weighing function

Wavelength (nm)	Aphakic ^a hazard function, $A(\lambda)$	Blue-light ^a hazard function, $B(\lambda)$	Retinal thermal hazard function $R(\lambda)$ (where λ is in nm)
300	6.00	0.01	—
305	6.00	0.01	—
310	6.00	0.01	—
315	6.00	0.01	—
320	6.00	0.01	—
330	6.00	0.01	—
335	6.00	0.01	—
340	5.88	0.01	—
345	5.71	0.01	—
350	5.46	0.01	—
355	5.22	0.01	—
360	4.62	0.01	—
365	4.29	0.01	—
370	3.75	0.01	—
375	3.56	0.01	—
380	3.19	0.01	0.01
385	2.31	0.0125	0.0125
390	1.88	0.025	0.025
395	1.58	0.050	0.05
400	1.43	0.100	0.1
405	1.30	0.200	0.2
410	1.25	0.400	0.4
415	1.20	0.800	0.8
420	1.15	0.900	0.9
425	1.11	0.950	0.95
430	1.07	0.980	0.98
435	1.03	1.000	1.0
440	1.000	1.000	1.0
445	0.970	0.970	1.0
450	0.940	0.940	1.0
455	0.900	0.900	1.0
460	0.800	0.800	1.0
465	0.700	0.700	1.0
470	0.620	0.620	1.0
475	0.550	0.550	1.0
480	0.450	0.450	1.0
485	0.400	0.400	1.0
490	0.220	0.220	1.0
495	0.160	0.160	1.0
500	0.100	0.100	1.0
505	0.079	0.079	1.0
510	0.063	0.063	1.0
515	0.050	0.050	1.0
520	0.040	0.040	1.0
525	0.032	0.032	1.0
530	0.025	0.025	1.0
535	0.020	0.020	1.0
540	0.016	0.016	1.0
545	0.013	0.013	1.0
550	0.010	0.010	1.0
555	0.008	0.008	1.0
560	0.006	0.006	1.0
565	0.005	0.005	1.0
570	0.004	0.004	1.0
575	0.003	0.003	1.0
580	0.002	0.002	1.0
585	0.002	0.002	1.0
590	0.001	0.001	1.0
595	0.001	0.001	1.0
600–700	0.001	0.001	1.0
700–1,050	—	—	$10^{(700-\lambda)/500}$
1,050–1,150	—	—	0.2
1,150–1,200	—	—	$0.2 \cdot 10^{0.02(1150-\lambda)}$
1,200–1,400	—	—	0.02

^aThe UVR extension of $A(\lambda)$ and $B(\lambda)$ at wavelengths below 380 nm are provided for the evaluation of optical spectra that may contain UVR. The aphakic hazard function, $A(\lambda)$, is normalized to correlate with the blue-light hazard function, $B(\lambda)$ for wavelengths above 440 nm.

Note: Table reprinted from Ziegelberger, G. (2013). ICNIRP guidelines on limits of exposure to laser radiation of wavelengths between 180 nm and 1,000 μm. *Health Physics*.
<https://doi.org/10.1097/HP.0b013e3182983fd4>

The effective retinal thermal radiance dose D_R can be acquired by multiplying L_R with exposure time t , assuming the radiance is constant over time (Ziegelberger, 2013b).

For focussed laser light, the ICNIRP has set up an additional set of guidelines which describe the exposure limit to lasers including those that emit in the IR-A spectrum (Ziegelberger, 2013a). This exposure limit EL is described as irradiance in watts per square meter ($W\ m^{-2}$). This value is calculated from the exposure limit of the wavelength that has the lowest limit (EL_{min}) multiplied by the spectral correction factor C_a and C_c . The values for C_a and C_c can be found in table 3. For an IR-A laser with an exposure time of $10s < t < 30ks$ the equation takes the following form

$$EL = EL_{min} \times C_a \times C_c$$

With EL_{min} having a value of 10 (table 3).

Table 3 - C_b as a function of EL

C_A	=	1.0 $10^{0.002(\lambda/1\text{ nm} - 700)}$ 5.0	for	400 nm \leq λ < 700 nm 700 nm \leq λ < 1,050 nm 1,050 nm \leq λ \leq 1,400 nm
C_B	=	1.0 $10^{0.02(\lambda/1\text{ nm} - 450)}$	for	400 nm \leq λ < 450 nm 450 nm \leq λ \leq 600 nm
C_C	=	1.0 $10^{0.018(\lambda/1\text{ nm} - 1150)}$ $8 + 10^{0.04(\lambda/1\text{ nm} - 1250)a}$	for	700 nm \leq λ < 1,150 nm 1,150 nm \leq λ < 1,200 nm 1,200 nm \leq λ \leq 1,400 nm

^a C_C becomes large as the wavelength approaches 1,400 nm. However, the calculated exposure limit from Table 5 must then be compared with the skin exposure limit or $2 \times$ the skin exposure limit in accordance with note C of Table 5. The lower of the two limits applies.

Note: Table reprinted from Ziegelberger, G. (2013). ICNIRP guidelines on limits of exposure to laser radiation of wavelengths between 180 nm and 1,000 μm. *Health Physics*.
<https://doi.org/10.1097/HP.0b013e3182983fd4>

Table 4 - Exposure limit as function of duration and wavelength

Wavelength (nm)	Exposure duration		Exposure limit	Restrictions
	Lower limit	Upper limit		
Visible				
for $t \leq 10$ s				
and $\alpha \geq \alpha_{\max}$				
$400 \leq \lambda < 700$	100 fs	10 ps	$0.17 \text{ kJ m}^{-2} \text{ sr}^{-1}$	All only for large sources with constant radiance
$400 \leq \lambda < 700$	10 ps	5.0 μs	$0.34 \text{ kJ m}^{-2} \text{ sr}^{-1}$	
$400 \leq \lambda < 700$	5.0 μs	0.625 ms	$3.1 t^{0.75} \text{ MJ m}^{-2} \text{ sr}^{-1}$	
$400 \leq \lambda < 700$	0.625 ms	0.25 s	$76 t^{0.25} \text{ kJ m}^{-2} \text{ sr}^{-1}$	
$400 \leq \lambda < 700$	0.25 s	10 s	$0.15 t^{0.75} \text{ MJ m}^{-2} \text{ sr}^{-1}$	
For $t > 10$ s; dual limits				
Photochemical				
Photochemical radiance EL valid for all α , but averaging of exposure level over γ_{ph}				
$400 \leq \lambda < 600$	10 s	10 ks	$1.0 C_B \text{ MJ m}^{-2} \text{ sr}^{-1}$	
$400 \leq \lambda < 600$	10 ks	30 ks	$100 C_B \text{ W m}^{-2} \text{ sr}^{-1}$	
Thermal for $\alpha \geq 100$ mrad				
$400 \leq \lambda < 700$	10 s	100 s	$0.15 t^{0.75} \text{ MJ m}^{-2} \text{ sr}^{-1}$	
$400 \leq \lambda < 700$	100 s	30 ks	$47 \text{ kW m}^{-2} \text{ sr}^{-1}$	
Short wavelength IRR				
for $\alpha \geq \alpha_{\max}$				
$700 \leq \lambda < 1400$	100 fs	10 ps	$0.17 \text{ kJ m}^{-2} \text{ sr}^{-1}$	
$700 \leq \lambda < 1400$	10 ps	5.0 μs	$0.34 C_A C_C \text{ kJ m}^{-2} \text{ sr}^{-1}$	
$700 \leq \lambda < 1400$	5.0 μs	0.625 ms	$3.1 t^{0.75} C_A C_C \text{ MJ m}^{-2} \text{ sr}^{-1}$	
$700 \leq \lambda < 1400$	0.625 ms	0.25 s	$76 t^{0.25} C_A C_C \text{ kJ m}^{-2} \text{ sr}^{-1}$	
$700 \leq \lambda < 1400$	0.25 s	10 s	$0.15 t^{0.75} C_A C_C \text{ MJ m}^{-2} \text{ sr}^{-1}$	
$700 \leq \lambda < 1400$	10 s	30 ks	$10 C_A C_C \text{ W m}^{-2}$	
$700 \leq \lambda < 1400$	10 s	100 s	$0.15 t^{0.75} C_A C_C \text{ MJ m}^{-2} \text{ sr}^{-1}$	
$700 \leq \lambda < 1400$	100 s	30 ks	$47 C_A C_C \text{ kW m}^{-2} \text{ sr}^{-1}$	

^at in seconds.

Note: Table reprinted from Ziegelberger, G. (2013). ICNIRP guidelines on limits of exposure to laser radiation of wavelengths between 180 nm and 1,000 μm . Health Physics. <https://doi.org/10.1097/HP.0b013e3182983fd4>

As with the incoherent light sources, no differentiation is made between infants and adult when calculating thermal limits. As such, it can be assumed that lasers rated as Class 1 (safe for adults to look straight into without protective eyewear) are also suitable for infants.

2.2.2 SOUND

In-uterus, high frequency sounds from outside are reduced in pressure by between 20dB to 35dB, with the sound the foetus experiences predominantly laying below a frequency of 500Hz (Krueger et al., 2012). Preterm infants, however, do not enjoy the protection against these stimuli that the uterus provides. Like light stimuli, sound stimuli can cause stress in the preterm infant (Newnham et al., 2009). Because of this, recommendations have been written that describe the maximum environmental sound pressure levels in the NICU. The Consensus Committee on Recommended Design Standards for Advance Neonatal Care recommends an maximum equivalent continuous sound pressure level (Leq) of 45 dB, an L10 level of 50dB, and an Lmax peak of 65dB (White et al., 2013).

However sound levels in the NICU of multiple hospitals already surpass this standard. One study found a noise level with an Leq of 58.1 dBA (S. W. Smith et al., 2018). A TU Delft study found an Leq of 58.15 dBA (Milette, 2010). (Peixoto et al., 2011) Found mean sound levels excess of 70dBA. In fact, noise levels inside incubators

like the Draeger Caleo (currently used by Erasmus) have an advertised internal sound pressure of 47dB when operating, without outside noise, already exceeding the recommended Leq.

Since sound pressure is cumulative, this means that the product would have operate completely silently for it adhere to the recommendations.

2.2.3 CONCLUSION

Though a visible light recommendation is now known, turning on a light of such intensity in, for example, a dark room would startle the infant and cause stress, which is what we are trying to prevent. Therefore, it is still important to keep additional light sources for image acquisition to a minimum and have light sources that are necessary come on in a gradual way. Since the pupils of early preterm infants do not yet adjust to light stimuli, there was no recommendation found on the speed with which such lighting should turn on.

IR-A lighting was originally thought to be unsuitable do to supposed damage to the infant's eyes. However, now that the IR-A guidelines are known, it seems very much possible, and perhaps even preferable to use this type of lighting for image acquisition: Since IR light is not visible to humans, its presence cannot cause stress with infants.

Though it might not be applicable as flood lighting to illuminate an image used for stereophotogrammetry (there would be no contrast for the software to determine features), IR projector can be used for pattern projection which aids in photogrammetry through the addition of texture to the subject, allows for depth perception through triangulation of the pattern, and allows for IR time of flight (ToF) systems to function.

Finally, for sound production it appears that the product needs to be completely quiet. In practice this means no moving parts, which will most likely culminate into not having active ventilation for cooling purposes.

2.3 GROWTH MONITORING

To ensure that the infant is developing correctly while in the NICU, the growth of the infant is measured in various ways. This research focusses on the measuring of cranial growth through the usage of the head circumference (HC) measurement. This measurement is performed to approximate the cranial volume, which indicates brain growth and thus neurological development (Cheong et al., 2008). In addition to this, HC can be used to estimate body growth as well (Geraedts et al., 2011), potentially removing the need for stressful length measurements.

2.3.1 METHODS

2.3.1.1 TAPE MEASUREMENT

The most used method for HC measurement, and the one used is Erasmus MC, makes use of a simple tape measure. At Erasmus, this process is performed by two nurses. One nurse lifts and holds the head of the infant in position while the seconds nurse puts the tape measure around the widest part of the head (Santander et al., 2020). Both than take a reading of the tape and agree upon a value which gets written down. This whole process takes place within the incubator, with both nurses standing on one side each, interacting with the infant through the opened side hatched (figure 15). For a more detailed procedure overview see Appendix A.



Figure 15 - Erasmus NICU nurses performing a head circumference measurement

ADVANTAGES

COSTS

The costs for this method of measurement are low. A regular, store-bought tape measure will suffice for this task, and specialty tapes made for this task are affordable.

DISADVANTAGES

PRECISION

This method requires multiple quick manual operations whose precision rely on the interpretation of the nurse. At the time of measurement, the nurse must:

- Determine the point of the cranium with the largest circumference, and place the tape in that position
- Make sure that the tape is aligned with the circumference of the cranium
- Make sure that the tape is in the same position as previous measurements.
- Pull the tape tight enough around the head for an accurate reading, but not too tight to cause discomfort for the infant.
- Read the tape measure correctly from whatever angle the infant may end up in.

This succession of steps whereby each step allows for a (small) error, can cause larger errors in the final written-down HC value. One study kept track of the HC measurements of 1105 low-weight (<2000g) infants in order to find the reliability of such measurements. They found that in 5% of measurements an inter-observer deviation of 2cm or more was recorded (Bhushan & Paneth, 1991)

An exchange with an Erasmus MC NICU staff member gave me a purported accuracy of “half a centimeter” (appendix B).

Precision can be increased by using specialized HC measuring tape (not currently used by Erasmus MC). However, a study with 71 infants still found a deviation of 0.65cm or more in 5% of the intra-observer measurements, with 95% being within 0.47cm of the true value, and 1.0cm or more in inter-observer measurements (Bartram et al., 2005)

INFANT STRESS

This type of measurement requires physical contacts. As described in appendix A, nurses need to lift and hold the head of the baby, while also keeping its extremities out of the way of the measurement. This causes a visible stress response in the infant (spontaneous movement of limbs), which is known to have negative effects on the neurological development of the child (G. C. Smith et al., 2011).

2.2.1.2 STEREOPHOTOGRAMMETRY

Santander et al. (2020) devised a method whereby a portable stereophotogrammetric camera (Figure 16) is used to image the head of the infant from multiple angles. These images are then fed to a computer program which reconstructs a 3D model of the infant’s head (Figure 17). This model can be used for determining the HC, as well as the direct approximation of the cranial volume.



Figure 16 - Canon stereophotogrammetry camera

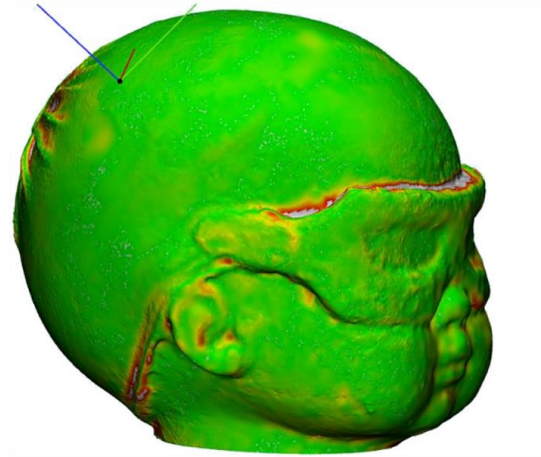


Figure 17 - Headscan using stereophotogrammetry camera. Reprinted from Santander, P., Quast, A., Hubbert, J., Horn, S., Meyer-Marcotty, P., Küster, H., & Dieks, J. K. (2020). Three-dimensional head shape acquisition in preterm infants - Translating an orthodontic imaging procedure into neonatal care. *Early Human Development*, 140, 104908. <https://doi.org/10.1016/j.earlhumdev.2019.104908>

The image acquisition process consists of the following steps.

1. The baby is given a thin, nylon cap which smooths out the infant's hair, keeping it from interfering with the 3D reconstruction. In addition to this, the cap has markers on it to help the reconstruction software with determining camera position relative to the subject. (Figure 18)
2. Eye protectors are put on the infant to protect its eyes from the camera's flash unit
3. The baby is taken out of the incubator for every side of the head to be photographed. This allows for the reconstruction of the entire head.
4. After image acquisition, infant is put back into the incubator
5. The nylon cap and protective eyeglasses are removed



Figure 18 - Infant doll wearing cap with reconstruction markers. Reprinted from Santander, P., Quast, A., Hubbert, J., Horn, S., Meyer-Marcotty, P., Küster, H., & Dieks, J. K. (2020). Three-dimensional head shape acquisition in preterm infants - Translating an orthodontic imaging procedure into neonatal care. *Early Human Development*, 140, 104908. <https://doi.org/10.1016/j.earlhumdev.2019.104908>

ADVANTAGES

ACCURACY & PRECISION

The models generated using this method allow for a highly accurate and precise measurement of the HC (-0.85mm to 0.38mm deviation), when compared to a tape HC measurement.

CLOSER APPROXIMATION OF CRANIAL VOLUME

3D reconstruction of the infant's head allows for a more thorough assessment of the cranial growth (and thus neurological development) than a 2D representation like HC does. One study created a model that predicts cranial volume with only HC as input. This achieved a predictive value of only 78% (Martini et al., 2018).

DISADVANTAGES

INFANT STRESS

This method does not reduce the stress experienced by the infant. Image acquisition requires multiple infant handling operations in addition to the ones needed for the tape HC measurement.

- A nylon cap must be put on the head of the infant
- Protective eyewear must be placed on the infant
- The infant must be taken out the warm environment of the incubator
- The infant must be handled to acquire images of all sides of the infant's head.

P. Santander et al. (2020) do suggest that images of the head may be acquired by a second or third nurse during routine procedures where the infant is already taken out of the incubator, in order to not at any more handling time for image acquisition alone.

MANUAL IMAGE ACQUISITION

The portable stereophotogrammetric camera requires an operator at all times to operate the camera, frame the shot, and decide what images are (yet) to be taken.

Image acquisition is not supported by any user interface which, for example, tells the nurse what parts of the head has already been photographed, or when the head is properly framed for an image to be taken. This means that nurses will have a steeper learning curve than they would have had if there were such a supporting interface, or if the image acquisition process were automatic.

HIGH COSTS

The Vectra H1 camera used in this experiment's setup costs (at the time of publishing) €9.950,- excluding VAT (Santander et al., 2020), compared to the <€1 costs of measuring tape.

EXTENDED PROCESSING TIME

photogrammetry has the high computational requirement. Camera position, image stitching, surface detection and more all have to be done in software after acquisition of the initial images. Santander et al. (2020) had a processing time of 49 minutes between the image acquisition and mesh output when using a desktop computer.

2.3.1.3 LASER SCANNING (STARSCANNER)

The STARscanner was introduced in 2001 by Orthomerica. The device scans infant heads for deformities with the intention to use the generated 3D models for the production of a custom therapeutic helmet (cranial orthosis), which forms the cranium back into the desired shape.

The scanner works using laser triangulation. 4 class 1 lasers project a line across the circumference of the head of the infant. 8 cameras use this line to determine a 2D shape of that "slice" cranium. By moving the assembly along the head of the infant, multiple slices are taken and then joined into a 3D reconstruction of the infant's head (Ifflaender, Rüdiger, Koch, et al., 2013), with an accuracy of about 0.5mm (*STARscanner – Orthomerica Products, Inc.*, 2020).

Ifflaender et al. (2013) Has applied this scanner to determine the HC and cranial volume of preterm infants, in an attempt to get more accurate and useful data compared to the traditional tape measure HC measurement.

The acquisition process is as follows:

1. The glass surface of the scanner is disinfected
2. The infant a nylon cap put on its head to flatten any hair that might interfere with the scan.
3. The infant is taken out of the incubator
4. The infant is placed on the glass bed of the scanner (Figure 19)
5. The infant is held completely still by nursing staff while the 3 second scan takes place
6. The infant gets placed back into the incubator
7. The nylon cap is removed from the infant



Figure 19 - Infant in Starscanner

ADVANTAGES

HIGH ACCURACY

Since the acquisition process is mostly automated, the scanner has a high accuracy and low interobserver variation. One study found an accuracy of 0.36mm (Geil & Smith, 2008), while the manufacturer claims an accuracy of 0.5mm (*STARscanner – Orthomerica Products, Inc., 2020*).

LOW INTEROBSERVER VARIATION

Since the acquisition process is mostly automated, the interobserver variation is lower than with HC tape measurement. For HC measurements a level of agreement (LoA) of -0.39% to 0.39% was reached, while for cranial volume a LoA of -0.8 to 3.6% was obtained (Ifflaender, Rüdiger, Koch, et al., 2013).

FAST ACQUISITION

The scan itself only takes 3 seconds, with infants spending a total of 20 seconds on the glass scanner bed, before being taken back to the incubator.

CLOSER APPROXIMATION OF CRANIAL VOLUME

Like with stereophotogrammetry, the 3D reconstruction of the infant's head allows for a more thorough assessment of the cranial growth (and thus neurological development) than a 2D representation like HC does

DISADVANTAGES

STRESS

This method of HC acquisition requires the infant to not only be removed from the incubator, but also be put on a hard, unheated glass service for 20 seconds. In addition to this, the infant must be restrained for the 3 seconds it takes for the scanner to fulfil its task.

2.3.2 CONCLUSION

Though attempts have been made at replacing the tape measure HC measurement with non-invasive 3d scanners, the procedures required for these scanners to acquire their data still requires interaction between the nurse and the infant, the infant even having to be removed from the incubator and in one case placed in a non-optimised environment.

Not only does this cause the stress that this product is trying to prevent, it also impossible to be safely removed from the incubator for the very early preterm infants (<26 weeks).

The product must thus be designed in such a way that the complete acquisition can be performed with the infant still inside of the incubator, in order to prevent stress in the infant.

What these 3D scanners do show is that it is possible to get equal or better results regarding HC and cranial volume with a 3D reconstruction, than it is with the 2d representation a tape measure provides.

Table 5 - Comparison of head circumference measuring methods

Method	Tape measure	Photogrammetry	Laser triangulation
Accuracy	5mm	1.23mm	0.36mm
Costs	~€1, -	€10,000	> €10,000
Availability	+	-	-
Precision	-	+	+
Infant Stress	-	+	+
Acquisition time	+	-	+

3D capture

-

+

+

2.4 PROGRAM OF REQUIREMENTS

The following is a list containing the requirements and wishes for the product, based on the above research. *Wishes are blue and italicized.*

1. PERFORMANCE

- 1.1. The product must make a contactless 3D scan of the infant's head
- 1.2. The product must successfully perform an acquisition with the infant still in the incubator
- 1.3. The product must successfully perform an acquisition without the infant being handled by any staff for the sole purpose of acquisition.
- 1.4. The use of the product must be less stressful for the infant than the use of a standard HC tape measure.
- 1.5. The product must produce a HC or equivalent measurement must be of the same or better performance than a mean standard tape measurement, meaning a deviation of less than 0.71cm
- 1.6. The product must have a depth deviation of $\leq 1\text{mm}$
- 1.7. The product may not produce any noise
- 1.8. The product must fit and function with the Draeger Caleo and Draeger Babyleo models of incubator
- 1.9. The product must comply with the (93/42/EEG) Class 1 guidelines for medical tools.
- 1.10. The product may not produce more than 600Lm of white light when acquiring data
- 1.11. The product must operate correctly in an environment with 0lm of visible light.
- 1.12. The product must remain its own entity, meaning that the solution must not be a permanent addition to the incubator
- 1.13. The product must operate on the outside of the incubator
- 1.14. *The product must be compatible with as many incubator models as possible*
- 1.15. *The product must be able to serve as a continuous monitoring device.*
- 1.16. *The product must be able to measure cranial volume in addition to head circumference.*
- 1.17. *Acquisition must be as fast as possible.*

2. MAINTENANCE

- 2.1. Outside of cleaning and charging, the product must be maintenance free
- 2.2. The product shall not contain any hard-to-clean services or creases that ay trap dirt or other contaminants.
- 2.3. The product must be able to be cleaned by the use of a microfibre cloth, an alcohol dilution, and the bare or latex-gloved hands of the hospital staff.

3. AESTHETIC, APPEARANCE & FINISH

- 3.1. The product may not cause any visual noise that is distracting to the nursing staff
- 3.2. *The product must be as unobtrusive as possible, in order to allow for easy observation of the infant around the product*

4. ERGONOMICS

- 4.1. The product must be able to be handled by a single nurse
- 4.2. The product may not obfuscate the infant from the nursing staff.
- 4.3. *Acquisition must take the least amount of cognitive effort possible*
- 4.4. *Acquisitions must take the least amount of physical effort possible*

5. SAFETY

- 5.1. The product must comply with the ICNIRP (2013a) guidelines on scattered IR-A radiation
- 5.2. The product must comply with the ICNIRP (2013b) guidelines on laser IR-A radiation
- 5.3. The product may never endanger or otherwise come in contact with the infant
- 5.4. The product may never endanger the operator

6. PRODUCT POLICY

- 6.1. *The product should integrate with the current pay-per-scan environment used with the Vectory3 Curatio*

2.5 TECHNOLOGY OVERVIEW

In order to acquire the data necessary for cranial measurements, the product needs to employ a surface scanning technology. Previous chapters discussed a selection of those technologies already used or tested for infant cranial measurement. This chapter will expand on the functioning of those technologies as well as additional options. The goal is to make a selection of one or more technologies that will be used for the ideation and prototyping phases. A full breakdown of each technology with advantages and disadvantages can be found in appendix D.

2.5.1 TYPES OF ACQUISITION

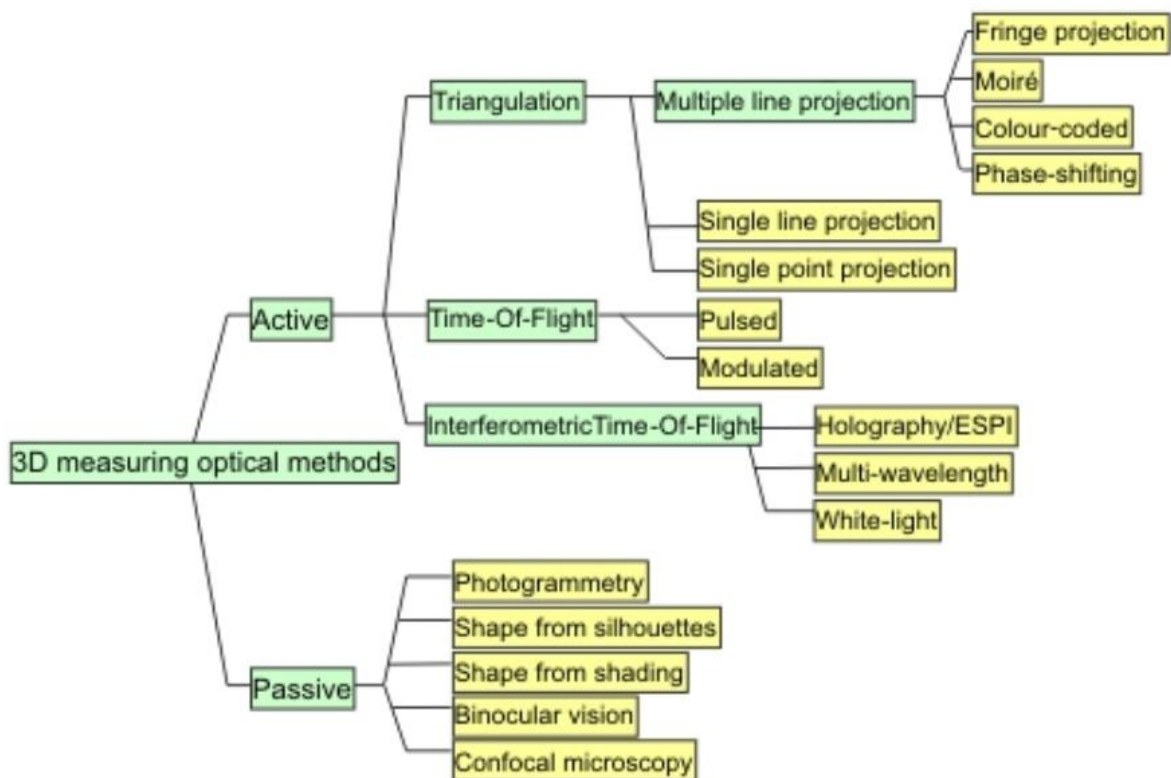


Figure 20 - Optical 3D measuring methods. Reprinted from Pezzati et al., in: "Handbook on the Use of Lasers in Conservation and Conservation Science", 2008

There are many different ways to acquire a surface scan. These are often divided into the *contact* and *non-contact* category, with the non-contact category being divided into *active* and *passive* acquisition (Figure 20) (Ebrahim, 2013).

This division allows us to immediately eliminate certain techniques as candidate. Contact methods, for example, require a physical instrument to interact with the infant in order to acquire data. Not only would touching the infant cause stress, it would also require that the device be placed within the incubator. Thus, only non-contact scanning methods will be discussed.

In addition, since only surface data is needed for measurement, volumetric scanning methods (e.g. MRI, CT), too, will not be considered due to their added complexity, and with that, higher cost and larger size. In addition, radiation from some of these devices could be harmful for the infant.

2.5.2 OVERVIEW

The following is an overview detailing each technique that is considered for the product. A short description of functioning and the intrinsic performance variables are provided. See appendix D for the full comparison.

2.5.2.1 LASER TRIANGULATION

Laser triangulation is a simple form of 3D scanning, whereby a single laser and a camera are used to acquire depth data along the path of the laser line. The basic principal is as follows:

- A laser and camera are positioned at a known angle α (Figure 21).
- Depending on the depth of the object the laser point hits, it's position on the camera sensor changes.
- Using triangulation, this shift in position on the sensor can be translated into an absolute depth of the point.

This concept can be expanded upon by projecting a laser line instead of a point using, for example, an oscillating mirror. This then give a depth “slice” of the object that is to be scanned. Moving the laser & camera setup, or the object, can be done to acquire multiple of these slices. Stitching these slices together forms a 3D surface scan of the object.

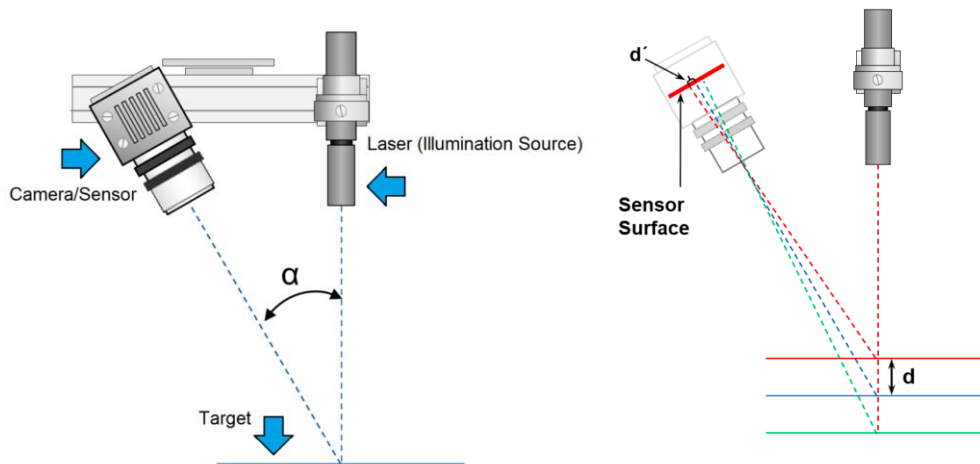


Figure 21 - Visual representation of triangulation

Laser triangulation is adequately accurate, with a depth accuracy of 0.04mm being claimed by one report (Vukašinović et al., 2010). At the same time, complete systems sell for a relatively low price. Murobo sells a turntable based model (where the to-be-scanned object is rotated instead of moving the laser assembly) for \$249,- (Murobo, n.d.).

INTRINSIC PERFORMANCE VARIABLES

- α : The value of α determines both the depth resolution of the setup, and the sensitivity of the setup to occlusion. The depth resolution and sensitivity to occlusion as a function of α are correlated. Thus, as α increases both depth resolution and sensitivity to occlusion increase, and vice versa.
- Laser line thickness: Influences the depth resolution of the system. The thinner the line, the easier the sensor can pick up small variation in the surface's depth.
- Sensor resolution: The higher the resolution of the used image sensor, the more detail it can pick up in the variations of the laser line height, which directly translates to increased depth resolution.
- Lens quality: A higher quality lens can resolve more detail, and therefore feed a higher resolution sensor with data.

2.5.2.2 STRUCTURED LIGHT

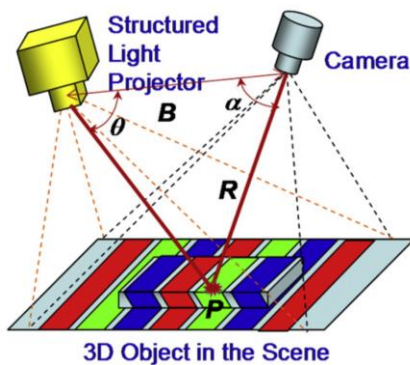


Figure 22 - Scanning a 3D object using structured light. Reprinted from Geng, J. (2011). Structured-light 3D surface imaging: a tutorial. *Advances in Optics and Photonics*, 3(2), 128. <https://doi.org/10.1364/aop.3.000128>

This scanning technique, like laser triangulation, uses triangulation to determine the depth of a point on the surface on the to-be-scanned object. Where the two techniques differ is that laser triangulation can only acquire one line (or slice) of depth data at any given moment, while structured light scanning allows for the simultaneous acquisition of an entire 3d surface. The basic operation is as follows:

- A light projector, placed at a known angle α and θ to the camera (as in figure 22), projects a pattern of sorts on the to-be-scanned surface.
- The camera captures the distortion of this pattern on the surface, which is influenced by the depth of each point of the surface
- Using one of the techniques outlined in figure 23, the software identifies each point of the pattern, comparing its shifted position to its original position.
- Triangulation is used to determine the depth value of each point based on the shift from its original position, from the viewpoint of the camera.

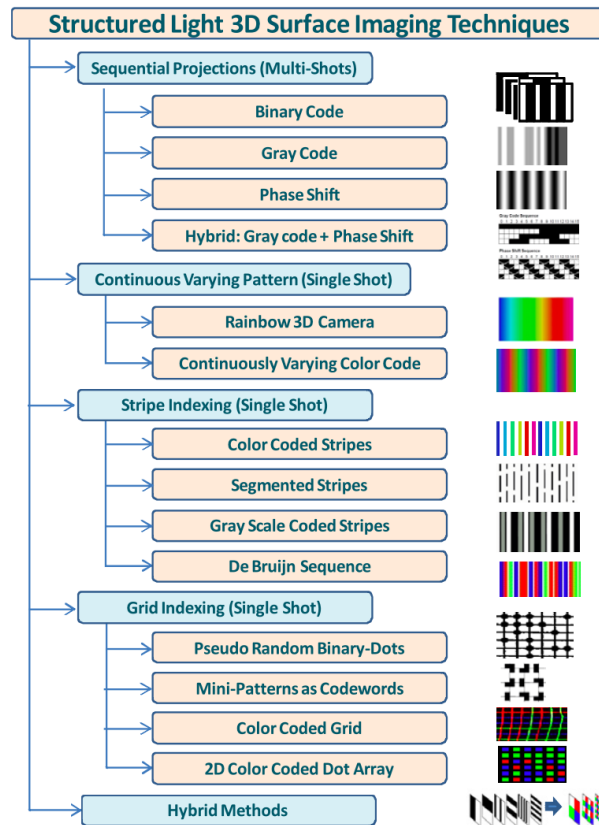


Figure 23 - Structured Light Surface Imaging Techniques. Reprinted from Geng, J. (2011). Structured-light 3D surface imaging: a tutorial. *Advances in Optics and Photonics*, 3(2), 128. <https://doi.org/10.1364/aop.3.000128>

Though all structured light scanners use the same principle of triangulation, various techniques exist for solving the problem of point recognition: For the scanner to determine the depth value of each point it must know the original position of the projected pattern point corresponding to it.

Thus, the scanner must be able to uniquely identify each point of the projected pattern. (Geng, 2011) grouped these techniques into *single-shot* and *multi-shot* methods (Figure 23). As the name suggests, single shot methods allow all necessary information to be captured by the camera in a single frame or 'shot', while multi-shot methods require multiple sequential frames to be captured in order for the pattern to be fully identified.

To illustrate the difference between the categories, the following is an overview of two predominant technologies, one of each of the two discussed categories

GRAY CODING (MULTI-SHOT)

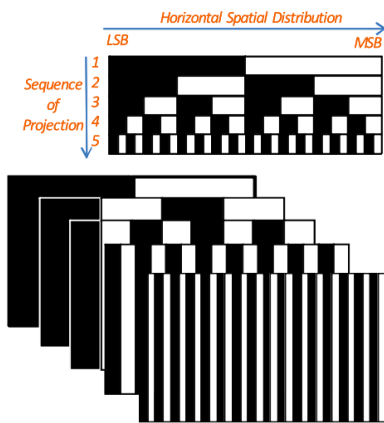


Figure 24 - Grey Coding projection pattern. Reprinted from Geng, J. (2011). Structured-light 3D surface imaging: a tutorial. *Advances in Optics and Photonics*, 3(2), 128. <https://doi.org/10.1364/aop.3.000128>

With Gray coding, the projection is divided up into vertical or horizontal lines which are either black (no projected light) or white. These represent the binary values 0 and 1 respectively. By projecting and capturing a sequence of frames, these bars can be used to create a unique identifier for each line. Since each frame represents one state, or bit, the number of possibilities is equal to 2^N , where N is the number of frames in a sequence. Thus, the more frames, the higher the amount of unique lines that can be identified, increasing the resolution of the scan until the camera sensor's resolution becomes the limiting factor.

PEUDO RANDOM BINARY DOTS / LIGHT CODING (SINGLE-SHOT)

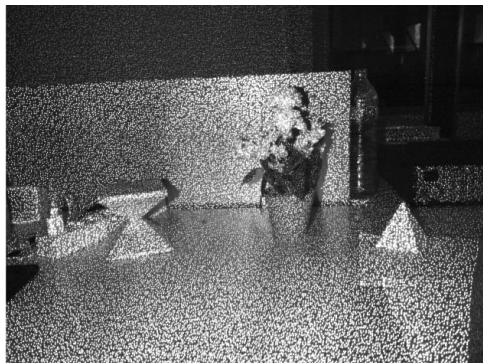


Figure 25 - Dot projection pattern from a Kinect v1 camera. Reprinted from Villena Martinez, Víctor & Guilló, Andrés & Azorin-Lopez, Jorge & Saval-Calvo, Marcelo & Mora-Pascual, Jeronimo & Rodríguez, José & Garcia-Garcia, Alberto. (2017). A Quantitative Comparison of Calibration Methods for RGB-D Sensors Using Different Technologies. *Sensors*. 17. 243. [10.3390/s17020243](https://doi.org/10.3390/s17020243).

This method, employed by the ubiquitous Kinect v1 camera, uses a laser generated pattern of pseudo random dots to identify areas of the pattern. The dots are arranged in such a way that a sub-area of a predetermined size sliding over the pattern would give this sub-area's absolute position in the pattern, regardless of its position (figure 25) (Geng, 2011). This is achieved by having the neighbouring dots of every dot in the pattern be in a unique relative position compared to the neighbouring dots of every other dot in the pattern.

At close range, a structure scanner like Occipital's Structure Mk2 has an accuracy of 0.2% of the measured depth (Occipital, 2020a), while costing a total of \$449,- (Occipital, 2020b).

INTRINSIC PERFORMANCE VARIABLES

- α & θ : As with laser scanning, the values of α and θ influence the setup's depth resolution as well as its sensitivity to occlusion. Decreasing α and θ increases both depth resolution and sensitivity to occlusion, and vice versa
- Pattern complexity: Increasing the complexity of the pattern increases the amount of uniquely indexed areas within this pattern, which in turn increases the resolution of the scan. This increase in complexity can take multiple shapes:
 - For single shot methods such as light coding, an increase in complexity would entail a higher resolution grid pattern, meaning more dots per area, which gives more unique sub-areas.
 - For multi-shot methods such as Gray coding, an increase in complexity would entail more frames added to the sequence to increase the amount of possible combinations for a line.
- Sensor resolution: The higher the resolution of the used image sensor, the more detail it can pick up in the projected pattern, which directly translates to increased depth resolution.

2.5.2.3 TIME OF FLIGHT

If an object travels at a constant speed, it is easy to determine the distance it has travel by timing the duration of the travel: multiplying its speed by the travel time gives the total distance travelled. This principal is applied in Time of Flight (ToF) scanners. These scanners use a projector to send out a pulse of light. Since the speed of light is constant, the time it takes for this light to return to the ToF sensor can then simply be multiplied by the speed of light to get the round-trip distance travelled. Halving this value gives the distance between the sensor and the object. This is known as *direct ToF* (Terabee, n.d.)

Indirect ToF makes use of the phase of the light being sent out by the projector vs the phase of the light being received by the sensor in order to gauge distance travelled (Terabee, n.d.). The projector sends out modulated light at a set frequency. For this example, the amplitude is modulated in a sinusoidal manner at 10MHz. This gives a wavelength of 30m. When the modulated light leaves the projector, its state is known. Depending on the distance the light has travelled before returning to the sensor, the phase will have shifted from its original projected state. Unlike direct ToF where the maximum measuring range is dependent on the intensity of the projector and the light sensitivity of the sensor, indirect ToF's range is determined by the modulation frequency: a 10MHz, 30m wave can only be used to measure distances up to 15m (wavelength divided by 2).

Two major types of ToF systems can be distinguished: LIDAR systems, and ToF cameras.

LIDAR

LIDAR (a portmanteau of Light and raDAR) uses a pulsing laser and simple single point ToF sensor to scan the depth of a surface. Since the laser only sends out a singular beam, this system requires continuous mechanical movement, moving the beam across the whole surface in order to capture a full 3D scan.

Recent close-range LIDAR systems such as Intel's L515 have a stated depth accuracy of <5mm (Intel, 2019). This unit is set to sell for \$349,- (Intel, 2020).

TOF CAMERA

A time of flight camera uses a 2-dimensional sensor and projector. Instead of a single laser point, multiple points of the surface are acquired at the same time. This means that unlike LIDAR, no mechanical system is needed to move the assembly, as long as the to-be-scanned surface fits within the conical field of view (FoV) of the sensor.

A study trying to improve the accuracy of ToF cameras through software reached a depth-accuracy of 4.6mm within its full range (He et al., 2017), which is inadequate for the intended application. However, the paper does not mention if the used point cloud is the result of a single acquisition of the Kinect, or if an average of multiple frames are used. If only a single acquisition was used, accuracy might be improved by instead averaging the depth of the point cloud points acquired over multiple sequential frames. Microsoft priced its newest ToF camera, a follow-up to the Kinect v2, at \$399,- (Microsoft, 2020).

INTRINSIC PERFORMANCE VARIABLES

- Clock resolution: The depth resolution of ToF based systems is dependent on the resolution of the clock. The smaller the time unit, the more smaller the steps between depth units (distance = constant speed / time).
- Sensor & projector resolution (ToF camera): The higher the resolution of the used image sensor and light projector, the more detail can pick up in the projected pattern, which directly translates to increased surface scan resolution.
- Polling rate (LIDAR): Influences the speed of acquisition. The higher the polling rate, the faster the laser may move over the surface for the same resolution, decreasing acquisition time which aids in capturing dynamic objects.

2.5.2.4 PHOTOGRAMMETRY

component-wise, photogrammetry is the simplest of the methods. This technique only requires standard CMOS sensors to capture RGB images of the to-be-scanned surface, from multiple angles. All 3D data is generated through software. Feature recognition is used to determine the position of each camera, after which multiple algorithms, amongst which is triangulation, are used to determine texture and geometry of the surface.

This makes photogrammetry an almost completely software-based solution. The advantage of this is that a single hardware setup may last for multiple generations, since increases in scan quality are generally achieved through software optimizations. However, since all the heavy lifting is done in software, this technique can be the most computationally intensive of all technologies discussed in this chapter. For illustration, Vectory3's Curatio scanner takes 20 minutes to deliver a 3D model, with off-site processing.

A study using the Curatio prototype reached an accuracy of 1.5mm with close-range photogrammetry (Smakman, 2014).

NEAR-IR PHOTOGRAMMETRY

Though Photogrammetry is usually performed using RGB cameras and light in the visible spectrum, it is possible to use cameras with an IR filter and IR light source to capture the subject. The advantage of this would be the ability to increase illumination of the infant using the IR light source to allow for better capture of the images, without disturbing the child with visible light.

A possible disadvantage of this technique is the reduced data per photo available for the algorithm to resolve the to-be-scanned surface: No colour data is available, possibly reducing contrast between parts of the image. Additionally, the resulting grayscale images would have a lower bit-depth than their colour counterparts (8bpp vs 24bpp, respectively).

However, one study comparing a near IR photogrammetry scan with a RGB scan using the same setup concluded that there is no difference in accuracy between the two, both reaching <1% deviation in measurement (Edelman & Aalders, 2018). This could thus be a viable option for the product.

INTRINSIC PERFORMANCE VARIABLES

- Number of cameras: Influences object scan detail. Increasing the number of (correctly placed) cameras allows the reconstruction software to more accurately and with more detail reconstruct the to-be-scanned object. Note that returns are diminished as the number of cameras increases.
- Sensor resolution: The higher the resolution of the used image sensor, the more detail it can pick up increasing the overall detail of the produced model.

2.5.3 CONCLUSION

Table 6 - Comparison of optical scanning techniques

Method	Structured Light	Photogrammetry	Laser Triangulation	Time of Flight	LIDAR
Depth Accuracy (as cited above in the representing <€1000 systems)	0.6mm	1.5mm	0.36mm	4.6mm	<5mm
Hardware costs	+	+	+	-	-
Hardware complexity	+	-	-	+	+(solid state)
Processing requirement	+	-	+	+	+
Multi-cam interference	-	+	-	+	+
Environmental light sensitivity	-	-	+	+	+
Occlusion sensitivity	-	+	-	-	-
Acquisition time	+	-	+	+	+
Resolution	-	+	+	-	-

Having looked at common technologies for 3D scanning, a decision will now be made on what technologies to use for the ideation and prototyping phase. The following is a brief overview of the decision argumentation for each technology.

LASER LINE TRIANGULATION

Laser line triangulation allows for adequate accuracy of the scan. Additionally, the technology does not require great computational power to deliver a timely result. However, human action is needed to place the laser line in the correct position of the head, which introduces a factor of human error into the measurement. This manual placement would also require the use of visible laser light, which can disturb the infant. This problem could be alleviated with a mechanical system that moves the scanning assembly, creating a 3D surface. However, introducing mechanical systems complicates the product, increases the amount of failure points, and potentially increases noise production, which is to be kept at a minimum.

Because of these disadvantages, this technology will not be explored further

STRUCTURED LIGHT

Structured light scanning allows for adequate accuracy of the scan. Like laser triangulation, the processing of depth information requires little computational power, though the indexing of the pattern required by this technology does increase complexity. Since this technology can make use of IR-A light for its projector, the infant should not be disturbed by the acquisition. Prices for existing technologies are acceptable, with a 0.1mm accuracy Structure scanner for €449.

This technology thus seems suitable for this application. However, since little information was found a unit must be acquired for testing this technology through the hood of the incubator, before ideation.

LIDAR

Though this technology can be used with IR-A light, thus reducing the impact on the infant, the mechanical system required to move the assembly increases product complexity, failure modes, and noise production. In addition, this technology does not have adequate depth resolution (<5mm) for a HC measurement that is equal to or more accurate than the tape-based HC measurement. Furthermore, like other active 3D scanning systems, tests would need to be performed to check the applicability of the technology when scanning through a curved, imperfectly transparent surface like that of the incubator.

This technology will thus not be explored any further.

TOF CAMERA

Though these cameras remove the mechanical component of LIDAR systems, accuracy stays below the required amount for an improvement upon current HC measuring techniques (4.6mm depth accuracy (He et al., 2017)). Additionally, like other active 3D scanning systems, tests would need to be performed to check the applicability of the technology when scanning through a curved, imperfectly transparent surface like that of the incubator.

Therefore, this technology will not be explored any further.

PHOTOGRAMMETRY

Though the accuracy of photogrammetry is dependent on the configuration, Vectory3 has reached accuracies of 0.15mm with their Curatio hand scanner, which is adequate for the proposed application. Furthermore, the system requires no moving parts and the components are relatively inexpensive (standard CMOS cameras).

Downsides are the product complexity due to the multiple cameras needed at multiple angles. The required computation time, too, is higher compared with all previously mentioned technologies. Vectory3 currently needs 20 minutes to process a Curatio scan off-site, which is before any measuring of the finished model. This would significantly impact the current procedure used for circumference measurement, whereby the result is immediately known to the NICU employee performing the measurement.

A faster alternative to basic photogrammetry, which uses the same basic principle of stereoscopy, but combines it with an IR dot projector for creating texture on the subject, can be found in the Intel D4xx series of depth sensing modules. These modules increase cost, but mitigate hardware setup complexity by integrating much of the electronics in a self-contained module, reduce processing time to mere milliseconds per frame thanks to a custom ASIC in the modules, and reduce the systems sensitivity to environmental light by the use of the integrated IR dot projector. This technology will therefore be chosen to represent the photogrammetry solution.

2.6 TECHNOLOGY CHOICE

In the Technology Overview chapter two potential candidates for the final product were chosen: Structured light scanning, and a hybrid photogrammetry-based approach based on the Intel RealSense D4xx series of hardware. In this chapter the two technologies will be compared, and a best fit chosen for the final product design.

2.6.1 HARDWARE

Table 7 - SR300 vs D435i comparison

	SR305	D435i
		
Technology	Structured Light	Photogrammetry with dot projector
Highest precision resolution	640x480	848x480
FoV	69° x 54°	86° x 57°
Claimed depth accuracy	<1mm	<2%
Depth range (m)	0.2 – 1.5	0.105 - 10
Price	€80	€175

To perform the tests, representative hardware for each of the two technologies first had to be sourced. For the hybrid-photogrammetry based technology, this meant a Intel D4xx depth sensor. Due to availability a D435i unit was chosen to perform the test. This unit costs €175,- and is widely available in component shops (*Mouser, 2020*)

For the structured light setup, a comparably priced device had to be found, which was preferably aimed at the same market as the D435i. Luckily, Intel produces this very sensor as part of their RealSense line-up, of which the D435i is also part. The SR305 is a structured light depth sensor that is, at the time of writing, sold for €80,-. Though this is significantly less expensive than the D435i, the difference is mostly made up by the more expensive setup needed for the photogrammetry process, as well as the integrated inertial unit which will not be used for this product.

When looking at the specifications, the cameras perform comparably, with the lower resolution of the SR305 being offset by its smaller field of view, resulting in a higher resolution per surface area for the SR305.

Since no access to the hospital could be granted after the start of the project, a setup was built at Vectory3 using a real Dräger Caleo incubator hood, combined with several infant dolls representing different gestation ages. More information about this setup can be found in appendix E.

2.6.2 PLANE FIT

Two tests were performed to find which technology would perform best. The first was a plane fit test, whereby the cameras were pointed at a flat surface with a clear contrasting pattern on it, through the hood of the incubator (figure 26). A plane was then fitted to the acquired geometry in order to find the depth error. This test was performed to find if either of the technologies was influenced by the curved top surface of the incubator. The RealSense Depth Quality Tool created by Intel was used for this purpose. A print featuring randomized grayscale noise was used as the scan surface, as recommended by Intel (Zabatani et al., 2019). Both cameras were setup to provide maximum depth accuracy as described by Intel (Zabatani et al., 2019).

SR305

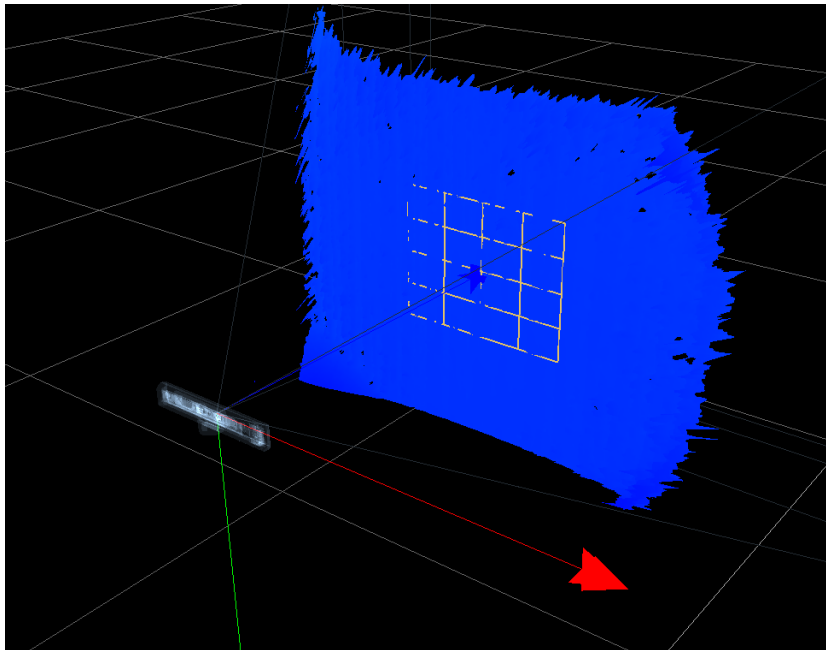


Figure 26 - SR305 plane scan

Figure 26 shows a mesh representing the depth output of the SR305 camera when aimed at the plane through the incubator hood. The image clearly shows that significant deformation is present near the edges of the FoV of the camera. However, considering that the infant must be placed near the centre axis of the incubator in order to maximize internal airflow efficiency, it is unlikely that the to-be-scanned object (the infant) will be found in these edge areas. Therefore, a region of interest (RoI) was chosen that approximates the likely area that the child is to be found in. The plane is only fitted to this RoI, thus the deformations at the edges are not taken into account for the depth accuracy calculation.

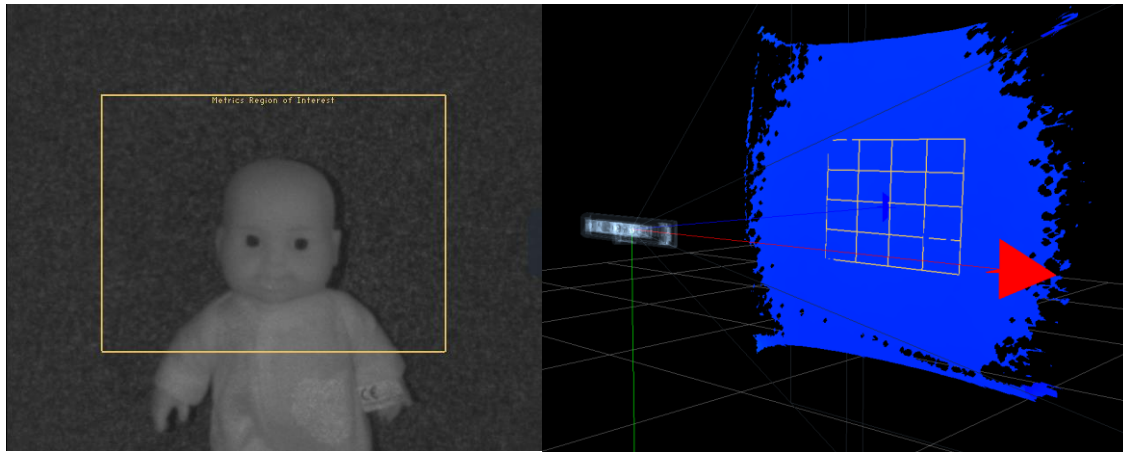


Figure 27 - region of interest shown on plane, with infant doll for reference

Figure 27 shows the Y8 output of the depth sensor of the SR305, with the yellow border representing the ROI in relation to the size of the baby doll. When taking into account only the ROI, the results are acceptable, with an RMS error of 0.14% deviation from the fitted plane relative to the distance from the plane (400mm), which translates to a 0.56mm RMS error, which is below the 1mm requirement.

D435I

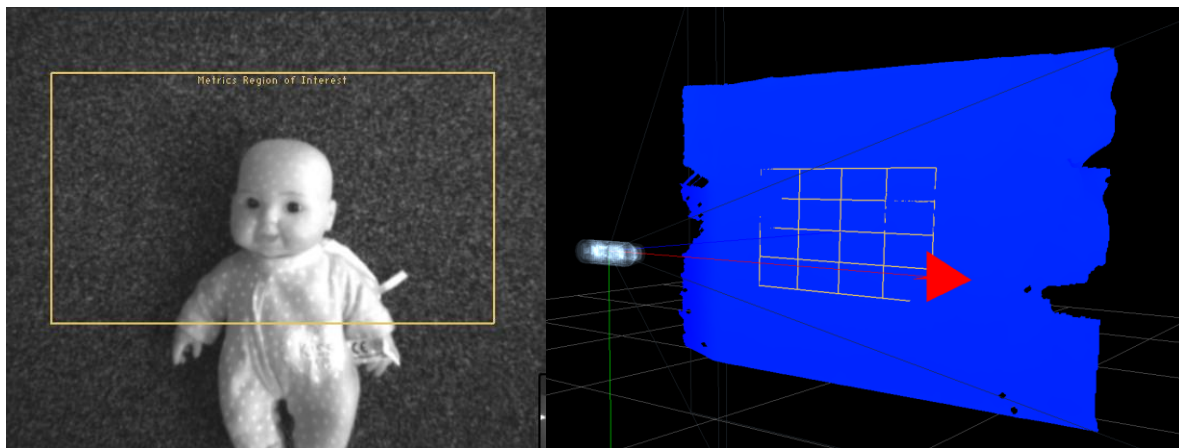


Figure 28 - region of interest shown on plane, with infant for reference

Figure 28 shows a mesh representing the depth output of the D435i camera when aimed at the plane through the incubator hood. Though deformation is still present near the edges of the FoV of the camera, it is less severe when compared to the SR305.

Comparing the error within the ROI (shown in figure 28 with a yellow border relative to the infant doll) the D435i manages a RMS error of 0.18% relative to the sensor to surface distance, which translates to a 0.72mm error. Larger than that of the SR305, but still within the 1mm requirement.

2.6.3 RECONSTRUCTION ACCURACY



Figure 29 - Artec Eva scan of infant doll

To determine which camera produced the most accurate reconstruction, a comparison between the cameras was made using the 24week infant doll. In order to provide a ground truth for the test, a base scan was made of the doll with an Artec Eva white-light scanner (figure 29). In order to reduce the number of variables, the incubator hood was not used for this test. Instead a small tripod was acquired to hold the cameras in multiple predetermined orientations to capture the full scene (figure 31). The used orientations can be seen in figure 30. In addition to this, small markers in the form of Go pieces were placed around the baby to help with alignment. The cameras were placed at the same distance from the child as they would have been when placed on the outside of the incubator looking in. The meshes were directly output by the Intel RealSense Viewer application, with the settings recommended by Intel.

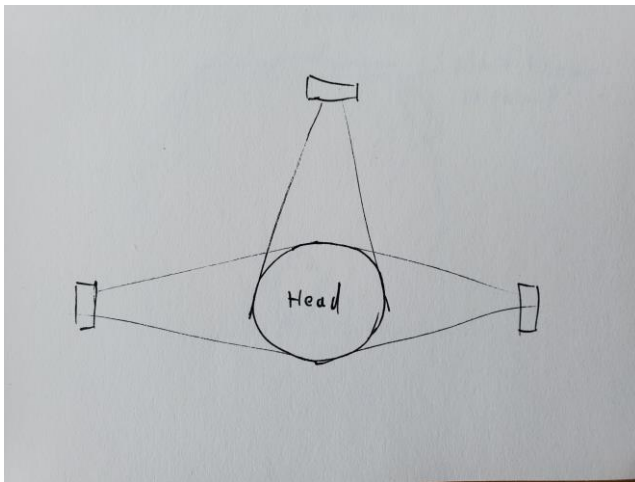


Figure 30 - Drawing of camera positions around the infant head



Figure 31 - Photo of tripod setup

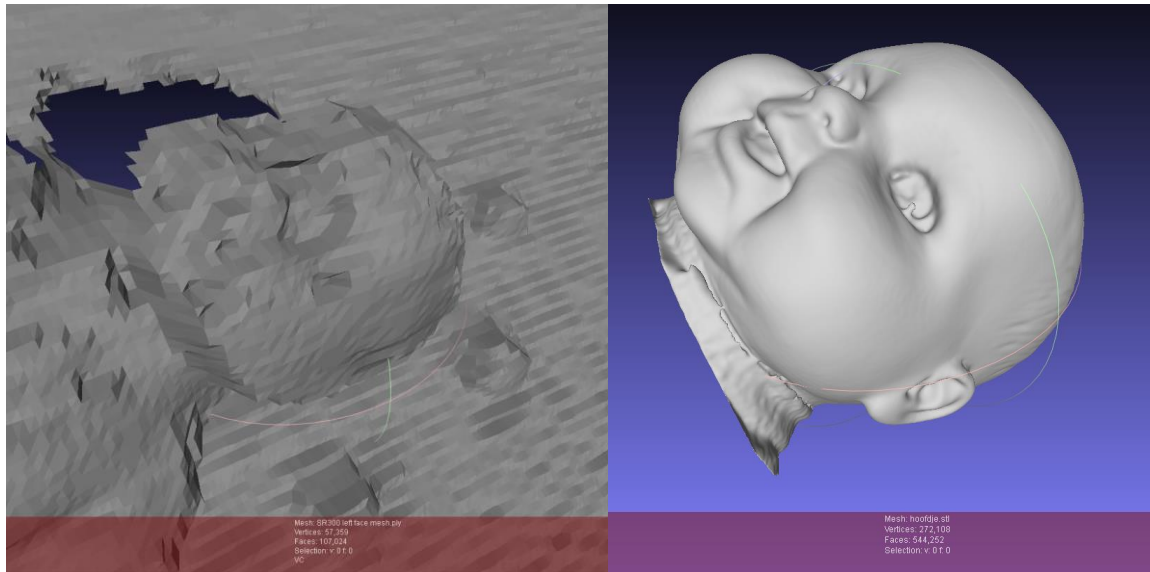


Figure 32 - Comparison between SR305 and Artec Eva scan

Figure 32 shows a comparison between the left camera acquisition using the SR305 and a similarly oriented reconstruction made using the Artec Eva. Though the general shape of the head is still recognisable, it is clear that no detail has been captured. None of the facial features of the doll are recognisable in the SR305 acquisition. Using all three acquisitions (left, top and right) a full reconstruction had been made using the Meshlab software (Cignoni et al., 2008) by aligning the meshes and manually cutting out the relevant geometry, after which the head was remeshed (figure 33). This mesh was then compared to the Artec scan using CloudCompare (CloudCompare, 2020).

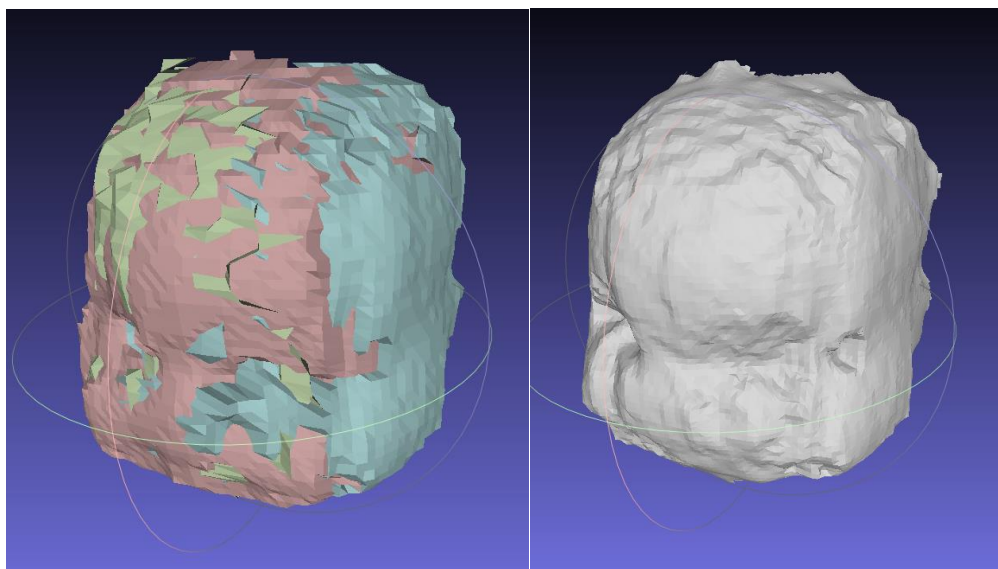


Figure 33 - (left) aligned meshes from SR305 acquisitions (right) remeshed geometry

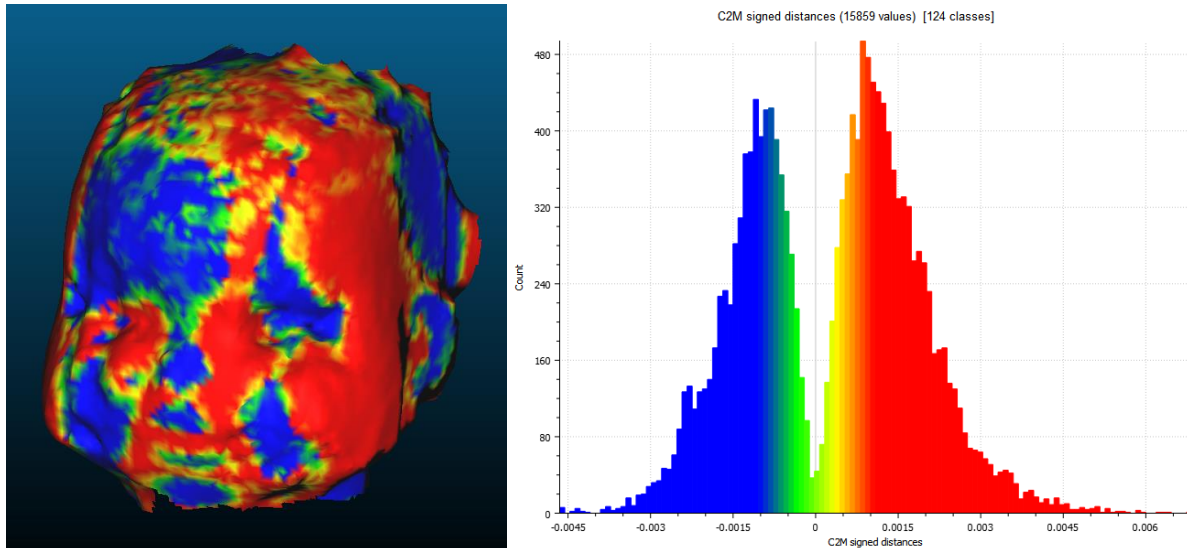


Figure 34 - distance map and accompanying histogram of SR305 scan compared to Artec Eva scan

Figure 33 shows the aligned geometry, with each colour representing a separate acquisition (top, left or right). Though the geometry is clearly low detail, thanks to the markers in the scene it was still possible to correctly align the acquisitions. The figure also shows the remeshed result. This result is noisy due to the lack of detail in the source geometry, as well as the artifacting around the eye area. Figure 34 shows a per vertex distance comparison to the Artec scan. The scale runs from solid blue (<-1mm deviation) to solid red (>1mm deviation). Here it can be seen that the model does not meet the 1mm requirement in most areas.

Additionally, it can be seen that the histogram shows two peaks on each side of 0, instead of 1 peak. This would normally indicate that the mesh has been linearly misaligned for the distance measurement, causing one half to fall outside of the reference mesh, and the other half to fall inside. However, the surface map shows no such clear misalignment.

D435I

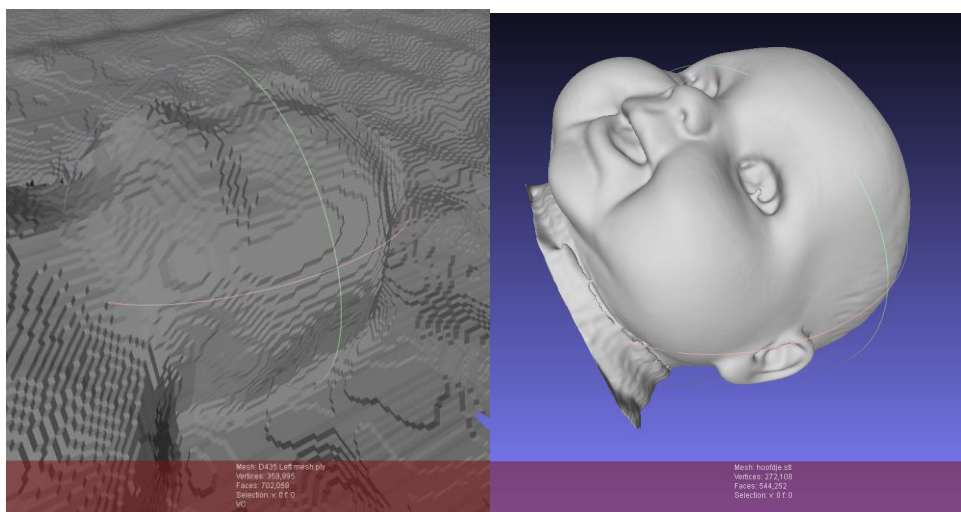


Figure 35 - Comparison between D435i and Artec Eva scan

Figure 35 shows the left camera acquisition using the D435i next to a similarly oriented reconstruction made using the Artec Eva. Here, more detail has been captured than with the SR305. Larger facial features, though smoothed over, are identifiable. This is against expectation, as the D435i has a lower resolution per area than the SR305. Both devices used the same software and processing for capture. A reason for this phenomenon has not yet been found. As with the SR305, using all three acquisitions (left, top and right) a full reconstruction had been made.

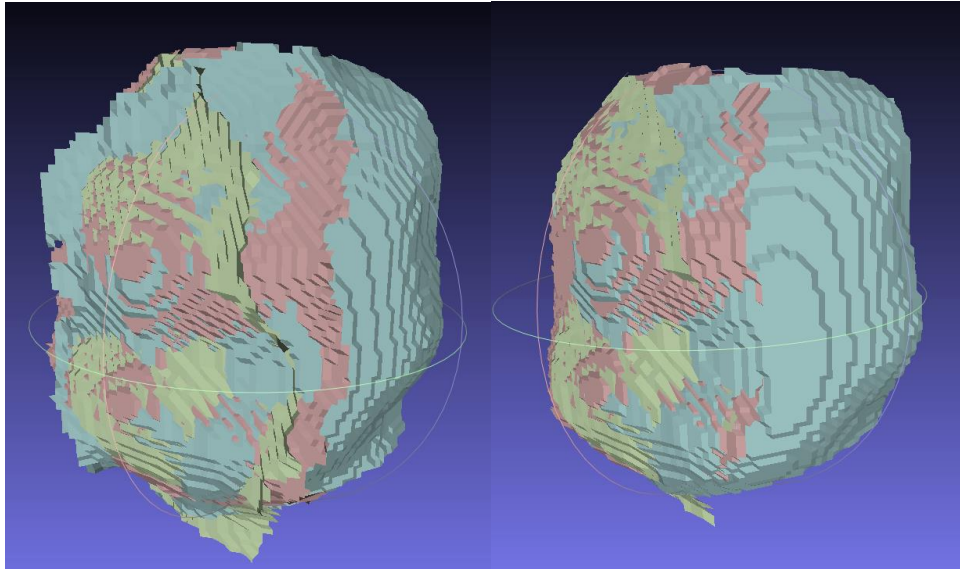


Figure 36 - D435i reconstruction showing scanning artifacts before and after trimming

Figure 36 shows the aligned geometry, with each colour representing a separate acquisition (top, left or right). Here, geometry was detailed enough for landmarks to be selected, and a point-based alignment could be made without the aid of the external markers in the scene. One noticeable artifact with the D435i is the “candy wrapper” like effect of the overlapping geometry. This was solved by removing 4 edge loops from each acquisition..

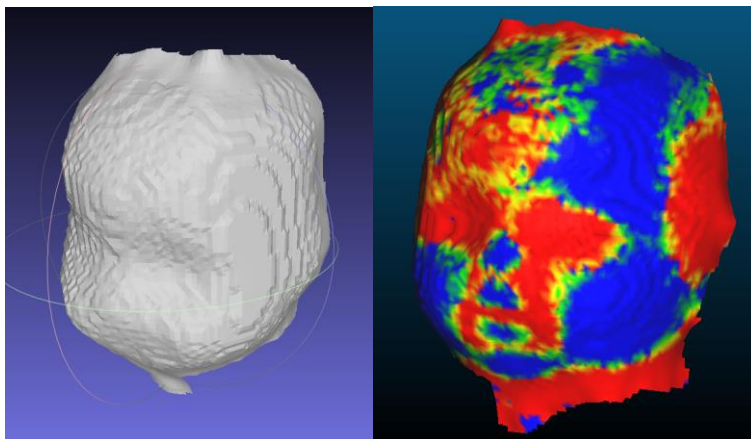


Figure 37 - remesh and distance map of D435i scan

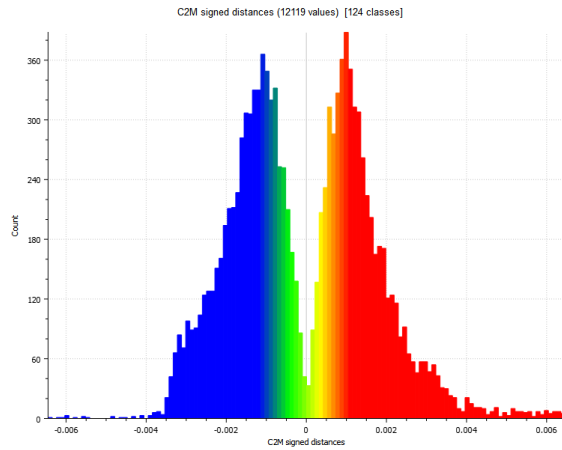


Figure 38 - Histogram of D435i distance map

Figure 37 shows the remeshed result. With the D415i the output mesh is not only more detailed, but also significantly smoother and free of artifacting when compared to the SR305. This does not, however, result in a significantly lower error when compared to the Artec Eva scan, as can be seen in figure 38.

2.6.4 CONCLUSION

In the distortion test, both scanners performed similarly in the RoI, with both staying below the 1mm requirement when capturing through the incubator hood. The SR305 reached a higher accuracy, while the D435i had less distortion near the edges of its FoV.

Regarding reconstruction, though the accuracy of the output mesh of the D435i was not significantly better than that of the SR305 when compared to the Artec scan, the D435i performed significantly better than the SR305, against expectation due to its lower pixel density. The output of the D435i features more resolved detail with clear landmarks and features carried over from the scanned doll, while the SR305's output was nearly unrecognizable, forcing the use of the external markers for aligning the separate acquisitions. In addition, the D435i featured less noise in the output mesh compared to the SR305.

Thus, the chosen technology will be the hybrid photogrammetry approach of the Intel D4x series of cameras.

3. DESIGN

This chapter is divided into 2 sections. **3.1 Concepts** gives a description of the 3 concepts that were considered for the product, concluding with the choice of one the concepts. **3.2 Embodiment** discusses the detail design of this concept, both in hardware and software.

3.1 CONCEPTS

This chapter will concisely cover the three developed concepts: LiveScan, FlexScan, and Monitor3d. An overview of each concept will be given. This overview contains a description of the design, the envisioned operation of the product, and the main advantages and disadvantages of the concept. Afterwards the final concept choice will be made based on which concept best adheres to the wishes of the PoR.

3.1.1 LIVESCAN

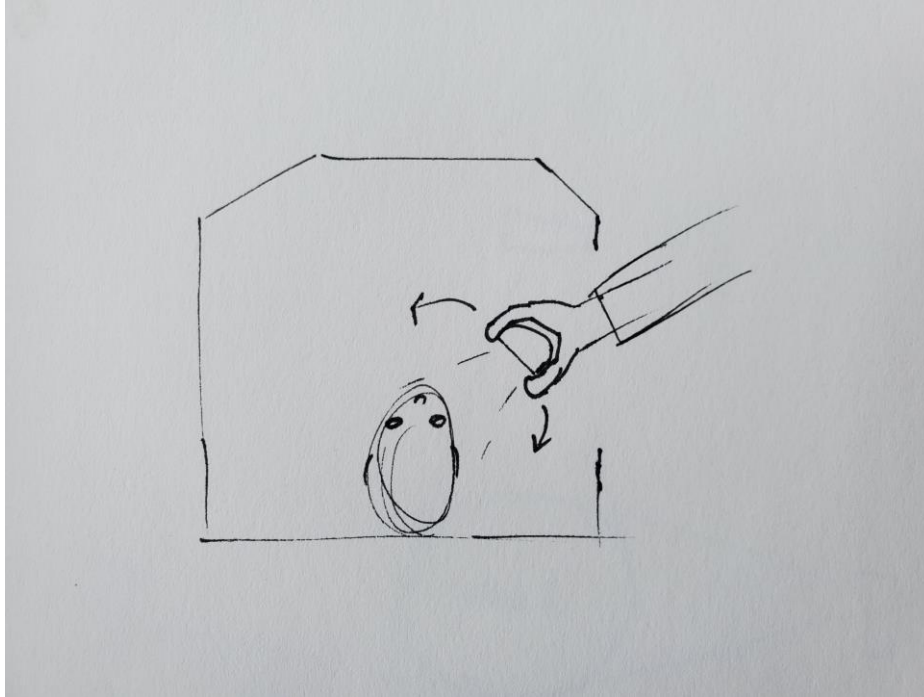


Figure 39 - Drawing of LiveScan concept

LiveScan is a handheld 3D scanner that operates by having the user move the scanner around the incubator during acquisition. This battery-operated device contains a single D435i scanning unit connected to a Raspberry Pi 4 single board computer (SBC). This setup allows for a theoretical 30fps capture and reconstruction of the scene in the FoV of the camera.

With this setup, acquisitions are performed in the following manner:

1. The user activates the LiveScan by pressing the singular button on the unit.
2. The unit connects to the Vectory3 servers, which relay the live reconstruction to the incubator-side computer, allowing the nurse to see the progress of the scan
3. The nurse slowly moves the scanner around the incubator, capturing as much of the head as possible
4. Acquisition can be stopped by pressing the button on the unit again
5. Further processing will be done on the Vectory3 servers, with the nurse being able to view and perform measurements on the finished model using either the bed-side computer or any other network connected PC.

•

3.1.2 FLEXSCAN

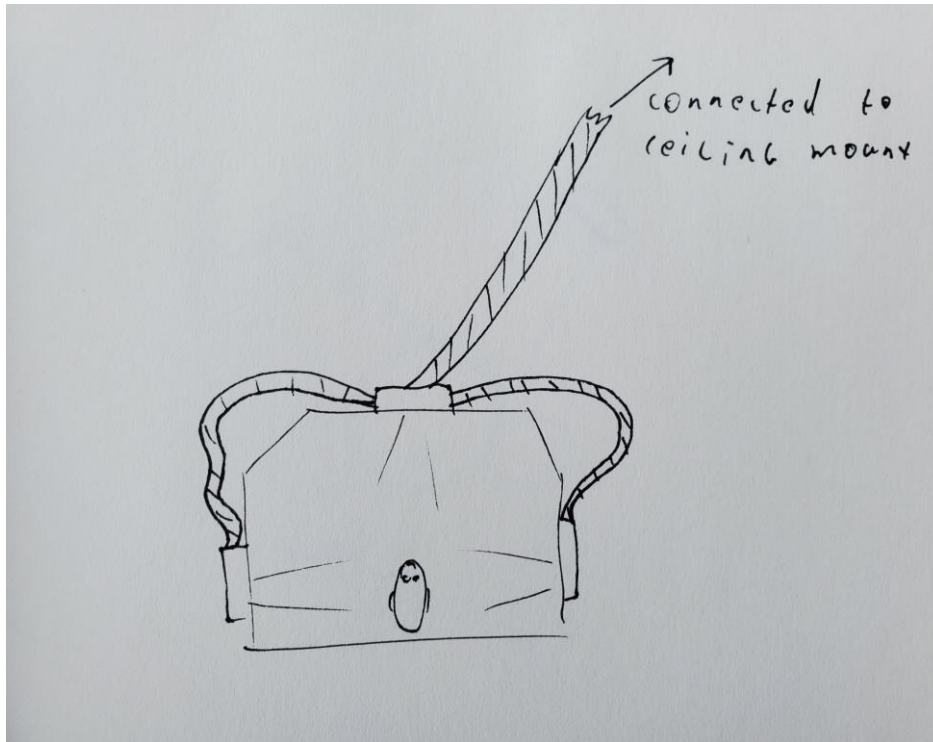


Figure 40 - Drawing of FlexScan concept

FlexScan is a multi-scanner, ceiling mounted solution that is part of the NICU station. The unit is suspended on a flexible arm, which allows users to easily pull down or push away the scanner from the incubator, depending on the requirements of the current situation. Since the unit is part of the NICU, no SBC is needed. Instead the unit is hardwired to the bed-side computer of its respective station.

With this setup, acquisition is performed in the following manner:

1. When the incubator is set-up and the child placed inside, the scanner is pulled down from the ceiling until the camera modules are in the correct position around the incubator
2. The user can control the scanner from the bed-side computer, allowing them to take an acquisition.
3. The mesh data will be sent to the Vectory3 servers, in order to be processed into a full model
4. When finished, the model is returned to the bed-side computer (or other network PC) where the user can perform measurements on it.
5. Whenever intervention is needed, the unit can be pushed away from the incubator, since it does not latch to it.

3.1.3 MONITOR3D

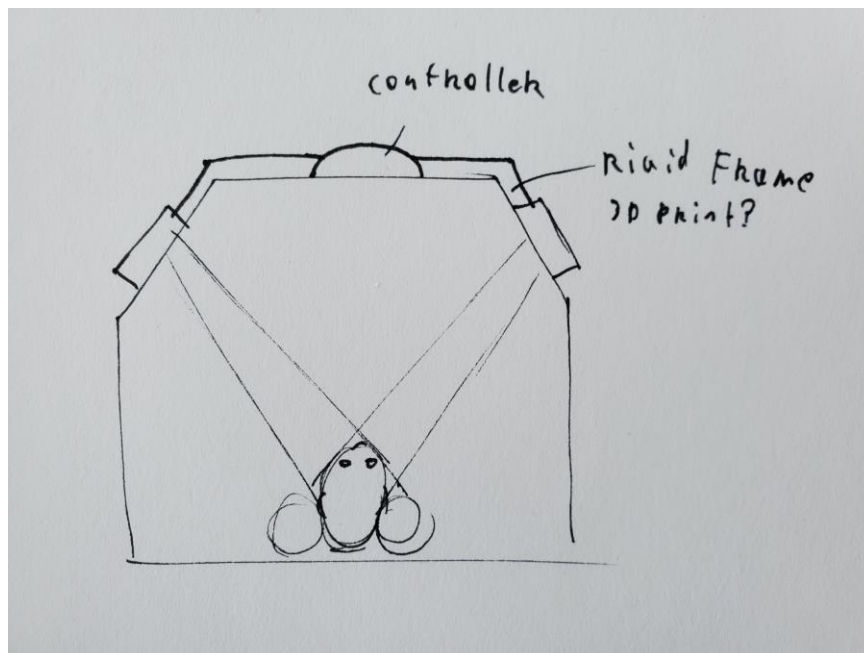


Figure 41 - Drawing of MONITOR3D concept

Monitor3d is a multi-camera, semi-portable scanner that is placed on top of the incubator by the user. After placement, the scanner can be left for multiple acquisitions, or until an intervention is necessary. Even though the scanner can easily be moved between incubators, it does not contain a battery, since it is intended to be left on an incubator after acquisition for the purpose of video monitoring of the child.

Like LiveScan, Moitor3d is a self-contained scanner, meaning it only requires power and a wireless network connection to function. To this end a Raspberry Pi 4 SBC is built-in to the unit for acquisition and communication with a wireless network, in order to contact the Vectory3 servers.

With this setup, acquisitions are performed in the following manner

1. The product is placed on top of the incubator and hooked up to the external power adapter
2. The user can control the product through a web interface on any computer with a network connection.
3. The mesh data will be sent to the Vectory3 servers, in order to be processed into a full model
4. When finished, the model can be requested from any PC with a network connection, where the user can perform measurements on it.
5. Whenever intervention is needed, the unit can be easily picked up from the incubator, since it does not latch on to it.

3.1.4 CONCEPT CHOICE

To decide on which concept will be chosen as the base for the final product, the *weighted objectives* method will be used (Roozenburg & Eekels, 1995). Here, the concepts will be ranked according to their score on the wishes of the program of requirements. These wishes are as follows (ranked from most to least important):

- 1.17 *The product must be able to measure cranial volume in addition to head circumference.*

- 1.16 *The product must be able to serve as a continuous monitoring device.*
- 6.1 *The product should integrate with the current pay-per-scan environment used with the Vectory3 Curatio*
- 1.15 *The product must be compatible with as many incubator models as possible*
- 3.2 *The product must be as unobtrusive as possible, in order to allow for easy observation of the infant around the product*
- 4.3 *Acquisitions must take the least amount of cognitive effort possible*
- 4.4 *Acquisitions must take the least amount of physical effort possible*
- 1.18 *Acquisition must be as fast as possible.*

Then the advantages and disadvantages of each concept were written down in order to determine the relative score of each concept in a weighted measure

LIVESCAN

Advantages of this concept are:

- The compact size of the unit, allows for easy handling and storage
- Battery operation removes wire clutter
- The effect of many cameras can be achieved with a single unit

Disadvantages of this concept are:

- No ability for continuous video monitoring of the child
- Lighting conditions are hard to control with the scanner not directly touching the incubator glass
- Acquisition process potentially requires skilled operator
- Comparatively more complex software development

FLEXSCAN

Advantages of this concept are:

- The ceiling mount allows the unit to be easily placed and stowed
- No battery or charging necessary
- Unit is always connected and ready
- Acquisition does not require direct control of the scanner.
- Ability to continuously video monitor the child

Disadvantages of this concept are:

- No placement flexibility: only stations with a FLEXSCAN unit can perform no-contact HC measurements.
- Mounting arm takes up space in the station
- Static multi-camera setup can more easily be obstructed than a moving single camera
- Multiple scanners required if all infants in the NICU need no-contact HC measurements

MONITOR3D

Advantages of this concept are:

- The compact size of the unit, allows for easy handling and storage
- Acquisition does not require direct control of the scanner.
- Ability to continuously video monitor the child
- The unit setup is quick, only having to be placed on the incubator
- Because it is portable, a single unit can be used in multiple stations on multiple incubators by simply placing it on top of the next incubator, only requiring the power to be reconnected.

Disadvantages of this concept are:

- Static multi-camera setup can more easily be obstructed than a moving single camera

Table 8 - Weighted objectives

Req.	Weight	LiveScan		FlexScan		Monitor3d	
		Score	Total	Score	Total	Score	Total
1.17	30	10	300	10	300	10	300
1.16	25	0	0	10	250	10	250
6.1	15	10	150	10	150	10	150
1.15	10	10	100	6	60	8	80
3.2	5	10	50	5	20	8	40
4.3	5	5	25	9	45	8	40
4.4	5	3	15	10	50	10	50
1.18	5	3	15	7	35	7	35
Total	100		655		910		945



Table 8 shows the results of the weighted objectives. Here the Monitor3d concept wins because it combines the best aspects of both the LiveScan and FlexScan products into a single design. Therefore, Monitor3d will be chosen as the final concept of this project.

3.2 EMBODIEMENT

The chosen concept is now to be embodied and detailed into a near-final product. This chapter covers the functional design of the scanner hardware, the design of the product's construction, and the design of the envisioned user experience (software).

3.2.1 SCANNING HARDWARE

Table 9 - Comparison between D435i and D415

	D415	D435i
		
Highest accuracy resolution	1280x720	848x480
FoV	65° x 40°	86° x 57°
Claimed depth accuracy	<2%	<2%
Depth range (m)	0.16 - 10	0.105 - 10
Price	€150	€175

Though the accuracy and distortion tests of this technology had been performed with a D435i, and the technology was chosen because it worked better than the SR305 structured light solution, the results were still not fully satisfactory. Resolved detail was lower than expected, hampering alignment through landmark selection, and accuracy when compared to the ground truth model was too low. Because of the large distance between vertices, these problems were both attributed to a too low sensor resolution per surface area. Therefore, a higher resolution alternative to the D435i was sought and found in the same series; the D415. As can be seen in table 9, the D415, which uses the exact same working principle as the D435i, improves upon the D435i by increasing resolution. In addition to this the FoV is lowered, which in means a higher significantly higher pixel count per surface area when compared to the D435i. Therefore, the D415 was chosen as a replacement for the D435i.

3.2.2 MODULE SETTINGS

In order to further optimize the acquisition process, the supplied software with the cameras (Intel RealSense Viewer) was used to implement multiple enhancements in the camera configuration, allowing for consistently better acquisitions. The main enhancements increasing scan quality are as follows (A full printout of the created config file can be found in Appendix P):

LASER POWER

The aforementioned D415 dot projector's intensity can be set from 0 to 255. Both too low and too high a value can cause scanning artifacts when environmental lighting conditions are suboptimal. Through trial and error testing a value was found that works in both the 0 Lux and 600 Lux conditions that are prescribed for NICU environments. Additionally, tests were performed on both the light- and dark-skinned infant dolls. The best value for all of these situations was found to be "180".

RESOLUTION

For the D415, Intel specifies that a depth camera resolution of 1280x720 gives the highest possible depth accuracy with this module (RealSense Technology, 2020)

DISPARITY SHIFT

The minimum rated Z value for the D415 of 0.2m is at a resolution of 640x480 (RealSense Technology, 2020). For the targeted 1280x720 resolution, this value is 0.44m, too high for the camera to capture the head of a full-term infant in the incubator. To solve this, the disparity shift function can be used. This allows the user to reduce of the max depth range of 10m while at the same time reducing the min depth. Because of lack of documentation of this feature, the correct value was found through trials and error. With a value of "110" all the dolls could be scanned.

DEPTH UNITS

The internal D4 VPU in the D415 module uses a 16bit integer to represent the depth value of each pixel of the depth sensor. By default, the unit this integer represents is set to 1000u, which gives a maximum precision of 1mm, and a maximum range of ~65m. However, the camera hardware itself is capable of higher precision, so the depth unit was set to "10u". This allows for a theoretical max precision of 0.01mm. This reduces the max measurable depth of the

3.2.3 SCANNER MODULE LAYOUT

Having a single scanner is not enough for a full acquisition of all sides of the infant's head. Multiple scanners must be used to capture as much of the visible had as possible, without the need for the head to be rotated. This ensures good overlap between acquisitions when the head is turned, and an additional set of acquisitions is taken to complete more of the model. This overlap is important because it aids in the alignment of the individual scans.

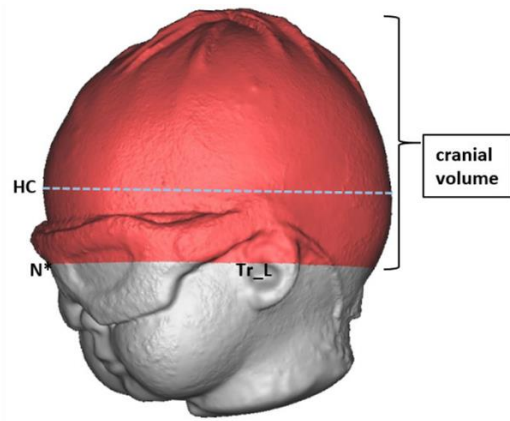


Figure 42 - Image showing region of interest for cranial volume measurements. Reprinted from Reprinted from Santander, P., Quast, A., Hubbert, J., Horn, S., Meyer-Marcotty, P., Küster, H., & Dieks, J. K. (2020). Three-dimensional head shape acquisition in preterm infants - Translating an orthodontic imaging procedure into neonatal care. *Early Human Development*, 140, 104908. <https://doi.org/10.1016/j.earlhumdev.2019.104908>

To determine this layout the relevant surface of the infant head must first be determined. For the HC, the place of measurement is described as “the level of maximum anterior-posterior head expansion”, which means its exact location is variable, but always above the eyes. Cranial volume is described as “the horizontal plane at nasion as well as right and left tragus” (Santander et al., 2020). Both these definitions are visualised in figure 42. It can be seen that, outside of landmark recognition for easy alignment, the facial area of the infant’s head is not needed for the actual measurement of both the HC and cranial volume.

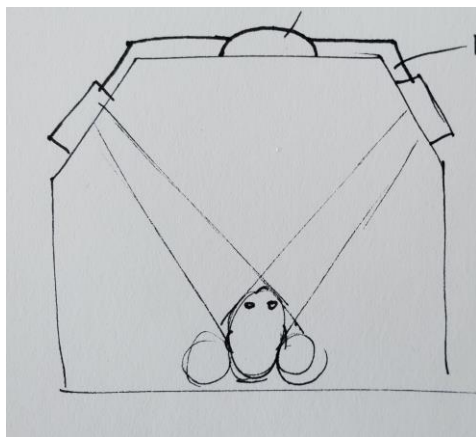


Figure 43 - Schematic drawing of incubator archetype

Another important factor in the camera layout is the shape of the incubator itself. Appendix C features an overview of currently available incubator designs, which shows that even though the exact measurements differ, a distinct archetype can be described that fits most of these designs. Figure 43 depicts this archetypical situation, whereby it is important to note the trapezoidal shape of the incubator hood in addition to the straight sides, as well as the rolled-up towel which is placed at a small distance around the infant’s body to stabilise it in case of movement.

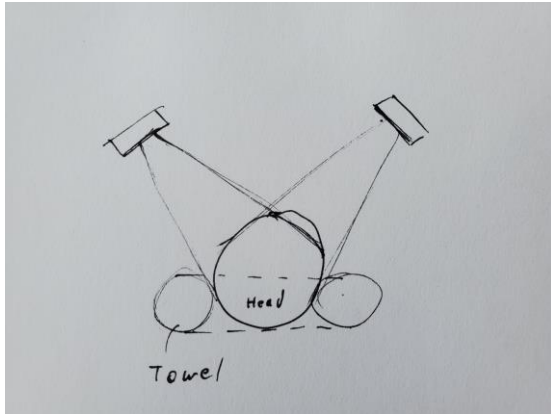


Figure 44 - Two camera scanning setup

In this situation, only 2 cameras would be enough to capture all the visible, relevant surfaces at once (figure 44). However, when performing initial tests with this setup it was quickly found that there was too little overlap of the two cameras' acquisitions to properly align the meshes without use of external markers. Additionally, this setup requires both cameras have a perfectly unobstructed view of the infant, as no significant overlap means that there is no redundancy in the acquisition process. Therefore, a "top" camera was added to both increase robustness of the capture, as well as simplify alignment of the meshes.

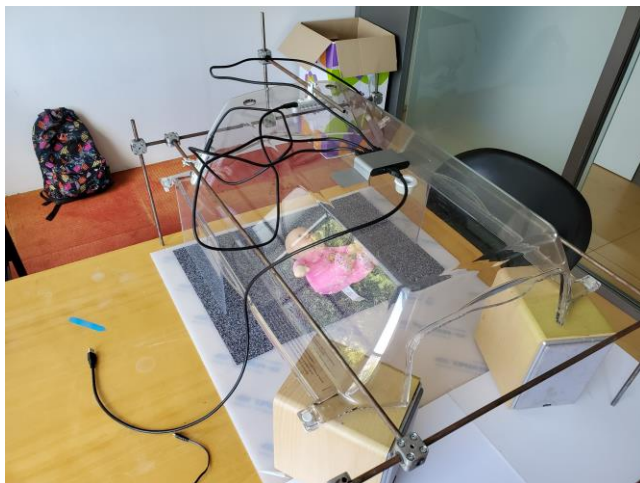


Figure 45 - Camera setup test rig

This three-camera setup was then used to determine the most effective relative layout of the cameras (Appendix H), using a special built rig which allowed for easy and quick placement and replacement of the cameras (figure 45). Multiple setups were tested, with the best performing setup being a linear setup whereby the cameras are placed parallel to the "glass" of the incubator hood, all on a single line to form a half-ring. This setup was chosen because, even though placing the cameras further back on the incubator and angling them towards the infant's head indeed gave a better capture of the absolute top of the head of the infant, the increased distance to the infant caused a drop in both detail (due to a decrease in pixel count for the to-be-scanned object when distance increases) as well as a drop in accuracy because of the relative depth-error of this particular technology (<2% of the distance from the object).

3.2.4. CONSTRUCTION

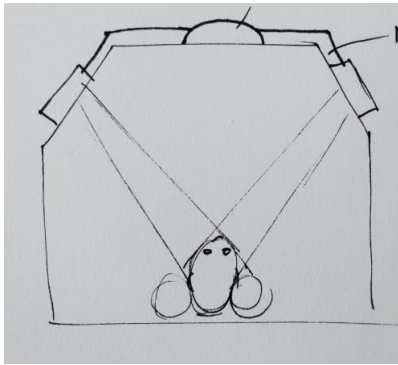


Figure 46 - Static setup

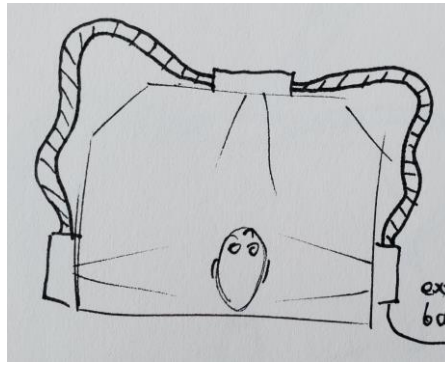


Figure 47 - Adaptable setup

One of the first major design considerations for this product was the incubator compatibility. Currently, many different designs are available and in circulation on the hospital market. Even though an archetype of these designs could be created, the precise dimensions differ per model. There were two main ways for this to be solved:

- Make the product adaptable to the incubator dimensions (figure 47)
- Make many different SKUs, one for each variation of incubator (figure 46)

Though the first option seemed the most obvious, multiple considerations led to the adoption of the second:

The low expected quantity of few tens of units in the first year of market introduction means that tooling costs must be kept at a minimum, or ideally be eliminated altogether. Furthermore, the stringent hygiene rules in the NICU make the implementation of moving parts difficult without creating seams and other dirt traps. Another important reason was that it was decided that a good way to speed up the post-acquisition mesh processing, was to factory calibrate the device, which would allow for automatic alignment of the three meshes of each acquisition, since the relative orientation and position of the camera modules would be a constant. Thus, rigidity of the device became a major factor of the design, eliminating the idea of an adaptable hinged system.

FRAME

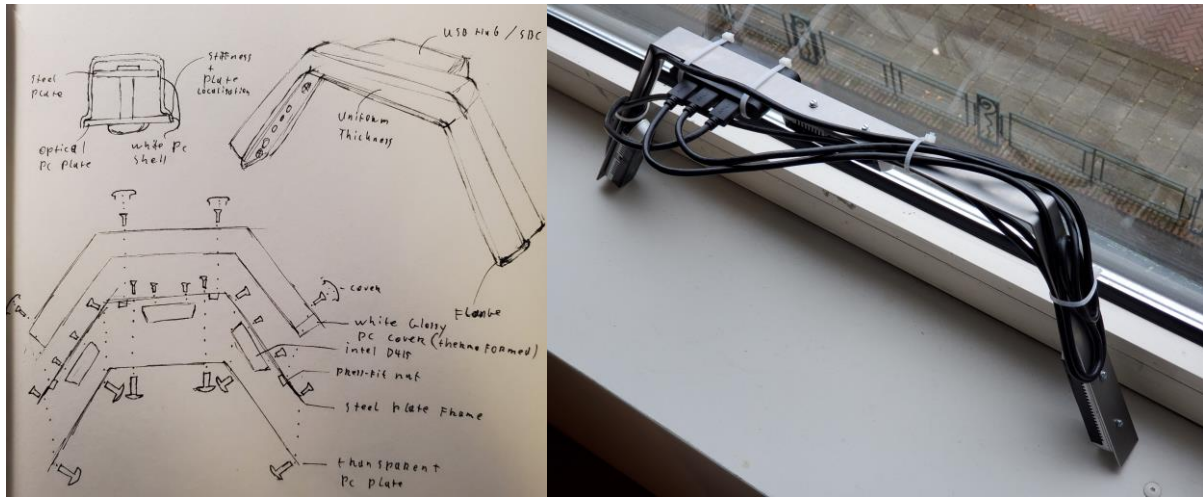


Figure 48 - Original construction design next to the first prototype of this setup

With the scanner layout known, a frame had to be designed in order to keep the relative positions of the camera constant during the life of the product. Since a plastic outer shell is not enough to provide this rigidity, an internal metal frame was chosen to which the cameras bolted directly. The first version of the design of this frame consisted of a single piece of 2mm steel plate, bent in two places to conform to the shape of the incubator hood (figure 48). All internal components of the scanner (the cameras, USB hub, and SBC) were to be mounted directly to this frame using screws.

A “barebones” prototype of this design was constructed to test functionality of major parts. This design consisted only of the 2mm steel frame, the 3 D415 units, and the USB hub (figure 48). Immediately while placing the prototype onto the incubator hood it was clear that the steel frame did not provide the required rigidity as was originally planned. Though deformation was small, any amount would cause the factory calibration of the relative orientation and position of the cameras to be non-representative of the truth, which in turn would cause errors in the scan results due to misalignment. The frame thus had to be redesigned.

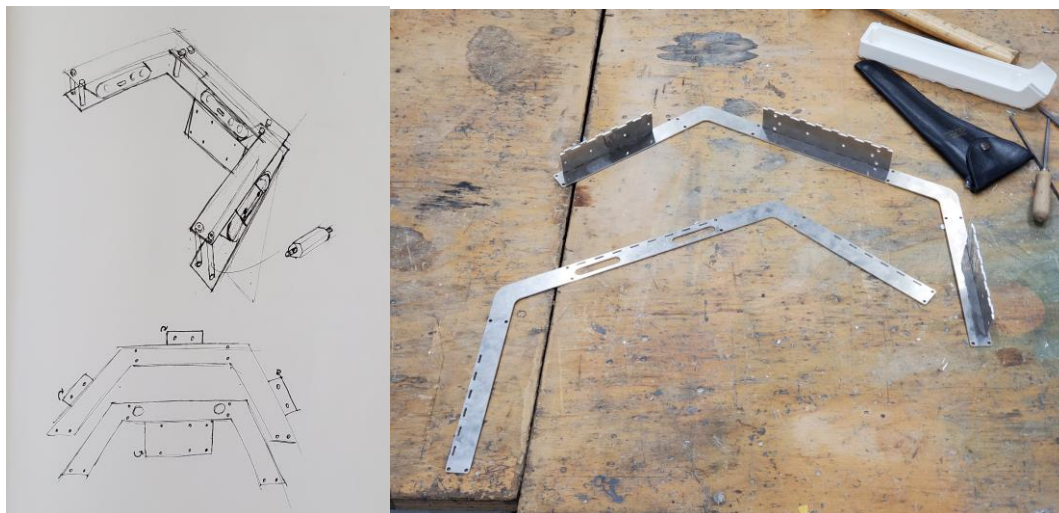


Figure 49 - Frame redesign showing three-dimensional layout

The redesign was to feature a 3-dimensional metal frame, which would increase rigidity. This entire frame was to be water cut from a 2mm aluminium plate with the individual components being held together with 30mm standoffs. Mounts for both the camera and the USB-hub/SBC were bent from this plate into the correct orientation (figure 49). However, it was decided to eliminate bending as a process altogether in order to reduce production methods to the minimum. Instead all parts including camera mounts were separate water cut elements from the aluminium plate, which were then mounted together using the 30mm standoffs and a slotted pattern in the pieces for mechanical fastening as well as locating (figure 50). Additionally, mounting points for handles were added, since the first prototype proved to be difficult to handle without.



Figure 50 - Constructed frame

ENCLOSURE

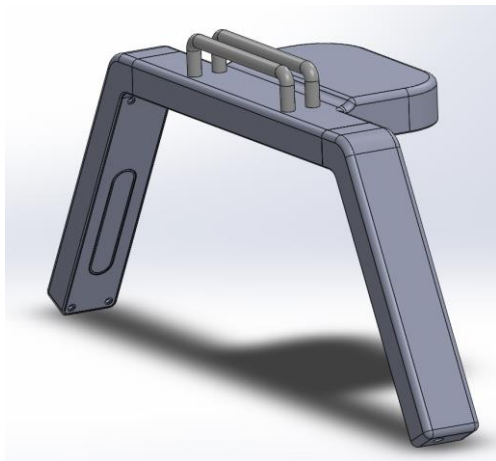


Figure 51 - CAD model of the complete device

For the case design multiple mood boards were created to determine the main aesthetical features that both NICU equipment, medical scanners and 3D scanners use. These mood boards can be found in Appendix J. The main takeaways from these mood boards were as follows:

- The device is to feature a matte white plastic casing
- Polished and brushed RVS are regularly used for frame and handle purposes
- Hospital equipment features smooth curves and shallow slopes

- Hospital equipment creates little visual noise

This combined with the requirements for low as possible interference with the NICU staff's view of the infant in the incubator, and the low tooling costs meant that the product would have to be fairly simple and minimalist in both shape and size.

Two ways were found to produce the plastic for the product case. The first choice was thermoforming, because of its low tooling costs and low volume possibilities. Since thermoforming does not allow for complex features such as ribs, this design featured an internal steel frame to provide the required rigidity. The bottom of the casing would be closed off using a bent transparent optical quality PC plate for the cameras. The top of the device featured an extended section where the USB hub and single board computer (SBC) for capture and wireless communication were housed.

However, it was soon found that the limitations of thermoforming regarding small details such as corners and edges were incompatible with the shape of this design. Therefore, the production process was transferred to 3D printing. According to Erasmus MC the only allowable form of 3D printing that meets the stringent NICU hygiene constraints is the SLS printing of PA12, which will then be coated in an epoxy resin to prevent porosity from causing any contaminant habitat. Though this process is more expensive per unit than thermoforming, there are no tooling costs, and product flexibility is increased in regard to fitting multiple incubators.

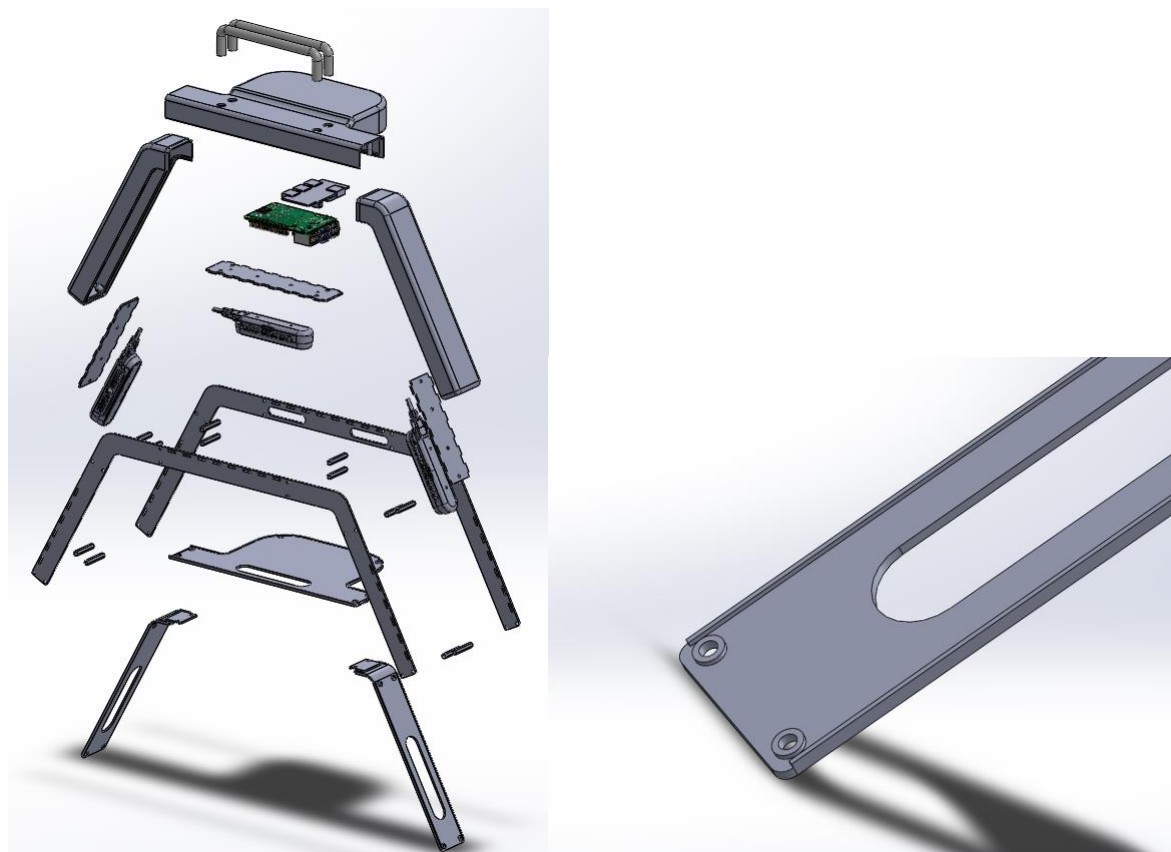


Figure 52 - Exploded view of the CAD model next to a closeup of some hygiene measures in the design

Figure 52 shows an exploded view of the final design of the product, excluding wiring and fasteners. Here the 6 interlocking case parts are clearly visible, along with the internal frame, standoffs, cameras, USB hub and SBC. The entire assembly is held together by 20 m3x5 torx screws, 2 m4.5x10 torx screws, and 2 m2.5x5 torx screws. Of these fasteners, 16 m3x5 torx screws are accessible from the outside of the device, on the bottom

side of the casing. In order to comply with NICU hygiene regulations, these screws are capped off with small white plastic disks, adhered with double sided tape.

Further hygiene measures include tight tolerances on the interlocking parts, as well as guiding slots and ridges like those depicted on the bottom case part in the same figure. These ridges ensure that no gaps appear when the case is forcefully deformed.



Figure 53 - Full render featuring materials used in the product

SUPPORT HARDWARE

As described in the Chapter 3.4.3, Monitor3d is a standalone device which requires only an internet connection and power. Therefore all supporting hardware must be built-in to the device. In the case of monitored this supporting hardware consists of the internal SBC, an internal USB 3.1 hub, and an external power adapter with barrel jack connection.

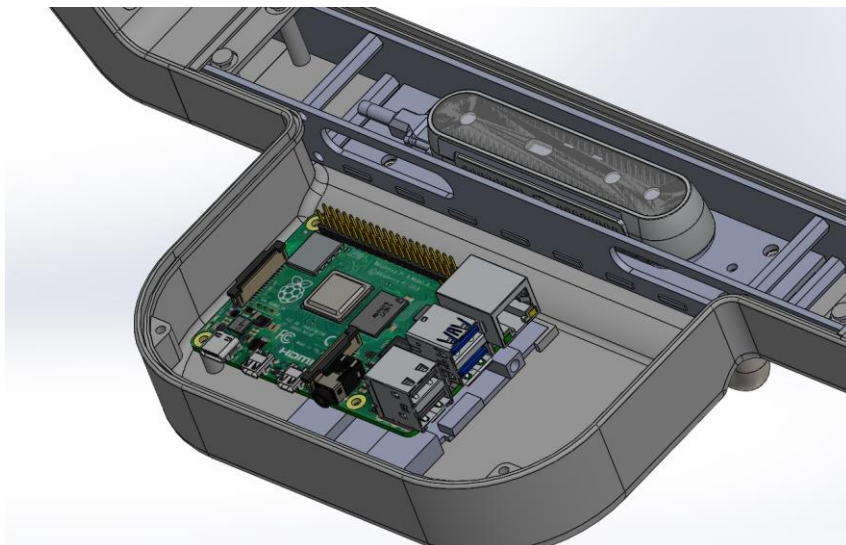


Figure 54 - internal view of the device showing the middle camera, as well as the USB hub and SBC

Vectory3 wants to integrate this scanner in their current pay-per-scan system used by their Curatio hand scanner. Curatio functions from an online environment hosted on Vectory3's servers, where all processing and data handling is done. In order for the product to be incorporated into this system a similar setup would be desirable. Therefore, it was chosen that a single board computer, in this case the Raspberry 4 (4GB) would be integrated. This SBC features the necessary connectivity (USB3.1, Wi-Fi) as well as software support by Intel for the RealSense modules. Figure 54 shows the SBC mounted inside the case, on top of the USB Hub.



Figure 55 - Close up of prototype showing the DC barrel connector

The scanner requires a 5V 3.5A power DC power supply to function. Originally, when the idea was to have an NICU use one unit and move this unit between beds for acquisition, this supply was meant to be internal in the form of a rechargeable lithium battery pack. However, since Vectory3 requested that the cameras of the device could also be used for monitoring, the design was changed to a more semi-permanent addition to the incubator during use, whereby each incubator has its own scanner unit. This not only meant that the unit had to be powered on continuously, which would increase size and cost of the battery, it also meant that the battery would not be needed due to longer periods of stationary use of the product. Therefore, the battery was dropped in favour of an external DC power adapter, which connects to the product using a barrel jack connector. Figure 55 shows the final prototype of Monitor3d with the DC adapter plugged into the side.

3.2.5 SOFTWARE

For the Curatio hand scanner, Vectory3 utilizes a pay-per-scan system, whereby all processing of the acquired data is performed off-scanner on Vectory3's servers. When the data has been processed, and a 3D reconstruction of the hand generated, the user can pay to acquire this scan, which can then be measured using local software on the user's computer.

Requirement 6.1 states: *"The product should integrate with the current pay-per-scan environment used with the Vectory3 Curatio"*. Therefore, a similar system will be used for Monitor3d. This system works as follows

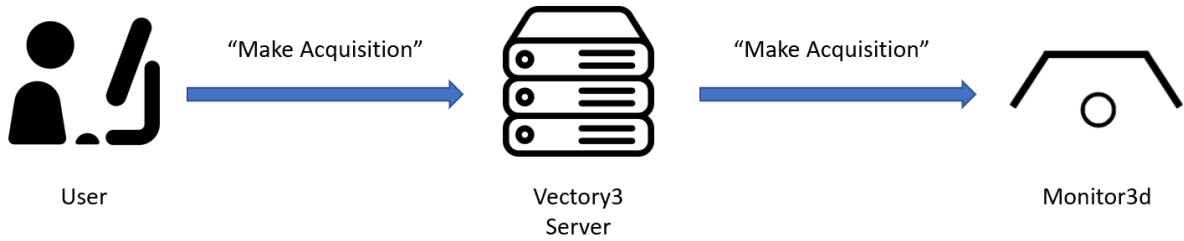


Figure 56 - User to device communication via V3 servers

Since Monitor3d features built-in processing and network connectivity, it never needs to be directly connected to the user's computer. Instead, Monitor3d connects directly to the Vectory3 servers. The user connects to these servers using a web portal, allowing them to make acquisitions and retrieve processed meshes. Figure 56 shows a simple diagram of a user sending the "Make Acquisition" command to the scanner. Note how this command is sent first to the Vectory3 server, after which it is relayed to the scanner.

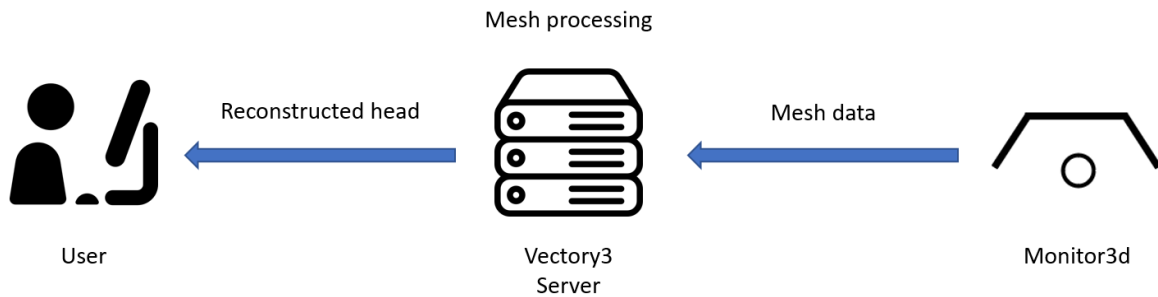


Figure 57 - Device to user communication via V3 servers

After acquisition, Monitor3d sends the acquired meshes to the Vectory3 server, where the meshes will ideally be automatically cleaned, aligned, and remeshed into the final reconstruction of the infant's head, depending on the feasibility of the software automation. The user can then view this reconstruction using the web portal and choose to download it if satisfactory (figure 57).

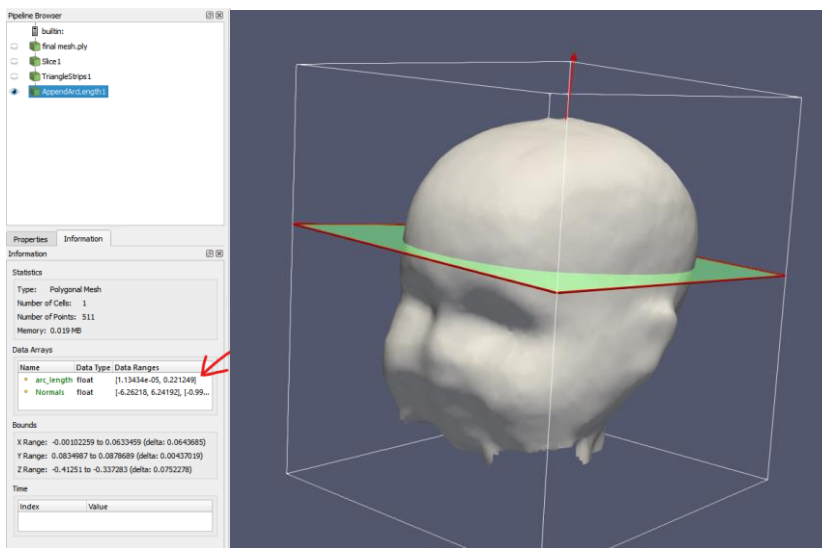


Figure 58 - Head circumference measurement being performed in ParaView

Finally, the user can use local software such as ParaView (figure 58) or a Vectomy3 developed application (like Metrix) to perform the required measurements.

4. EVALUATION

Now that the design is finished, the product must be validated in order to find if it meets the goal set at the beginning of the project. In order to accomplish this, a prototype will be built and tested against the Program of Requirements.

This chapter consists of the following parts: **4.1 Prototype** describes the creation of the prototype used for validation, as well as an overview of the software workflow currently required for mesh processing. **4.2 Measure Accuracy** evaluates the accuracy of the scans created with the product in the test incubator setup, and a 0 lux setup. **4.3 User Experience: Positioning** looks at the current workflow for placing and correctly positioning the device for a scan session through a physical user test. **4.4 User Experience: Mesh Processing** looks at the ability for users to perform the current mesh processing workflow using a 15 minute video demo divided into 5 parts.

4.1 PROTOTYPE

Having embodied the design of Monitor3d, a prototype was created in order to evaluate the design. This chapter describes the construction of this prototype, detailing changes made in both hardware and software compared to the design.

4.1.1 HARDWARE

Two parts of the prototype are to be custom produced for the product: the enclosure, and the frame. All other parts are of-the-shelf.



Figure 59 - Parts of aluminium frame next to the assembled model

Figure 59 shows the prototype frame. Though dimensions of the produced parts are exactly as described in the design and the correct material is used, production of the parts was done differently than originally planned, as the production company decided to use laser cutting instead of the explicitly specified water cutting. This should not have an effect on the representativeness of the prototype, however



Figure 60 - FDM print of case showing the split middle case part

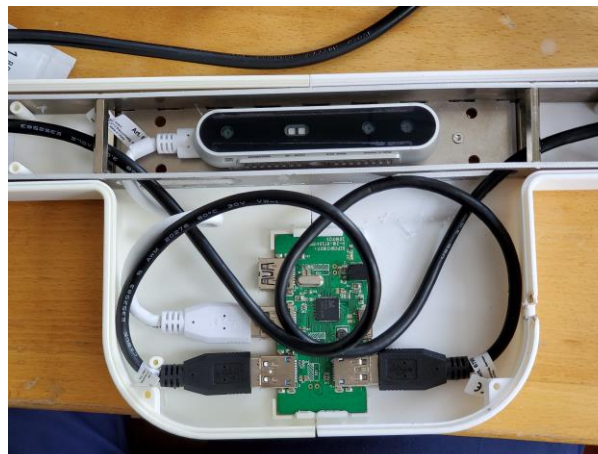


Figure 61 - Internal view of the final prototype showing the lack of an SBC due to overlength cables being used

Regarding the enclosure, multiple changes were made. First and foremost, the material was changed from PA12 to PLA, and the printing method from SLS to FDM. This was done because of availability of the printer and material in a short timeframe. Furthermore, as can be seen in figure 60, the middle sections of the enclosure have been split in half. This was done to fit the pieces to the print bed of the used printer (Ultimaker 2+).

Figure 61 shows that in addition to this, the SBC is not present in the prototype. This had two reasons: The software for the prototype did not require an internal computer, since the prototype would be hooked up to an external computer during testing. Additionally, as can be seen in figure 61, USB cables of the correct length could not be sourced in time, necessitating longer cable to be used. Because of this, no space was left for implementing the SBC



Figure 62 - Close up of prototype showing hardwired USB cable protruding from the device

Figure 62 shows that a permanent USB cable was added to the prototype. This was done because of the deletion of the SBC, and software changes that will be discussed in the next section.

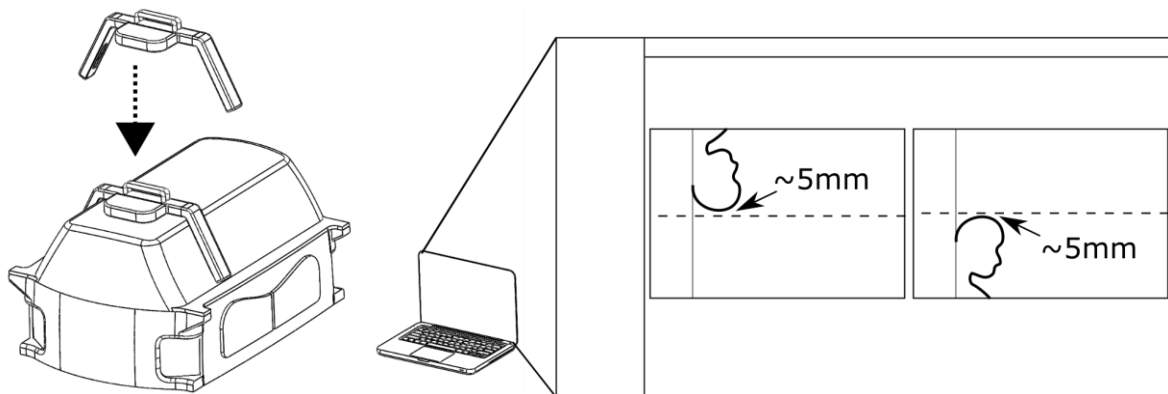


Figure 63 - Image of the instructional sticker featured on the prototype, displaying the correct placement and positioning method.

Figure 63 depicts a quick explanation label that is adhered to the back of the unit, facing the user. This label consists of two sections. The first to the left displays the correct placement for the device on the incubator hood. The second to the right shows a schematic representation of the software interface, displaying the desired position of the heads on the viewfinder on the monitor.

4.1.2 SOFTWARE

Since there was no time to create the custom software necessary to achieve the designed user experience, an alternative method of usage was created using available, open-source software. This method does away with the need for a server, and instead relies on the user connecting the prototype directly to a computer, after which all mesh processing is done manually.

This section gives a concise overview of the operation of the prototype. For the full step-by-step manual, see appendix E. Operations are divided into five sections: **Hardware setup**, which is concerned with the placement and initialisation of the prototype. **Acquisition**, which describes how the prototype is used to capture the scene. **Obtaining Full Reconstruction**, which details how multiple acquisitions are used to reconstruct a 3D model of the entire infant head. **Mesh Processing**, which describes the operations necessary to isolate and combine relevant geometry into the final model. And finally **Measuring Circumference**, which explains how the actual measurement is performed on the 3D model.

HARDWARE SETUP

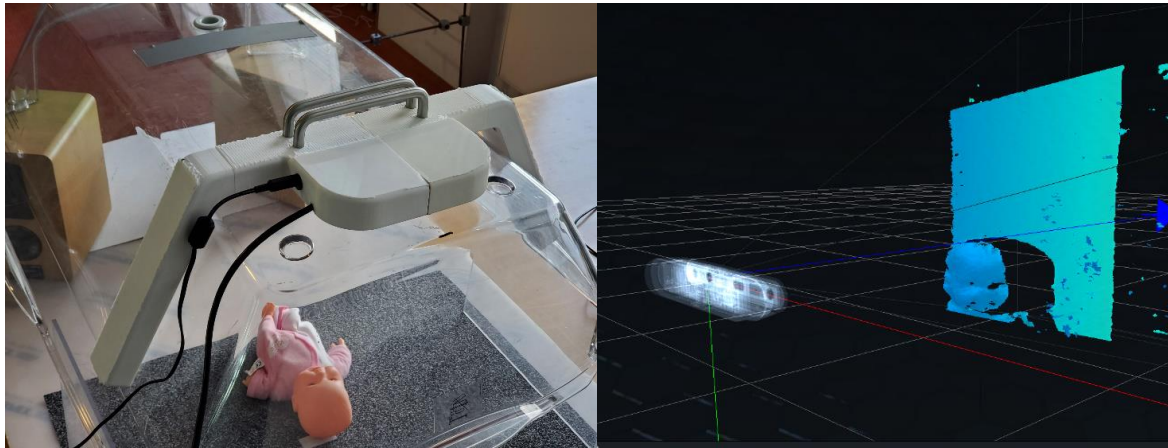


Figure 64 - The prototype plugged into a computer running the RealSense viewer software

The prototype features an integrated USB 3.1 Type A cable, which must be plugged into a computer running the required software, which will be detailed later. Figure 64 also shows an additional DC power cable which can be plugged into the device in case the computer cannot provide the required power over USB (~2A @ 5V).

The user can then place the device on top of the incubator using the handles on top of the product. Using the Intel Realsense software, the user can display a live preview of the output of one of the three integrated cameras. This preview is used to ensure a correct placement of the device, so it can capture the full head of the infant.

ACQUISITION

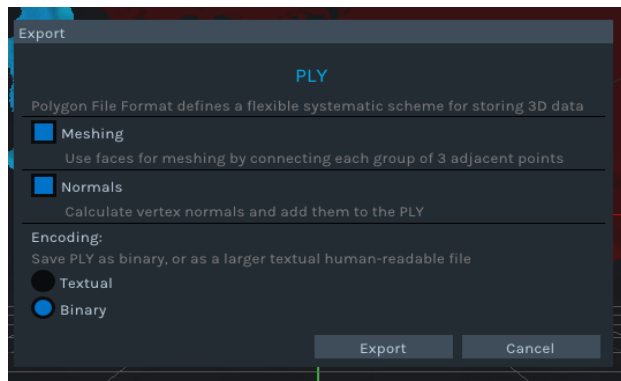


Figure 65 - RealSense mesh export dialogue

Using the Intel RealSense Viewer software (RealSense Technology, 2020), the user can directly export a 3D mesh of each of the three camera's current views (figure 65). The created files contain all geometry withing the FoV of the cameras, which include that of the infant's head.

ACQUIRING THE ENTIRE HEAD

One of the biggest hurdles to overcome was capturing the entire head of the infant. As discussed earlier, the infant is lying on an opaque mattress, which always hides part of the head from the cameras' view. This makes capturing the full head without interacting with the child challenging. Appendix G discusses the considered solutions for this problem in detail.

It was determined that the best way of acquiring data from all sides of the infant's head was to take multiple acquisitions, each one with the head in a different orientation: Facing up, facing to the left, and facing to the right. The total of these acquisitions then contains all the data needed for a full head reconstruction. Additionally, acquisitions do not have to be taken directly after one another. Instead, the current NICU procedure of rotating the infant's head multiple time a day, in order to prevent deformations in the cranium as it grows, can be used to obtain these additional head positions, fully eliminating any physical contact needed specifically for the HC measurement.

MESH PROCESSING

After all acquisitions have been made, the relevant geometry (i.e. the geometry that is part of the infant's head) must be isolated from all other captured data. After this the separate meshes will be puzzled together (aligned) in order to form the infant's head. Then, the edges of each mesh will be trimmed by a set amount in order to remove false data. Finally, the collection of meshes will be merged and remeshed into a final, representative model of the head.

CUTTING

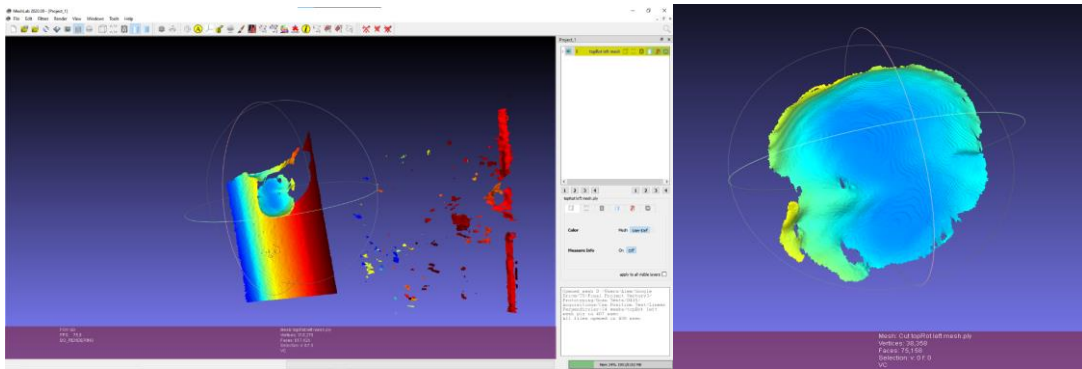


Figure 66 - Image depicting mesh before and after cutting away irrelevant geometry

Since the cameras capture the entire scene, a lot of irrelevant data, such as geometry of the mattress, surrounding equipment and noise, is contained within each file. This irrelevant data must be cut away before the meshes can be aligned together. To this end, the Meshlab software is used (Cignoni et al., 2008). Meshlab allows the user to manually drag boxes to select parts of the geometry. The user is to select irrelevant parts of the mesh and delete these, until only the head of the infant remains (figure 66).

ALIGNMENT

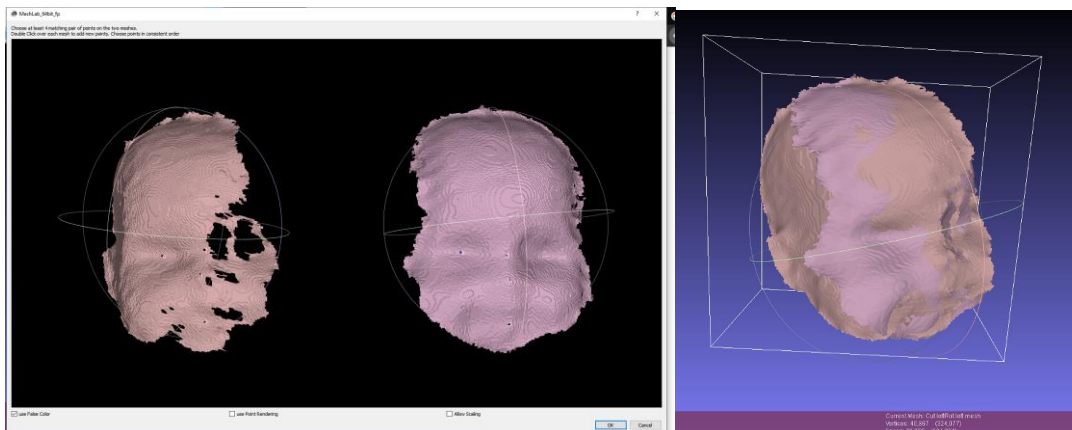


Figure 67 - Screen capture of MeshLab gluing dialogue

Using the same Meshlab software, the separate meshes must now be aligned by the user. This happens in pairs through point-based gluing. Figure 67 shows two meshes in the gluing dialogue. The user is to select four corresponding landmark points on these meshes, after which the software aligns them automatically (figure 67). This process is repeated for all meshes, until the full head has been reconstructed.

TRIMMING

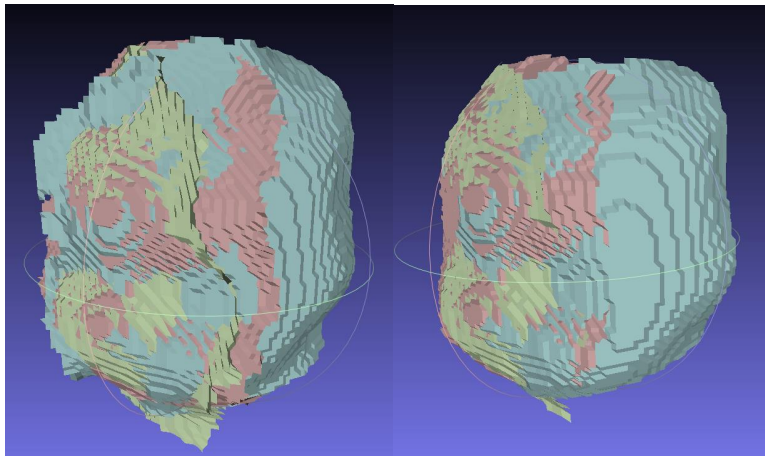


Figure 68 - Aligned mesh before and after trimming excess geometry

The vertices on the edges of each acquired mesh are not true to the scanned head which causes the aligned meshes to display a “candy-wrapper” like effect of overlapping geometry. To remedy this, 8 loops of the outer edge of each mesh are removed using Meshlab. Figure 68 shows the aligned meshes before and after trimming. Note the reduced overlap in the geometry.

REMESHING

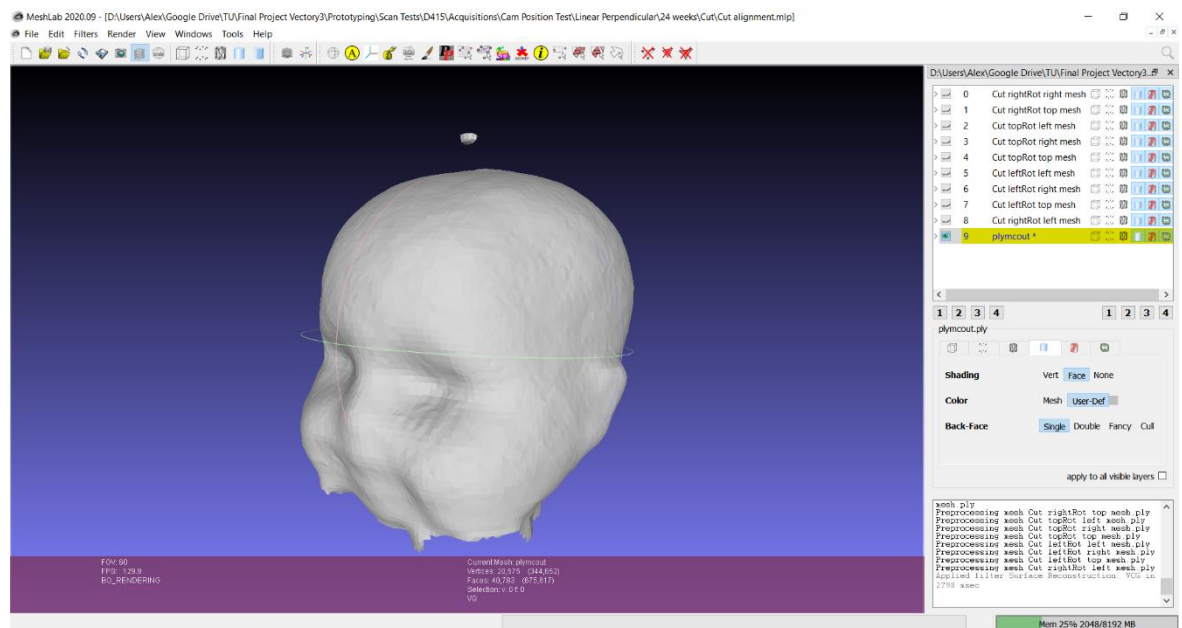


Figure 69 - MeshLab window showing the end result of remeshing the aligned meshes

Finally, now that the data has been fully cleaned and aligned, the multiple meshes can be merged, smoothed and remeshed using MeshLab’s VCG reconstruction algorithm. The result of this can be seen in figure 69. Stray geometry can be removed by the user using the same box select method as used when cutting the original meshes.

MEASURING CIRCUMFERENCE

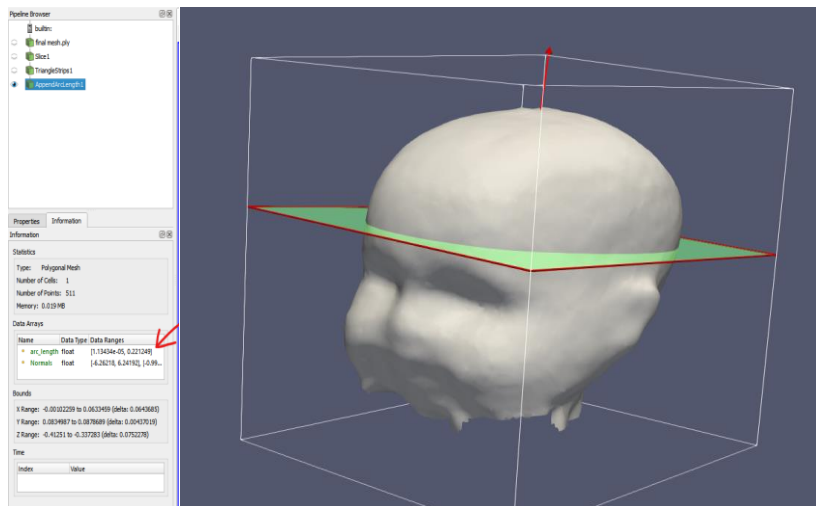


Figure 70 - ParaView displaying the resulting head circumference after a measurement

Now that the 3D model of the infant has been created, the head circumference measurement can be performed using the ParaView software (Ahrens et al., 2005). The user can place a green plane representing the “slice” of the head along which the measurement will be performed. The software then displays the HC value as depicted in figure 70.

4.2 MEASURE ACCURACY

For the device to replace the current measuring method for head circumference (the tape measure) it must meet or exceed that method's accuracy in order to be considered. This accuracy was set at an HC deviation of <math><0.73\text{cm}</math> (PoR 1.5), which translates to a radius deviation of <math><1\text{mm}</math> (PoR 1.6). The product was also tested to function in a 0 lux environment as per PoR 1.11.

4.2.1 METHOD

For this test, scans were made in two situations to test the product in a realistic scenario.



Figure 71 - Setup for situation 1

Figure 71 depicts situation 1. The incubator is placed in an environment with 562 lux environmental light (sun + CFL). The child is not obstructed from view of the scanner. Originally, the child is lying on a flat, white surface. This was changed after the pilot to a 4cm raised platform due to technical issues with the prototype. This will be further explained in 4.2.4 Discussion.

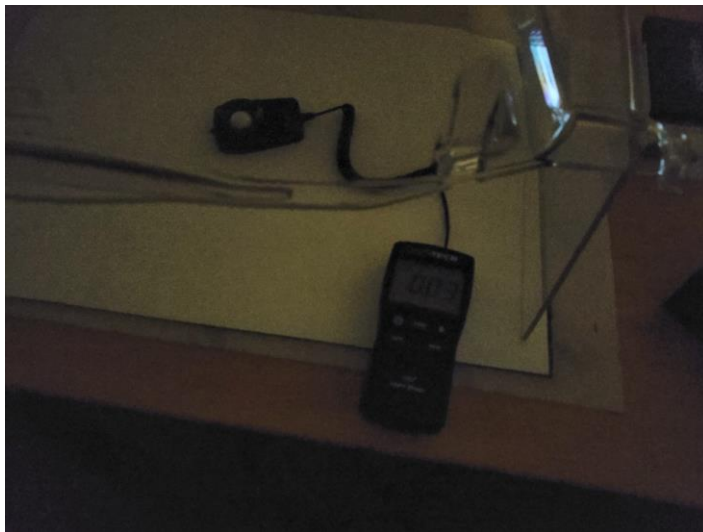


Figure 72 - Low light conditions for setup 2

Figure 72 depicts situation 2. This situation uses the same incubator setup, with the only change being the lighting condition. These were reduced to near-zero lux to simulate hospital environments where the child is kept in complete darkness for as long as possible (e.g., the situation at the Erasmus MC NICU).



Figure 73 - 24 week infant doll with HC tape measurement showing

The scan subject is a doll depicted in figure 73. Figure 29 shows a scan of the doll's head made with an Artec Eva scanner. This scanner has a 0.1mm accuracy. Its scan is used as the ground truth for this test, meaning that all scans produced by the product will be compared to this scan.

The doll was scanned 5 times in each scenario. The scans were processed according to the method described in Appendix E. The Artec scan and the product scans were aligned and distance-measured using the CloudCompare software. The comparison between the tape measure HC and the scan HC was made in the ParaView software.

4.2.3 RESULTS

Table 10 - Results scans situation 1 (light)

Scan#	1	2	3	4	5
Mean Signed Distance (mm)	0.066	0.060	0.063	0.067	0.071
Mean Absolute Distance (mm)	1.116	1.110	1.113	1.116	1.132
RMS (mm)	1.482	1.471	1.480	1.482	1.453
HC Deviation (mm)	2.51	2.46	2.48	2.51	2.53

The results for situation 1 are given in table 10. All values are close together as expected, with RMS ranging between 1.453mm and 1.482mm, and mean absolute distance ranging from 1.110mm to 1.132mm. Head circumference deviated from the tape measurement by 2.48mm to 2.53mm.

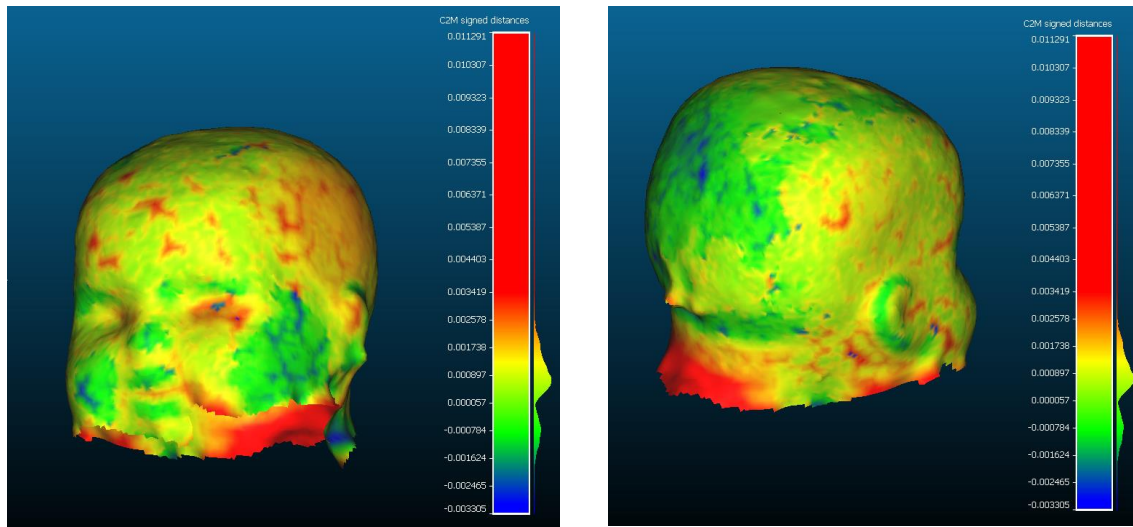


Figure 74 - Distance map of scan 2 of situation 1

Figure 74 shows that again the neck of the infant shows the greatest deviation. It also displays the histogram which shows a less pronounced double peak around 0.

Table 11 - Results scans situation 2 (dark)

Scan#	1	2	3	4	5
Mean Signed Distance (mm)	0.018	0.018	0.016	0.017	0.016
Mean Absolute Distance (mm)	1.130	1.131	1.123	1.128	1.125
RMS (mm)	1.283	1.284	1.285	1.280	1.287
HC Deviation (mm)	0.43	0.41	0.39	0.40	0.40

The results for situation 2 are given in table 11. All values are close together as expected, with RMS ranging between 1.280mm and 1.287mm, and mean absolute distance ranging from 1.122mm to 1.131mm. Head circumference deviated from the tape measurement by 0.39mm to 0.43mm.

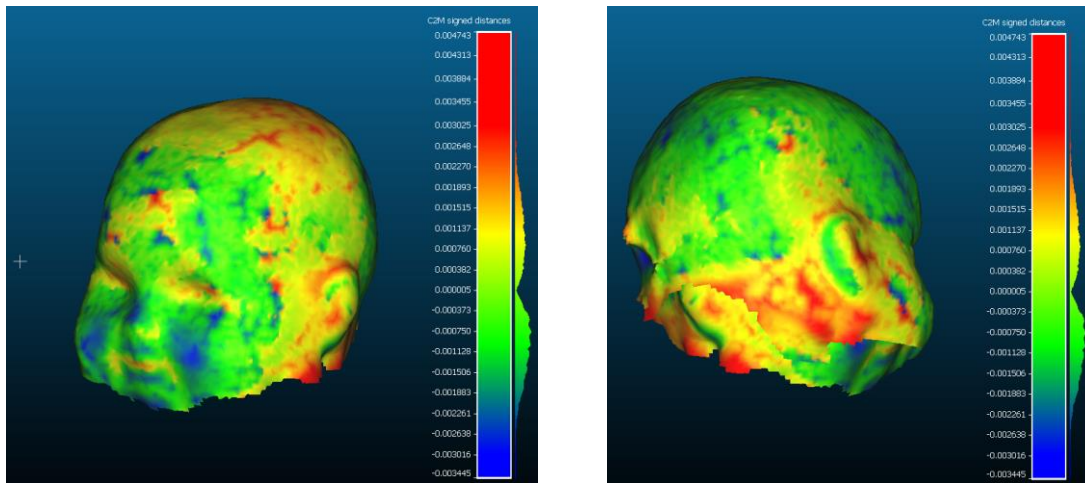


Figure 75 - Distance map of scan 4 of situation 2

Figure 75 depicts that the neck of the infant shows the greatest deviation. It also displays the histogram which clearly shows two peaks around the 0.

4.2.4 DISCUSSION

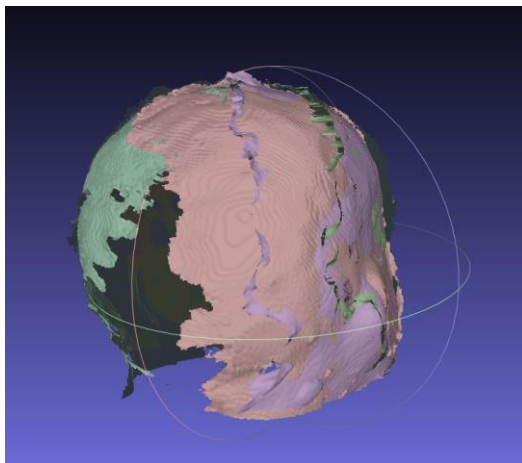


Figure 76 - Image showing missing geometry due to a design flaw in the prototype

During initial testing it became clear that there was an issue with the image acquisition. Figure 76 shows the rear side of model after the alignment step. The rear two acquisitions which are supposed to overlap instead show a large gap. This made it impossible to recreate a full 3D model of the head. The cause was determined to be a twofold design flaw. Firstly, due to erroneous measurements of the incubator hood, the device was too small, causing it to be lifted $\sim 1\text{cm}$ from the surface of the incubator. Additionally, the side cameras were mounted too high in the construction in order to make place for fasteners and a power plug. This added up to the side cameras of the device being placed $\sim 5\text{cm}$ higher than they were placed in the camera setup experiment. Because of this, the conical FoV of the cameras caused scannable the area on the surface of the incubator bedding to be reduced severely enough that the entire head could no longer be captured.

To mitigate this problem fully, a redesign of the prototype is necessary. Unfortunately, this was not possible due to time constraints. In order to still determine the setup's accuracy, the child was raised the lost 5cm by lying it on a small platform in the incubator. This way the test could still be performed.

Looking at the data some interesting observation can be made. The histograms of both scenarios show two separate peaks, one on each side of the chart. In Scenario 2, these are of near equal size. This can also be seen in the mean signed distance values in that scenario. The fact that these are close to 0 means that even though there is a deviation in both directions from the Artec scan, the total volume of the scan should be near identical between the two. This effect is less pronounced, but still clearly visible in scenario 1. Though similarities between areas either having a negative or positive deviation from the Artec scan can be found between scenarios (e.g., the ears, neck, cheeks, etc.) as of yet no full explanation of the occurrence of the double peak has been found.

From the relevant figures it is clear that some areas of the head are more prone to deviation than other. Both scenarios show the neck area having the largest deviation of the scan. This is because of the setup of the cameras (which are optimized for capturing the cranium) making it so that the device is positioned slightly above the head, reducing detail in the neck area. Additionally, the VCG reconstruction algorithm used to re-mesh the scan consistently “fans” out the geometry when a hole is encountered, as is the case in the neck area. This effect can also be seen in the small protrusion on the back of the head in both scenarios. This protrusion originates from a hole created through a lack of camera data in that area.

This lack of data is due to a combination of 2 factors: the earlier discussed small FoV of the camera, and the improper rotation of the child’s head. For these (and previous) tests the child’s head had always been rotated until the side of the was parallel tot the bedding of the incubator. This apparently is not enough to consistently capture the full head of the child. Though this is not important for the HC measurement, since the blind spot sits below the region of interest for those type of measurements, it could reduce accuracy when the device is used for cranial volume scans.

4.2.3 CONCLUSION

The product can scan with an accuracy that meets and exceeds that of the currently used tape measure, with am HC deviation between 0.39 and 2.53mm. This means that the product meets PoR 1.5. PoR 1.6, however, was not met. None of the RMS values got below the 1mm mark set in the requirement. This means that the product might potentially not meet volumetric scanning requirements for future cranial volume exams. However, the low signed distance between the Artec and product scan suggests that the total volume of the should indeed be near that of the ground truth.

4.3 USER EXPERIENCE: POSITIONING

The device needs to be setup before it can be used to make an acquisition. An important step of this setup is the correct placement of the device on the incubator hood. The device must be placed in such a way that all relevant parts of the infant are in view of all the cameras. To accomplish this, a setup method was devised that makes use of a live preview of the scanner's output on a connected computer, allowing users to directly see the influence of their actions on the scanner's output, allowing them to place the device correctly and confidently. To test this method, a short experiment was setup that allows participants to place the device using the described method in order to find out their experience of the process.

In this test a distinction is made between placement and positioning of the device. Placement entails picking up the device and roughly placing it in the correct position on the incubator hood. Positioning entails minor adjustments made to the position of the device after initial placement on the incubator hood.

4.3.1 RESEARCH QUESTIONS

- 1) Is the placement of the hood intuitive to the user?
- 2) Is the positioning of the hood intuitive to the user?
- 3) How does the user score the positioning of the device regarding comfort?
- 4) How does the user score the confidence in having placed the device correctly?

4.3.2 METHOD



Figure 77 - the test setup for the placement test

A setup was built using the test incubator setup as pictured in figure 77. The product is lying next to the incubator, already connected to a laptop running the live preview software. The laptop is positioned in such a way that it mimics the position of the bedside computer at the Erasmus MC NICU. A video camera was used during testing for processing of the results. This video was deleted after the results have been gathered.

The participant is given an oral explanation of the test, explaining its purpose. The participant is then given an oral explanation about the head circumference measurement in preterm infants, including the infant's

sensitivities. Finally, the function of the device is explained, without explicitly telling the user how it is operated. The first test then begins:

INTUITIVENESS TEST

- 1) The user is positioned next to the incubator, on the side of the product and the live preview.
- 2) The participant is asked to “Place the product on the incubator”
- 3) The participant is asked to “Adjust the placement of the device on the incubator, until they think it is correct”
- 4) The participant is now asked to rate their “comfort of placement on scale from 1 to 7, 7 being very comfortable, 1 being very uncomfortable
 - a) The user is asked to motivate their score
- 5) The participant is now asked to rate their “confidence in having place the device correctly on scale from 1 to 7, 7 being very confident, 1 being very unconfident
 - a) The user is asked to motivate their score
- 6) The participant is asked for any additional remarks.

USABILITY TEST

The user is now given a full explanation of the intended use of the device, including an explanation on how to use the live preview on the laptop, and an explanation of what a correct placement is. The test is then repeated as follows.

- 1) The user is positioned next to the incubator, on the side of the product and the live preview.
- 2) The participant is asked to “Place the product on the incubator”
- 3) The participant is asked to “Adjust the placement of the device on the incubator, until they think it is correct”
- 4) The participant is now asked to rate their “comfort of placement on scale from 1 to 7, 7 being very comfortable, 1 being very uncomfortable
 - a) The user is asked to motivate their score
- 5) The participant is now asked to rate their “confidence in having place the device correctly on scale from 1 to 7, 7 being very confident, 1 being very unconfident
 - a) The user is asked to motivate their score
- 6) The participant is asked for any additional remarks.

4.3.3 RESULTS

Table 12 - Comfort and Confidence scores of participants pre- and post-instruction

Participant #	Pre-Instruction		Post-Instruction	
	Comfort	Confidence	Comfort	Confidence
1	7	5	4	6
2	5	5	5	6
3	6	5	6	7
4	7	6.9	7	6.9
5	6	3.5	6	7
6	7	4	7	7
7	5	4	5	7
8	5.5	6	5.5	7

Table 12 shows the scores each of the 8 participants gave to the comfort and confidence of using the device before and after having received instructions on its intended functioning. Comfort scores varied between 4 and 7, while confidence score varied between 3.5 and 7. Comfort scores did not improve after instruction, and in one case even dropped due to the participant not liking the intended way of placing the device by the handle. The confidence score rose an average of 2 points after instruction was given.

Table 13 - Participant remarks and behaviour during the test

Positive Remarks	# of mentions
Easy to handle	4
Understood the sticker once I saw the monitor	4
Placing was instantly clear through the sticker	7
Placing was instantly clear through the shape of the device	2
Improvement points	
Too heavy	2
Handle should allow for two hands	4
I don't know whether I placed it at exactly 5 mm	2
I tried to replicate the physical measurement digitally [referring to placing the positioning line across the widest part of the skull as if it were a measuring tape]	1
I didn't notice the second picture on the sticker/correlate it to the laptop screen	4
I want to use my second hand to steady the device while precisely positioning	4

Table 13 shows a breakdown of the comments and behaviors made by users while operating the device. Since most participants had the same remarks, these remarks were written down with a number indicating the frequency of it being mentioned by different participants.

4.3.4 DISCUSSION

Though it was expected that the confidence score would vary between participants before instruction, it was surprising to see that the comfort score, too, was varying between 4 and 7 points. Looking at the remarks made by the participants, the biggest culprit seems to be the way the handle is designed. 4 out of 8 participants tried to either grab the device by its sides instead of the handle, or tried to otherwise incorporate their second hand while positioning the device. Asking about this, all participants gave the same answer: "control". Since it was their first time using the device, and the movement of the device in relation to the camera feedback was not yet clear, participants were careful to precisely position the device in the way they thought was correct. Half of these participants felt the urge to use a second hand in order to better control the device, and thus exert more control over its exact position. A redesign of the grip must thus be considered in order to allow for this behavior, which would in turn increase the perceived comfort of the device.

2 out of 8 participants also noted the high weight of the unit. The device weighs about 1kg, which isn't much when handling or carrying it close to you. However, since the incubator is a large object with little freedom of positioning yourself around it, users would have to outstretch their arms for a short period of time while placing the device on the incubator hood.

Confidence scores seemed to mostly be influenced by participants' understanding of the sticker included on the device. The two steps displayed on the sticker had a large variation in their success to convey the use of the product. The first part, indicating the placement of the device on top of the incubator, was successfully communicated to 6 of the 8 participants, with the other 2 finding the placement out through the shape of the device. The second part, however, did not fair as well. Only 4 out of 8 participants noticed the correlation between that part of the sticker and the laptop screen. The other 4 either did not understand its meaning, or outright ignored the drawing.

4.3.5 CONCLUSION

Through this test three clear directions for improvement were found: Creating the ability for people to handle the device with two hands, Reducing the strain generated on the arm of people by adjusting the way the device is handled, and modifying the second part of the sticker by more clearly conveying the correlation between the drawing and the laptop screen.

Outside of these improvements, the product performed well. While not perfect, the product was able to be used correctly in half the cases without any prior training or explanation. Though this is not a scenario that will occur in real life (hospital staff is always trained on equipment) the test proves that using the product does not require a great cognitive load from the user, satisfying PoR 4.1 through 4.4.

4.4 USER EXPERIENCE: MESH PROCESSING

Even though the mesh processing steps of the prototype are not at a level of automation envisioned for the final product, they are developed far enough to produce a usable outcome when followed. It is, however, unrealistic to expect NICU nursing staff to perform the relatively lengthy process (compared to the current measuring tape-based HC measurement) in a life NICU setting. Therefore, the ability for people to use the product in its current form is limited to researchers and their supporting staff, who wish to use the data this product generates for study.

A test was devised to determine the ability of people with varying levels of familiarity with 3D scanning and processing. This test consists of a shortened version of the mesh processing manual, whereby each step must be performed a reduced number of times when compared to a regular acquisition and processing process.

4.4.1 RESEARCH QUESTION

- 1) How much time does it take people to complete a (shortened) mesh processing sequence?
- 2) How difficult do people find the process?
- 3) How clear are the provided instructions?

4.4.2 METHOD

For this test, an online questionnaire was setup using Google Forms. This form contains links to the programs necessary to complete the mesh processing, as well as a folder which contains all the necessary mesh files to proceed with the processing. After installation of these programs, the participant can go to through the questionnaire. Each of the 5 sections of mesh processing (Cutting, Aligning, Cleaning, Remeshing, and Measuring) are represented by an own section in the questionnaire, featuring a short (~3 minutes) instructional video. After watching this video, the participant is asked to follow the process explained in the video while timing their progress. Afterwards, the user answers questions about their performance, the difficulties they had, and the quality of the instructional video. After the final questions, the user is asked to create an archive of their work folder, which will then be sent over for me to check their output. To make sure participants do not get stuck on a single part of the video, all 5 parts would feature their own premade project files (where applicable) in order for them to continue even if they fail a previous step.

A copy of the form including all responses from participants can be found in appendix K.

4.4.3 RESULTS & DISCUSSION

The mesh processing tutorial performed above expectation. All participants where able to fully complete all the steps, even those with no prior knowledge of any 3D software. The following is a per section breakdown of the feedback received. Though positive feedback was abundant, this section will mainly focus on points of improvement.

1. MESH CUTTING

Though relatively simplistic in execution, mesh cutting was for some participants their first introduction to the use of 3D processing software. Because of that, completion times varied from 4 minutes to 20 minutes.

The task itself was considered “very easy” by most participants with 3 of the 12 rating it 5 or higher on the 1 to 7 difficulty scale. The main trouble with this step seemed to be the general control system of Meshlab. Participants did note that after some practice this issue disappears on its own as the participant gets used to the control scheme of MeshLab

All twelve participants rated the instructional video a 5 out of 7 or higher on the 1 to 7 clarity scale. A recurring request that comes up for the first time at this point is that for a “voice over”. The current videos are silent with a text overlay detailing the steps. However, participants note that it would be easier to follow if they could listen to the instructions while also looking at their own screen, instead of having to focus continuously on the video.

2. MESH ALIGNING

The most difficult step, mesh alignment took participants 2 to 25 minutes to complete. The main reason for this disparity is because of the sensitivity of the MeshLab software. If the steps are not executed exactly as on screen, the program has a chance of misaligning the meshes, which is a problem that is hard to recover. At that point, it can be quicker to restart MeshLab and try again from the beginning.

This difficulty is reflected in the difficulty score, with only 5 participants rating this task as 1 “very easy”, while 4 rated it a 6 or higher. Participants seemed to be split through the middle. When the software operated as intended the task was found quick and easy. However, as soon as something went wrong, a long process of recovering and retrying began.

Though ratings of the video were mostly positive, with 9 participants rating it a 6 or higher on clarity, this also ties into the main comments on the instructional video. Participants experienced problems were not given the tools to solve these problems in the video, leaving them to either find it out for themselves, or trying again from the start entirely. Another important point that was brought up was the inclusion of a overview of the results at the beginning of the video. Currently the videos start without showing the user what they are working towards. Showing this in the beginning of the video could put the users at ease by giving them a concrete idea of what they are trying to achieve.

3. MESH CLEANING

Mesh cleaning is a nearly fully automated step. The participant only needs to select a mesh and then run a script from the MeshLab software in order to execute it. This resulted in the step taking only 7 minutes at the longest, an 50 seconds at the shortest.

The task was rated and a very easy 2 or lower by 11 out of 10 participants, with one participant giving it 6. This participant encountered an as of yet unreproduced error that caused the script to create long ridges on the provided mesh files.

The instructions were found to be clear by most participants, with 11 participants rating it a 6 out of 7.

4. REMESHING

Remeshing was another, fully automated step that required no skill from the user. As such this step took users between 20 seconds and 5 minutes to complete.

Participants universally rated this step as easy, with all participants giving it a 2 or lower on the difficulty scale.

The instructional video was rated 6 out of 7 or higher by 10 of the participants. One important tip that came in was the clarifying of the selection system. Though the basic selection system is explained, it is not clarified that, because of MeshLab's split between mesh visibility and mesh activity, an invisible mesh can still be active and edited even if it is not on screen. Not knowing this can make it difficult for users to troubleshoot their seemingly unresponsive software

5. MEASURING

Though not difficult in execution, this step requires its own software suite: ParaView. Since this is the first time most participants used ParaView, some additional difficulty from the unfamiliar interface is to be expected. Nevertheless, all participants managed to clear this step between 1 and 15 minutes.

Task difficulty was spread evenly from 1 to 4, with some participants finding the task "straightforward" while others had difficulty with the new interface. Specifically, the long lists of filters took some participants some time to get through to find the right command. Another hurdle was the control of the slicing plane. This plane uses its own unique control scheme that takes some time to get used to. Time that the participants did not have in this single measurement.

The video itself was rated as "Quite clear" with all participants giving it a 5 out of 7 or above.

An important additional data point in this step is the actual head circumference value that the participants got. As can be seen in Appendix K, all participants got the HC value down to the same millimeter, showing that all were capable of taking the measurement.

4.4.4 CONCLUSION

Though there is still room for improvement, the videos have succeeded in their task to get even inexperienced people to successfully process the mesh and take an HC measurement by breaking down the process into more simple individual steps. On average the steps took 5 minutes to complete, with only the alignment step being an outlier (12 minutes) due to its increased difficulty and reliance on precision work.

5. CONCLUSION & RECOMMENDATIONS

At the start of this project, we set out to create a tool that would allow medical staff in the NICU to take contactless head circumference measurements of preterm infants, thereby protecting them from the stress that accompanies physical touch. The goal was for this product to be producible by Vectory3, and usable by the NICU staff.

With MONITOR3D, this tool has been created. Though there is still work to be done before this device can be put into full NICU use, this report has shown that the technology is robust and capable. The software, though unfinished and slower than the current tape-based HC measurements, is easy to use, understandable by untrained personnel through a short video tutorial, and ultimately produces a result that exceeds the accuracy of the current tape-based solution.

For the continued development of MONITOR3D, this research also found some recommendations for follow-up studies and developments.

Firstly, on the hardware side, it is important that the frame of the device is redesigned in such a way that the side cameras get pushed down into the corners as far as possible. This increases the size of the bounding box which determines the scannable area, allowing for more freedom in placing the infant in the incubator.

A solution should also be found for the current handle setup on the device. During user testing participants made it clear that a second grip or handle would increase their (sense of) control over the precise positioning of the device. This could be done through, for example, a second handle on the side of the device, or a melded-in grip.

More research needs to be done on the effect of obstructions in the incubator on the scanner. Though a test was performed with a full incubator setup, including wiring and tubing to the infant doll, this could not be included due to the before mentioned hardware design issue, and the limited amount of captures we were able to take (one).

The largest developments are to be considered for the software solution. Currently the workflow is based around readily available, standard open-source software such as the Intel RealSense Viewer, MeshLab and ParaView. Though this workflow can successfully produce results that meet the requirements (as shown in this report) the amount of manual work required to get to these results is still higher than that necessary for the current tape-based HC measurement. Therefore, time needs to be spent on automating as much of the workflow as possible to reduce this workload on the end user. Though some parts of this automation are not foreseen to be difficult, such as the automatic aligning of captures between the three cameras, others are likely to be more challenging, like the automatic cutting of the head from the surrounding geometry.

Finally, it is recommended to run trials with actual NICU staff, in order to get a better idea of the specific needs of the actual end user.

6. REFERENCES

- Ahrens, J., Geveci, B., & Law, C. (2005). ParaView: An end-user tool for large-data visualization. In *Visualization Handbook*. <https://doi.org/10.1016/B978-012387582-2/50038-1>
- Akiyama, S., Ohta, H., Watanabe, S., Moriya, T., Hariu, A., Nakahata, N., Chisaka, H., Matsuda, T., Kimura, Y., Tsuchiya, S., Tei, H., Okamura, K., & Yaegashi, N. (2010). The Uterus Sustains Stable Biological Clock during Pregnancy. *The Tohoku Journal of Experimental Medicine*, *221*(4), 287–298. <https://doi.org/10.1620/tjem.221.287>
- American Academy of Pediatrics AAP Task Force on Infant Positioning and SIDS: Positioning and SIDS. (1992). *Pediatrics*, *89*(6 Pt 1), 1120–1126. <http://www.ncbi.nlm.nih.gov/pubmed/1503575>
- Ancel, P. Y., Goffinet, F., Kuhn, P., Langer, B., Matis, J., Hernandorena, X., Chabanier, P., Joly-Pedespan, L., Lecomte, B., Vendittelli, F., Dreyfus, M., Guillois, B., Burguet, A., Sagot, P., Sizun, J., Beuchée, A., Rouget, F., Favreau, A., Saliba, E., ... Kaminski, M. (2015). Survival and morbidity of preterm children born at 22 through 34 weeks' gestation in France in 2011: results of the EPIPAGE-2 cohort study. *JAMA Pediatrics*, *169*(3), 230–238. <https://doi.org/10.1001/jamapediatrics.2014.3351>
- Bartram, J. L., Rigby, A. S., & Baxter, P. S. (2005). The “Lasso-o” tape: Stretchability and observer variability in head circumference measurement. *Archives of Disease in Childhood*, *90*(8), 820–821. <https://doi.org/10.1136/adc.2004.063743>
- Bhushan, V., & Paneth, N. (1991). The reliability of neonatal head circumference measurement. *Journal of Clinical Epidemiology*, *44*(10), 1027–1035. [https://doi.org/10.1016/0895-4356\(91\)90004-S](https://doi.org/10.1016/0895-4356(91)90004-S)
- Blencowe, H., Cousens, S., Oestergaard, M. Z., Chou, D., Moller, A. B., Narwal, R., Adler, A., Vera Garcia, C., Rohde, S., Say, L., & Lawn, J. E. (2012). National, regional, and worldwide estimates of preterm birth rates in the year 2010 with time trends since 1990 for selected countries: A systematic analysis and implications. *The Lancet*, *379*(9832), 2162–2172. [https://doi.org/10.1016/S0140-6736\(12\)60820-4](https://doi.org/10.1016/S0140-6736(12)60820-4)
- Brandon, D. H., Silva, S. G., Park, J., Malcolm, W., Kamhawy, H., & Holditch-Davis, D. (2017). Timing for the Introduction of Cycled Light for Extremely Preterm Infants: A Randomized Controlled Trial. *Research in Nursing and Health*, *40*(4), 294–310. <https://doi.org/10.1002/nur.21797>
- Cheong, J. L. Y., Hunt, R. W., Anderson, P. J., Howard, K., Thompson, D. K., Wang, H. X., Bear, M. J., Nursing, B. A., Inder, T. E., & Doyle, L. W. (2008). Head growth in preterm infants: Correlation with magnetic resonance imaging and neurodevelopmental outcome. *Pediatrics*, *121*(6), e1534–e1540. <https://doi.org/10.1542/peds.2007-2671>
- Cignoni, P., Callieri, M., Corsini, M., Dellepiane, M., Ganovelli, F., & Ranzuglia, G. (2008). MeshLab: An open-source mesh processing tool. *6th Eurographics Italian Chapter Conference 2008 - Proceedings*.
- CloudCompare* (2.11.1). (2020). <http://www.cloudcompare.org/>
- Ebrahim, M. A.-B. (2013). 3D Laser Scanners' Techniques Overview. *International Journal of Science and Research*.
- Edelman, G. J., & Aalders, M. C. (2018). Photogrammetry using visible, infrared, hyperspectral and thermal imaging of crime scenes. *Forensic Science International*, *292*, 181–189. <https://doi.org/10.1016/j.forsciint.2018.09.025>
- Geil, M. D., & Smith, A. (2008). Accuracy and reliability of a system for the digital capture of infant head shapes in the treatment of cranial deformities. *Journal of Prosthetics and Orthotics*, *20*(2), 35–38.

<https://doi.org/10.1097/JPO.0b013e318169c439>

- Geng, J. (2011). Structured-light 3D surface imaging: a tutorial. *Advances in Optics and Photonics*, 3(2), 128. <https://doi.org/10.1364/aop.3.000128>
- Geraedts, E. J., Van Dommelen, P., Caliebe, J., Visser, R., Ranke, M. B., Van Buuren, S., Wit, J. M., & Oostdijk, W. (2011). Association between head circumference and body size. *Hormone Research in Paediatrics*, 75(3), 213–219. <https://doi.org/10.1159/000321192>
- Hamer, R. D., Dobson, V., & Mayer, M. J. (1984). Absolute thresholds in human infants exposed to continuous illumination. *Investigative Ophthalmology & Visual Science*, 25(4), 381–388. <http://www.ncbi.nlm.nih.gov/pubmed/6706502>
- He, Y., Liang, B., Zou, Y., He, J., & Yang, J. (2017). Depth Errors Analysis and Correction for Time-of-Flight (ToF) Cameras. *Sensors*, 17(1), 92. <https://doi.org/10.3390/s17010092>
- Henderson, R. (2006). *Wavelength Considerations*. https://web.archive.org/web/20071028072110/http://info.tuwien.ac.at/iflt/safety/section1/1_1_1.htm
- Ichihashi, M., Ueda, M., Budiyanto, A., Bito, T., Oka, M., Fukunaga, M., Tsuru, K., & Horikawa, T. (2003). UV-induced skin damage. In *Toxicology* (Vol. 189, Issues 1–2, pp. 21–39). Elsevier Ireland Ltd. [https://doi.org/10.1016/S0300-483X\(03\)00150-1](https://doi.org/10.1016/S0300-483X(03)00150-1)
- Ifflaender, S., Rüdiger, M., Koch, A., & Burkhardt, W. (2013). Three-Dimensional Digital Capture of Head Size in Neonates – A Method Evaluation. *PLoS ONE*, 8(4), e61274. <https://doi.org/10.1371/journal.pone.0061274>
- Ifflaender, S., Rüdiger, M., Konstantelos, D., Wahls, K., & Burkhardt, W. (2013). Prevalence of head deformities in preterm infants at term equivalent age. *Early Human Development*, 89(12), 1041–1047. <https://doi.org/10.1016/j.earlhumdev.2013.08.011>
- Intel. (2019). *LiDAR Camera L515* (Issue December).
- Intel. (2020). *LiDAR Camera L515*. <https://store.intelrealsense.com/buy-intel-realsense-lidar-camera-l515.html>
- Jarus, T., Bart, O., Rabinovich, G., Sadeh, A., Bloch, L., Dolfin, T., & Litmanovitz, I. (2011). Effects of prone and supine positions on sleep state and stress responses in preterm infants. *Infant Behavior and Development*, 34(2), 257–263. <https://doi.org/10.1016/j.infbeh.2010.12.014>
- Krueger, C., Horesh, E., & Crossland, B. A. (2012). Safe Sound Exposure in the Fetus and Preterm Infant. *JOGNN - Journal of Obstetric, Gynecologic, and Neonatal Nursing*, 41(2), 166–170. <https://doi.org/10.1111/j.1552-6909.2012.01342.x>
- Kuhn, P., Zores, C., Pebayle, T., Hoeft, A., Langlet, C., Escande, B., Astruc, D., & Dufour, A. (2012). Infants born very preterm react to variations of the acoustic environment in their incubator from a minimum signal-to-noise ratio threshold of 5 to 10 dBA. *Pediatr Res*, 71(4 Pt 1), 386–392. <https://doi.org/10.1038/pr.2011.76>
- Liu, L., Oza, S., Hogan, D., Chu, Y., Perin, J., Zhu, J., Lawn, J. E., Cousens, S., Mathers, C., & Black, R. E. (2016). Global, regional, and national causes of under-5 mortality in 2000–15: an updated systematic analysis with implications for the Sustainable Development Goals. *The Lancet*. [https://doi.org/10.1016/S0140-6736\(16\)31593-8](https://doi.org/10.1016/S0140-6736(16)31593-8)
- Martini, M., Klausling, A., Lüchters, G., Heim, N., & Messing-Jünger, M. (2018). Head circumference - a useful single parameter for skull volume development in cranial growth analysis? *Head and Face Medicine*, 14(1). <https://doi.org/10.1186/s13005-017-0159-8>
- Microsoft. (2020). *Buy the Azure Kinect developer kit – Microsoft*. <https://www.microsoft.com/en-us/p/azure->

kinect-dk/8pp5vxmd9nhq?activetab=pivot%3Aoverviewtab

Milette, I. (2010). Decreasing Noise Level in Our NICU. *Advances in Neonatal Care*, 10(6), 343–351.
<https://doi.org/10.1097/ANC.0b013e3181fc8108>

Mouser. (2020).
<https://nl.mouser.com/ProductDetail/Intel/82635D435IDK5P?qs=PqoDHHvF64%252B5RxJ3DyHflg%3D%3D>

Murobo. (n.d.). Retrieved May 5, 2020, from <http://store.murobo.com/atlas-3d-kit/>

Newnham, C. A., Inder, T. E., & Milgrom, J. (2009). Measuring preterm cumulative stressors within the NICU: The neonatal infant stressor scale. *Early Human Development*.
<https://doi.org/10.1016/j.earlhumdev.2009.05.002>

NW Newborn Clinical Guideline - Care of the baby in an Incubator. (n.d.). Retrieved April 15, 2020, from <http://www.adhb.govt.nz/newborn/Guidelines/Admission/BabyInIncubator.htm>

Occipital. (2020a). *Structure Accuracy*. <https://support.structure.io/article/377-how-precise-is-structure-sensor-mark-ii>

Occipital. (2020b). *Structure Costs*. <https://www.makepoint.nl/nl/structure-sensor-mark-ii-standalone-100525845.html>

Peixoto, P. V., de Araújo, M. A. N., Kakehashi, T. Y., & Pinheiro, E. M. (2011). Sound pressure levels in the neonatal intensive care unit. *Revista Da Escola de Enfermagem*, 45(6), 1309–1314.
<https://doi.org/10.1590/S0080-62342011000600005>

Perined | Home. (n.d.). Retrieved January 7, 2020, from <https://www.perined.nl/>

Positioning your premature baby. (2016). <https://www.tommys.org/pregnancy-information/pregnancy-complications/premature-birth/your-babys-time-hospital/positioning-your-premature-baby>

RealSense Technology, I. (2020). *Intel® RealSense™ TM Product Family D400 Series Datasheet Intel® RealSense™ Vision Processor D4, Intel® RealSense™ Vision*. www.intel.com/design/literature.htm.

Rivas-Fernandez, M., Roqué i Figuls, M., Diez-Izquierdo, A., Escribano, J., & Balaguer, A. (2016). Infant position in neonates receiving mechanical ventilation. In *Cochrane Database of Systematic Reviews* (Vol. 2016, Issue 11). John Wiley and Sons Ltd. <https://doi.org/10.1002/14651858.CD003668.pub4>

Rivkees, S. A. (2004). Emergence and influences of circadian rhythmicity in infants. In *Clinics in Perinatology* (Vol. 31, Issue 2, pp. 217–228). Elsevier. <https://doi.org/10.1016/j.clp.2004.04.011>

Robinson, J., Moseley, M. J., & Fielder, A. R. (1990). Illuminance of neonatal units. *Archives of Disease in Childhood*. https://doi.org/10.1136/adc.65.7_Spec_No.679

Rozenburg, N. F. M., & Eekels, J. (1995). *Product Design: Fundamental and Methods*. Wiley.

Santander, P., Quast, A., Hubbert, J., Horn, S., Meyer-Marcotty, P., Küster, H., & Dieks, J. K. (2020). Three-dimensional head shape acquisition in preterm infants - Translating an orthodontic imaging procedure into neonatal care. *Early Human Development*, 140, 104908.
<https://doi.org/10.1016/j.earlhumdev.2019.104908>

Sliney, D. H. (1994). UV radiation ocular exposure dosimetry. *Documenta Ophthalmologica*, 88(3–4), 243–254.
<https://doi.org/10.1007/BF01203678>

Smakman, P. (2014). *Curatio: Development of a low-cost, dedicated 3D Hand Scanner*.
<http://resolver.tudelft.nl/uuid:a4202d21-6174-4994-a6ea-828392836c54>

- Smith, G. C., Gutovich, J., Smyser, C., Pineda, R., Newnham, C., Tjoeng, T. H., Vavasseur, C., Wallendorf, M., Neil, J., & Inder, T. (2011). Neonatal intensive care unit stress is associated with brain development in preterm infants. *Annals of Neurology*, 70(4), 541–549. <https://doi.org/10.1002/ana.22545>
- Smith, S. W., Ortmann, A. J., & Clark, W. W. (2018). Noise in the neonatal intensive care unit: A new approach to examining acoustic events. *Noise and Health*, 20(95), 121–130. https://doi.org/10.4103/nah.NAH_53_17
- Spong, C. Y. (2013). Defining “term” pregnancy: Recommendations from the defining “term” pregnancy workgroup. In *JAMA - Journal of the American Medical Association* (Vol. 309, Issue 23, pp. 2445–2446). <https://doi.org/10.1001/jama.2013.6235>
- STARscanner – Orthomerica Products, Inc. (2020). <https://www.orthomerica.com/products/starband/starscanner/>
- Szczepański, M., & Kamianowska, M. (2008). The illumination intensity in the neonatal intensive care unit. In *Archives of Perinatal Medicine* (Vol. 14, Issue 2).
- Terabee. (n.d.). *A Brief Introduction to Time-of-Flight Sensing*. Retrieved May 1, 2020, from <https://www.terabee.com/a-brief-introduction-to-time-of-flight-sensing-part-2-indirect-tof-sensors/>
- Vos, J. J., & Van Norren, D. (1994). Weighing the relative significance of three heat dissipation mechanisms to produce cataract. *Lasers and Light in Ophthalmology*, 6(2), 107–117.
- Vukašinić, N., Korošec, M., & Duhovnik, J. (2010). The influence of surface topology on the accuracy of laser triangulation scanning results. *Strojnski Vestnik/Journal of Mechanical Engineering*.
- Watanabe, S., Akiyama, S., Hanita, T., Li, H., Nakagawa, M., Kaneshi, Y., Ohta, H., & Japan RED filter study group. (2013). Designing artificial environments for preterm infants based on circadian studies on pregnant uterus. *Frontiers in Endocrinology*, 4(SEP), 113. <https://doi.org/10.3389/fendo.2013.00113>
- White, R. D., Smith, J. A., & Shepley, M. M. (2013). Recommended standards for newborn ICU design, eighth edition. *Journal of Perinatology*, 33(SUPPL. 1), S2–S16. <https://doi.org/10.1038/jp.2013.10>
- Willinger, M., Hoffman, H. J., Wu, K. T., Hou, J. R., Kessler, R. C., Ward, S. L., Keens, T. G., & Corwin, M. J. (1998). Factors associated with the transition to nonprone sleep positions of infants in the united states: The national infant sleep position study. *Journal of the American Medical Association*, 280(4), 329–335. <https://doi.org/10.1001/jama.280.4.329>
- Zabatani, A., Surazhsky, V., Sperling, E., Ben Moshe, S., Menashe, O., Silver, D. H., Karni, T., Bronstein, A. M., Bronstein, M. M., & Kimmel, R. (2019). Intel® RealSense™ SR300 Coded light depth Camera. *IEEE Transactions on Pattern Analysis and Machine Intelligence*, 1–1. <https://doi.org/10.1109/tpami.2019.2915841>
- Ziegelberger, G. (2013a). ICNIRP guidelines on limits of exposure to laser radiation of wavelengths between 180 nm and 1,000 μm. *Health Physics*. <https://doi.org/10.1097/HP.0b013e3182983fd4>
- Ziegelberger, G. (2013b). ICNIRP guidelines on limits of exposure to incoherent visible and infrared radiation. In *Health Physics* (Vol. 105, Issue 1, pp. 74–96). <https://doi.org/10.1097/HP.0b013e318289a611>